

**DESIGN, ANALYSIS, TESTING, AND EVALUATION OF A
PROSTHETIC VENOUS VALVE**

A Thesis
Presented to
The Academic Faculty

by

Daniel Edward Tanner

In Partial Fulfillment
of the Requirements for the Degree
Master of Science in the
School of Mechanical Engineering

Georgia Institute of Technology
May 2013

COPYRIGHT © DANIEL EDWARD TANNER 2013

**DESIGN, ANALYSIS, TESTING, AND EVALUATION OF A
PROSTHETIC VENOUS VALVE**

Approved by:

Dr. David N. Ku, Advisor
School of Mechanical Engineering
Georgia Institute of Technology

Dr. Rudolph Gleason
School of Mechanical Engineering
Georgia Institute of Technology

Dr. Luke Brewster
Department of Surgery
Emory University

Date Approved: April 4, 2013

ACKNOWLEDGEMENTS

First and foremost, I would like to thank Jennifer, my wife and sweetheart. She has been more than supportive of the long hours required of graduate work, and yet has always been there to help me live a balanced life. I will always remember and treasure the many walks we took through campus together and the discussions we had regarding the latest development of my research, the affairs of the day, or our plans for the future. She inspires me to aim high in my goals and to do my very best in everything I do. I am grateful for her ability to discern which things matter most and for her help to prioritize my efforts.

I would like to thank my parents, Keith and Valarie Tanner, for raising me in a stable and loving home and for teaching me the value of education and diligent work. I would like to thank them for making learning fun for me as a child and for the many hours they spent doing schoolwork with me, as this ultimately enabled me to pursue higher education. They have supported me in every phase of my education, for which I am extremely grateful. I would also like to thank them for their example of how to budget time and money wisely.

I would like to thank my brother Brian for being the ideal hero for me, his younger brother. I appreciate the many unspoken lessons his example taught me about the importance of making time to care for and help others.

I would like to thank my lab mates, both past and present, who never ceased to amaze me with the endless wealth of knowledge they so willingly imparted to me: Andrea Para, Mark Livelli, Marmar Mehrabadi, Lauren Casa, John Glisson, Kathleen Bernhard, and Susan Hastings. I would especially like to thank Alex McIntire for the many hours he spent assisting me with the fabrication and testing of valve prototypes.

Finally, I would like to thank my advisor, Dr. David Ku, for all the mentoring and opportunities he has given me which have laid the foundation for me to work in the medical device industry. I appreciate his efforts to strengthen my creativity, critical thinking, and ability to problem solve. He has instilled in me a desire to seek continuous improvement, and his imprint will be felt for years to come in both my personal and professional life.

TABLE OF CONTENTS

ACKNOWLEDGEMENTS	iii
LIST OF TABLES	xi
LIST OF FIGURES	xiii
SUMMARY	xx
CHAPTER 1: INTRODUCTION	1
Chronic Venous Insufficiency	1
Prevalence and Economic impact	1
Quality of Life.....	3
Main Contributors to Venous Hypertension.....	3
Quantifying Symptom Severity	11
Approaches to Treatment.....	13
Exercise.....	14
Compression	15
Medication	16
Vein Disabling	16
Venous Stenting	17
Surgical Correction	17
Prosthetic Venous Valves	19

Remaining Issues	39
CHAPTER 2: DESIGN SPECIFICATIONS	41
Competency	41
Fatigue Life	42
Closing Time	42
Distal Pressure Rise	43
Outflow Resistance	43
Thrombogenicity	44
Stagnation Zones	44
Regions of High Shear	45
Material Biocompatibility	46
Blood Flow Loop	46
Deliverability	47
Summary	47
CHAPTER 3: PROPOWED VALVE DESIGN AND FABRICATION	49
Material Selection	49
Geometry	50
Manufacturing	55
Mold Creation	56

Stent Preparation.....	59
Valve Fabrication.....	59
Intended Use	60
CHAPTER 4: COMPUTATIONAL ANALYSIS	61
Finite Element Model	61
Material Properties.....	61
Model Creation	61
Boundary Conditions	62
Mesh Refinement and Convergence	63
Results.....	66
Computational Fluid Dynamics Model.....	69
Material Properties.....	69
Model Creation	69
Boundary Conditions	70
Mesh Refinement and Convergence	74
Results.....	77
CHAPTER 5: VERIFICATION TESTING.....	84
Preparation	84
PVA Tube Fabrication and Valve Fixation	84

Glycerol Solution Preparation and Properties.....	84
Reflux Flow Rate	85
Methods.....	85
Results.....	87
Smallest Competent Diameter	89
Methods.....	89
Results.....	89
Fatigue.....	89
Methods.....	89
Results.....	92
Closing Time.....	95
Methods.....	95
Results.....	95
Distal Pressure Rise Test	96
Methods.....	96
Results.....	98
Outflow Resistance	98
Methods.....	98
Results.....	99

Washout Test	101
Methods.....	101
Results.....	101
Buckling Test	103
Methods.....	103
Result	104
Blood Flow Loop Test	105
Methods.....	105
Results.....	106
Deliverability	107
Methods.....	107
Results.....	109
Summary.....	109
CHAPTER 6: PROPOSED VALIDATION TESTING AND SIZING	111
Purposes	111
Animal Testing.....	111
Proposed Methods.....	112
Human Testing.....	113
Location	113

Proposed Methods.....	117
Valve Sizing.....	121
Determining Vein Diameter for Sizing.....	121
Minimum Vein Diameter.....	121
Maximum Diameter.....	122
Stent Size.....	124
Valve Sizing for Sheep.....	124
Valve Sizing for Humans.....	126
Clinician Procedure.....	131
CHAPTER 7: EVALUATION AND DISCUSSION.....	133
Valve Design Evaluation.....	133
Main Contributions:.....	143
Valve Design.....	144
Design Specifications and Verification Testing.....	144
Computational Analysis.....	145
Valve Placement.....	146
Future Work.....	146
References.....	148

LIST OF TABLES

Table 1: Examples of CEAP classes C1, C2, C4, and C6 (recreated from [51]).....	12
Table 2: Relationship between CEAP class and VCS score (combined data from [55] and [56]).....	13
Table 3: Mean percent change in hemodynamic parameters from elastic compression use; all values are statistically significant ($p < 0.01$) (recreated from [38]).....	16
Table 4: Baseline and follow-up mean VCS scores for various vein disabling procedures.	17
Table 5: Summary of design specifications for a prosthetic venous valve.....	48
Table 6: Views of the original and finite element model geometry.	62
Table 7: Element characteristics of meshes constructed during mesh refinement for the finite element model.....	64
Table 8: Orifice area of the original and deformed valve geometries at specified distances above the shoulder.....	66
Table 9: Element characteristics of meshes constructed during mesh refinement for the CFD simulation.	75
Table 10: Measured time average reflux flow rates for five valve prototypes at 30 and 160 mmHg.....	88
Table 11: Time average reflux flow rates for valves before and after 500,000 cycles.....	93
Table 12: Valve closure time results for three valves.....	96
Table 13: Measured average flow rates, total outflow resistances, and resistance added by the valves results.	100

Table 14: Summary of design specifications and verification testing results for the proposed venous valve.	110
Table 15: Experimental results of the minimum height of water required to close a valve. The applied hydrostatic pressure and the height of blood needed to cause this pressure (equivalent to the minimum distance between valves in a vein) were calculated.....	114
Table 16: Occurrence of reflux in deep vein segments in ulcerated limbs (data from [42]).	115
Table 17: Comparison of ulcer healing rates for the surgical correction of single and multiple deep venous valves with primary and secondary incompetence (data from [45]).	116
Table 18: Suggested set of valve sizes with the calculated minimum and maximum D^* of each.	129
Table 19: Sizing guide for the suggested valve set.....	130
Table 20: Performance comparison of prosthetic venous valves which underwent experimental testing (data extracted from [102, 122, 123, 132, 137, 140, 142, 143, 145]). The valve presented in this work is referred to as "Tanner".	135

LIST OF FIGURES

Figure 1: In healthy veins, muscle contractions efficiently pump blood back to the heart while venous valves close to prevent reflux (left). Factors which lead to the development of CVI include incompetent venous valves which allow reflux, outflow obstruction which increases outflow resistance, and calf muscle pump dysfunction (right).....	2
Figure 2: Relationship between ambulatory venous pressure and the incidence of ulceration (image from [18])......	4
Figure 3: Veins in the Deep Venous System (image from [46]).	6
Figure 4: Veins in the superficial and perforating venous systems (image from [46]).	7
Figure 5: Normal venous flow paths with unidirectional venous valves. Blood flows from the feet (b) towards the heart (a). Perforating veins (f) connect superficial and deep venous systems (image from [9]).	8
Figure 6: Proximal (left) and distal (right) views of an open saphenous venous valve (image from [19])......	8
Figure 7: Ultrasound images of a venous valve in the great saphenous vein at the ankle. Distal (a, b) and side (c, d)views of valve leaflets when open (left) and closed (right) (image from [47])......	9
Figure 8: View of a closed venous valve (image from [19]).	9
Figure 9: CEAP classification system (image from [51])......	12
Figure 10: Revised Venous Clinical Severity Score (image from [4])......	12
Figure 11: A simplified overview for the diagnosis and treatment of CVI (image from [68])......	14
Figure 12: Before (left) and after (right) the transposition of an incompetent femoral vein into a competent great saphenous vein (image from [93])......	19

Figure 13: Taheri valve (image from[12]).	20
Figure 14: Umbilical valve created by Hill (image from Hill 1985 [107]).	21
Figure 15: Replacement valve made by Ofenloch (image from [94]).	22
Figure 16: Replacement valve made by Gomez-Jorge (image from [110]).	23
Figure 17: BVV1 (image from [110]).	24
Figure 18: BVV2 before (left) and after (right) implantation cellularization (images from [117]).	25
Figure 19: BVV3 before (left) and after (right) implantation and cellularization (images from [110]).	25
Figure 20: PAVV valve developed by Pavcnik (image from [121]).	26
Figure 21: PVVB developed by Venpro (image from [125]).	27
Figure 22: Stented valve made by Dijkstra (image from [131]).	29
Figure 23: Tissue engineered vein containing valve scaffolds made by Liu (image from [132]).	29
Figure 24: Reflux flow rate of tissue engineered venous valve developed by Liu at various pressures. The vertical axis is reflux (mL/min) and the horizontal axis is pressure (mmHg) (image from [132]).	30
Figure 25: Tissue engineered vein containing venous valve made by Wen (image from [133]).	30
Figure 26: Pellethane valve developed by Hill (image from [107]).	31
Figure 27: Uflacker monocusp valve (image from [110]).	31

Figure 28: Nadzeyka valve (image from [135]).	32
Figure 29: Sail valve (image from [136]).	32
Figure 30: First generation prosthetic venous valve prototype developed by researchers from the University of Akron (image from [140]).	34
Figure 31: Second generation prosthetic valve developed by researchers from the University of Akron (image from [138]).	34
Figure 32: Third generation prosthetic venous valve developed by researchers from the University of Akron (image from [140]).	35
Figure 33: Parabolic shaped valve developed by Sathe (image from [141]).	35
Figure 34: Forward flow of rhodamine solution through the Moriyama valves: bPVV (left) and oPVV (right) (image from [142]).	36
Figure 35: Sathe valve when closed (left) and open (right) (images from [141]).	37
Figure 36: Midha valve (left) with views of the valve cut along the major (middle) and minor (right) axes (image from [145]).	38
Figure 37: Drawings and dimensions of proposed valve.	54
Figure 38: Isometric views of the proposed valve geometry (left) and halved along the major (middle) and minor (right) axes.	55
Figure 39: Views of rapid prototype with steel shim and PVA valve on top of cylindrical spacer from the front (top) and side (bottom).	58
Figure 40: Venous valve mold (left). Individual mold halves (right).	58
Figure 41: Bottom of mold prior to spacers being inserted (Left). Bottom of valve mold with three of the four spacers inserted into the mold (Right).	59

Figure 42: Proximal views of the prototype valve when open (left) and closed (right).	60
Figure 43: Mesh Convergence for the finite element model. The circled mesh was selected for the finite element model.	64
Figure 44: Selected mesh for the finite element simulation.	65
Figure 45: 2D plots of total displacement magnitude on the first (left) and second (right) planes of symmetry of the finite element model with the valve's base displaced in the normal direction by 0.5 mm. Black wireframe lines indicate the original geometry.....	67
Figure 46: 3D plot of total displacement magnitude in of the finite element model with the valve's base displaced in the normal direction by 0.5 mm. Black wireframe lines indicate the original geometry.	68
Figure 47: 3D plot of points extracted from the deformed finite element simulation (left). CAD model of the expanded valve created from the extracted points (right).	72
Figure 48: View of entire fluid domain used in the CFD simulation (left). Zoomed in view of the portion of the fluid domain inside the deformed valve (right).....	73
Figure 49: Mesh Convergence for the CFD simulation. The circled mesh was selected for the CFD simulation.	75
Figure 50: View of entire selected mesh for the CFD simulation (left). Zoomed in view of the portion of the mesh near the deformed valve (right).....	76
Figure 51: 2D Contour plots of y velocity on the first (left) and second (right) planes of symmetry.....	78
Figure 52: 2D Contour plots of y velocity on the first (left) and second (right) planes of symmetry. Only regions of reverse flow are shown.	79
Figure 53: Wireframe view of fluid domain with a horizontal plane, marked in red, intersecting the domain 9 mm above the valve's shoulder (left). 2D contour plot of y velocity on this plane (right); reversed flow, indicated by shades of blue, is into the page.....	80

Figure 54: 3D plot of streamlines behind the valve's leaflets with (left) and without (right) the valve's internal orifice wall and leaflet slit shaded gray. Streamlines indicate that flow is circulating behind the leaflets.....	81
Figure 55: 3D view of deformed valve's geometry with the inner walls and leaflet slit highlighted in purple (left). 3D contour plot of shear rate on the valve's inner walls and leaflet slit (right).	82
Figure 56: 2D contour plots of shear rate on the first (left) and second (right) planes of symmetry emphasizing regions of low shear. Shear rates higher than 50 s^{-1} are dark red.....	83
Figure 57: Mold components (left) used to fabricate PVA tubes (right).	85
Figure 58: Schematic of reflux flow rate test. A column of glycerol induces a pressure to close the valve. The reflux flow rate is then measured using a scale and a stopwatch.	86
Figure 59: Average reflux flow rate for the proposed valve at low (30 mmHg) and high (160 mmHg) retrograde pressures. The valve meets the specification of having a reflux flow rate of less than 3 mL/min.	88
Figure 60: Schematic of fatigue test. Pulsatile flow is created by a column of water creating a 40 mmHg retrograde pressure head which closes the valve and a roller pump which induces forward flow to open the valve. The valve closes whenever the roller pump is not inducing full forward flow.	91
Figure 61: Prototype valve before (left) and after (right) being placed on a connector in preparation for fatigue cycling or washout test.	92
Figure 62: Valve after undergoing 500,000 cycles at 6 Hz.	94
Figure 63: Valve before and after undergoing 500,000 cycles at 3 Hz.	94
Figure 64: Example of Frames used to determine valve closure time. Frame 0 (Left). Frame 2 (Right).	96
Figure 65: View of valve and pressure transducer in the distal pressure rise test.	97

Figure 66: Schematic of outflow resistance test. A 15 mmHg pressure head is induced by a column of glycerol solution 19 cm above the valve's shoulder. Flow rate is measured visually using a graduated cylinder and a stopwatch.....	99
Figure 67: Comparison of outflow resistance added by the valve and venous obstruction Grade 1 at 15 mmHg (obstruction data from [48]).	100
Figure 68: Flow loop used for the washout test.....	102
Figure 69: Green hydrophilic dye behind the leaflets (left) completely washes out under a forward flow rate of 400 mL/min (right).	103
Figure 70: Valve inserted into a 7 mm inner diameter rigid tube does not radially buckle (left) but buckles in a 6.5 mm tube (right).	104
Figure 71: Blood flow loop.....	105
Figure 72: View valve's inlet after being in the blood flow loop for three hours.	106
Figure 73: Outside view of valve after being in the blood flow loop for three hours.	107
Figure 74: 10mm valve placed in 16 Fr (5.3 mm) inner diameter tube.....	109
Figure 75: Schematic of deep vein junctions between the groin and below the knee (image from [32]) Stars indicate the proposed locations of the prosthetic valve to be implanted in the femoral and popliteal veins.	117
Figure 76: Views of a stented 9 mm valve expanded to 12 mm (approximately the size of the largest vein diameter this valve is suggested to be placed in) compared to an unexpanded valve.	124
Figure 77: Probability density, assuming normality, of the sheep jugular vein diameter. A 10.4 mm diameter valve would fit into diameters ranging from 9.4 to 14.6 mm, which covers 94% of the expected diameter sizes.	126
Figure 78: Probability density, assuming normality, of the CFV's fully distended diameter. The percent probability of a diameter falling in the range of selected valve sizes is indicated.	130

Figure 79: Probability density, assuming normality, of the popliteal vein's fully distended diameter. The percent probability of a diameter falling in the range of selected valve sizes is indicated. 131

Figure 80: Flow chart for clinicians for human testing..... 132

Figure 81: Comparison of reflux flow rate of prosthetic venous valves which underwent experimental testing (data extracted from [102, 122, 123, 132, 137, 140, 142, 143, 145]). The valve presented in this work is referred to as "Tanner". 143

SUMMARY

Chronic Venous Insufficiency (CVI) is characterized by chronic venous hypertension from blood pooling in the lower limbs. The resulting symptoms include leg pain, varicose veins, fatigue, venous edema, skin pigmentation, inflammation, induration, and ulceration. Reflux from incompetent venous valves is a factor in up to 94% of individuals with CVI. Current treatments of CVI include compression stockings, drug therapy, vein disabling, venous stenting, and surgical correction with varying rates of success. However, a minimally invasive correction of deep venous reflux does not currently exist. A transcatheter prosthetic venous valve has the potential to be an effective, minimally invasive treatment for deep venous reflux which could treat up to 1.4 million individuals in the United States suffering from venous ulceration and make more than 1.7 billion dollars each year. Previously developed prosthetic venous valves have had problems with competency, patency, thrombogenicity, biocompatibility, and incorrect sizing. To meet the clinical need a prosthetic valve needs to be developed which succeeds where previous valves have failed.

This thesis describes the design, analysis, pre-clinical testing, and evaluation of a novel prosthetic venous valve. Design specifications for an effective prosthetic venous valve were created. Verification tests were developed and performed which demonstrated that the valve met every design specification. Finite element and computational fluid dynamics simulations were performed to analyze the valve and calculated a maximum shear rate of 2300 s^{-1} in the valve during the high forward flow after a Valsalva maneuver. The valve is made of a biocompatible material that has low thrombogenicity, Poly(vinyl-alcohol) cryogel. On the average, the valve allows less than 0.5 mL/min of reflux at low and high retrograde pressures even after 500,000

cycles, indicating that it will reduce the reflux of individuals with venous reflux by more than 99.4%. The valve closes in less than 0.07 seconds and allows the distal pressure to rise to an average of 7% of the equilibrium pressure 30 seconds after a simulated ankle flexion. The valve increases the outflow resistance an average of 2.3 mmHg*min/L which is much less than obstruction levels, ≥ 5 mmHg*min/L. The valve can fit in a 16 French catheter and is capable of percutaneous delivery. The base of the valve is 1.5 times the diameter of the vein in which it is to be implanted to help correct orientation upon deployment. Fluid behind the valve's leaflets is ejected with a forward flow rate of 400 mL/min, suggesting that thrombus formation will not occur at this location. A stented valve remained patent in a porcine blood flow loop for 3 hours. The valve remains competent without buckling in a constricted vein at rest. The valve can expand to fit a vein with a maximum diameter 1.4 times the valve's initial diameter with low risk of tearing or leaflet prolapse.

An IACUC protocol for a 12 week study to test the valve in sheep was prepared and approved. A study to evaluate the valve in humans is proposed with endpoints that can be tested for statistical significance and compared with other treatments for CVI. A set of valves which will correct reflux in the majority of common femoral, femoral, and popliteal deep veins is proposed and a sizing guide for surgeons is provided. The minimum distance between prosthetic valves placed in the same vein segment is 13 cm.

A comparison of this valve with previously developed prosthetic venous valves and recommendations for work to be performed in the future are given. The valve proposed in this work is the only valve to meet all design specification for an effective prosthetic venous valve, and therefore shows great potential to be a minimally invasive treatment for deep venous reflux.

CHAPTER 1: INTRODUCTION

Chronic Venous Insufficiency

Chronic Venous Insufficiency (CVI) is characterized by chronic venous hypertension from blood pooling in the lower limbs [1, 2]. In healthy veins, muscle contractions efficiently pump blood back to the heart while venous valves close to prevent reflux (see Figure 1) [3]. Venous hypertension and CVI can develop in the presence of venous reflux, venous obstruction, and calf muscle pump dysfunction (see Figure 1) [1]. The resulting symptoms include leg pain, varicose veins, fatigue, venous edema, skin pigmentation, inflammation, induration, and ulceration [4].

Prevalence and Economic impact

The risk of developing CVI increases with age, body mass index, height, family history of CVI, European ancestry, Hispanic ethnicity, pregnancy, prolonged standing, straining during bowel movements, being female, and residing in an industrialized country [5-10].

Studies on the prevalence of varicose veins have varied from 2-57% and < 1-73% for men and women respectively depending on the ancestry and degree of industrialization of the population studied as well as the disease criteria of the individual study [9]. These studies have also reported < 1-4.7% and < 1-5.5% of men and women respectively have a history of venous ulceration [9]. In the United States More than 7 million individuals have CVI with an estimated 2.5 million having venous ulcers [11, 12]. The United States spends up to 3 billion dollars annually treating venous ulcers [13]. It is estimated that every year 1.5-2% of the total health care budget for the United Kingdom, France, and West Germany is spent on treating venous

disease [14]. One study reported the onset of chronic leg ulceration to occur by age 40 for 24%, age 50 for 39%, and age 60 for 58% of individuals [15]. With the life expectancy in the United States being approximately 80 years, individuals with CVI may require treatment for 20-40 years, resulting in large lifetime cost of treatment per patient [16].

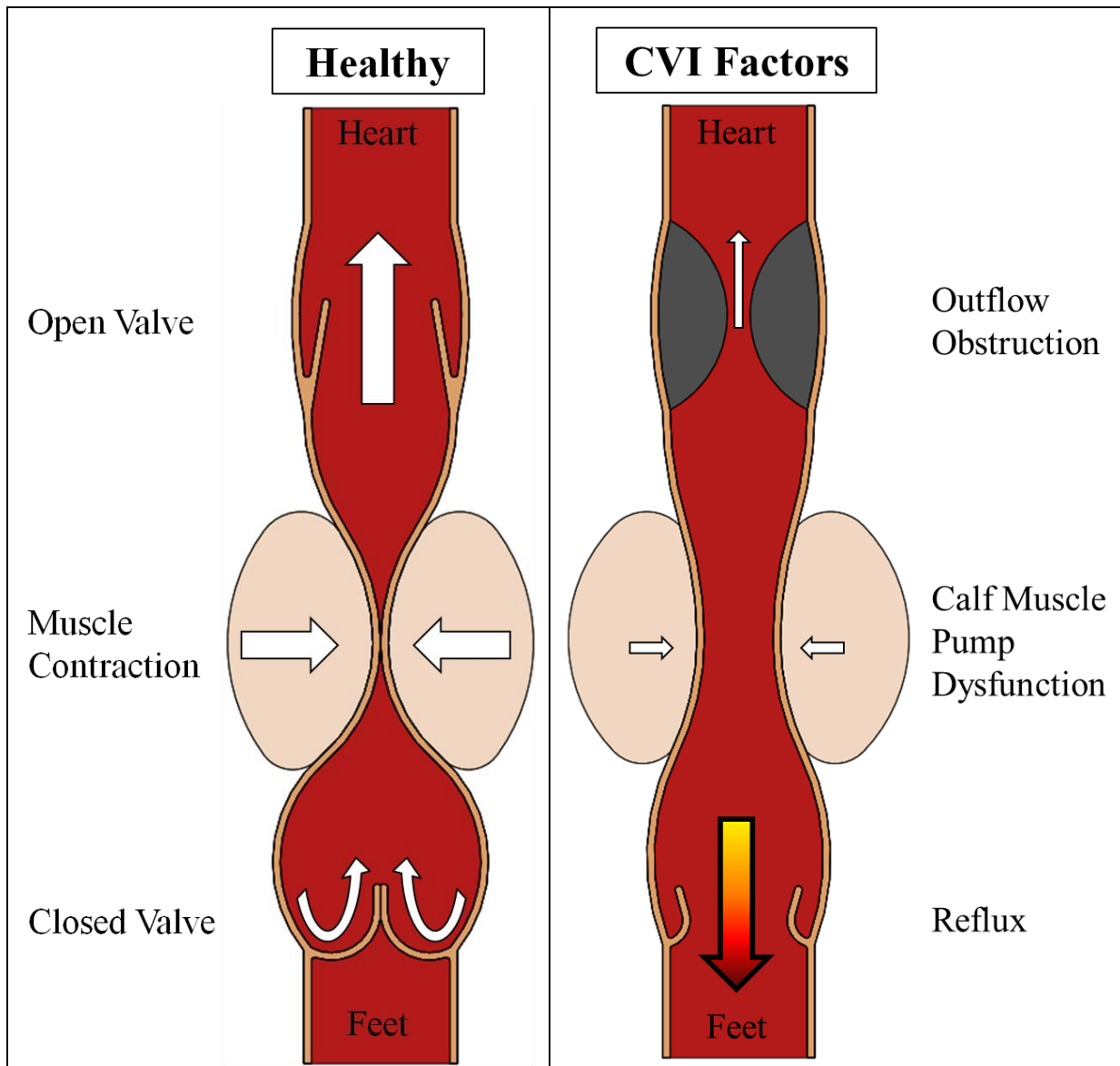


Figure 1: In healthy veins, muscle contractions efficiently pump blood back to the heart while venous valves close to prevent reflux (left). Factors which lead to the development of CVI include incompetent venous valves which allow reflux, outflow obstruction which increases outflow resistance, and calf muscle pump dysfunction (right).

There are additional indirect costs not included in the previous estimates. For instance, each year, an estimated 2 million work days are lost in the United States because of leg ulceration [11]. One study reported that 21% of working age individuals with chronic leg ulceration were severely limited or unable to work [17].

Quality of Life

In addition to the economic impact, the quality of life of individuals with CVI is decreased. Beyond concerns with the symptoms of CVI, patients also report having concerns with mobility, odor, cosmetic appearance, social embarrassment, and depression [11, 14]. Treatment of chronic ulcers has been correlated with a reduction in anxiety, depression, hostility, and cognitive impairment in patients [14].

Main Contributors to Venous Hypertension

The three main contributors to the chronic venous hypertension which results in CVI are venous reflux, venous obstruction, and calf muscle pump dysfunction (see Figure 1) [1]. Venous hypertension can be quantified by measuring a patient's ambulatory venous pressure (AVP), which is the mean pressure in the foot or lower leg during exercise [1]. There is a strong correlation between higher AVP measurements and ulceration (see Figure 2) [1, 18].

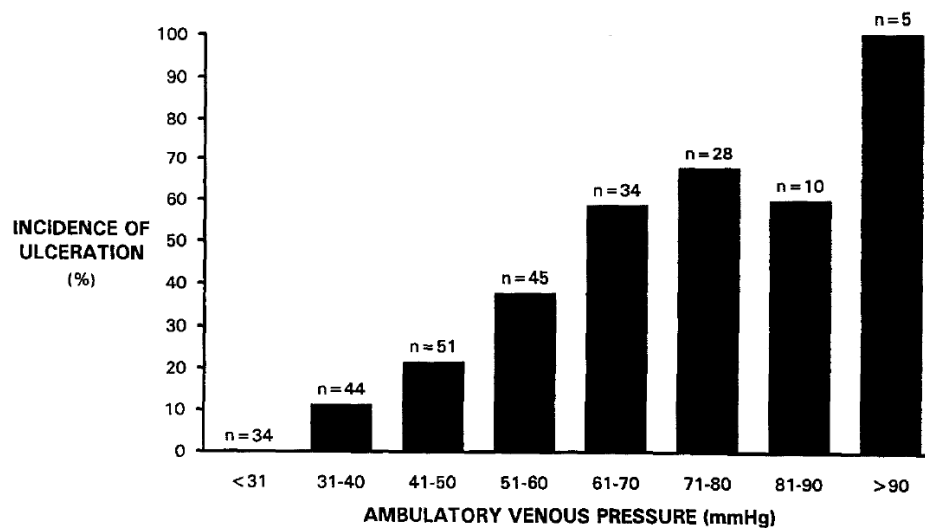


Figure 2: Relationship between ambulatory venous pressure and the incidence of ulceration (image from [18]).

Venous Reflux

Three venous systems of concern with CVI are the deep, superficial, and perforating veins. The deep venous system is composed of large diameter veins deep inside the leg, these include the iliac, common femoral (CFV), femoral, and popliteal veins (see Figure 3). The superficial venous system is composed of smaller diameter veins located in the leg closer to the skin, these include the great saphenous and small saphenous veins (see Figure 4). Perforating veins connect the deep and superficial veins throughout the calf and thigh (see Figure 4). Venous valves are located in each of these systems which allow unidirectional flow back to the heart (see Figure 5). These valves are naturally open and do not significantly impede forward flow to the heart (see Figure 6) [19, 20]. The leaflets of normal valves come together in response to retrograde pressure to close the vein and prevent reflux (see Figure 7 and Figure 8) [21-23].

Venous reflux occurs when valves become incompetent and allow retrograde flow. Primary valvular incompetence results from age related structural changes in the valve, such as

thinning of the leaflets. Secondary incompetence occurs when valves are damaged after deep vein thrombosis (DVT) and recanalization (restoration of the vein's lumen).

Venous reflux is present in 77-97% of symptomatic limbs, suggesting it is a major contributor to CVI [24-29]. The symptom severity of individuals with CVI is related to the total amount of reflux and the location of the refluxing vein segments.

Reflux is commonly quantified by measuring the reflux duration or a patient's venous filling index (VFI). Healthy native venous valves typically close in less than 0.5 seconds under retrograde pressure [30, 31]. While increased valve closure time is not highly correlated with increased symptom severity, it is common clinical practice to deem a valve incompetent if it takes more than 0.5 seconds to close [31-34]. The median valve closure time for an individual with CVI is 3.6 seconds [32]. VFI is the average filling rate of all the veins in the calf when an individual changes from the supine to the standing position and is measured using plethysmography (PG) and is the combined measurement of arterial inflow and venous reflux. A normal VFI is less than 2 mL/s, with higher measurements correlated with increased symptom severity [1, 35-39]. This suggests that the total amount of reflux is indicative of the symptom severity of a patient. Individuals with incompetent popliteal veins typically have a VFI greater than 5 mL/s, with skin changes and ulceration occurring with a VFI greater than 10 mL/s [35].

The location of refluxing vein segments also plays a significant role in the symptom severity of a patient. The risk of skin changes and ulceration for individuals with reflux in the deep venous system is higher than in those with superficial or perforator reflux [27, 33, 36, 40]. Approximately 43-74% of individuals with CVI and 49-88% with ulceration have deep venous reflux [25, 40-44]. The risk of skin changes and ulceration also increases when reflux is present in more than one venous system [25, 33, 40, 42].

Correction of deep venous reflux often leads to a drastic reduction of symptoms, with one study reporting a 78% ulcer healing rate when refluxing valves were surgically corrected and remained competent [45].

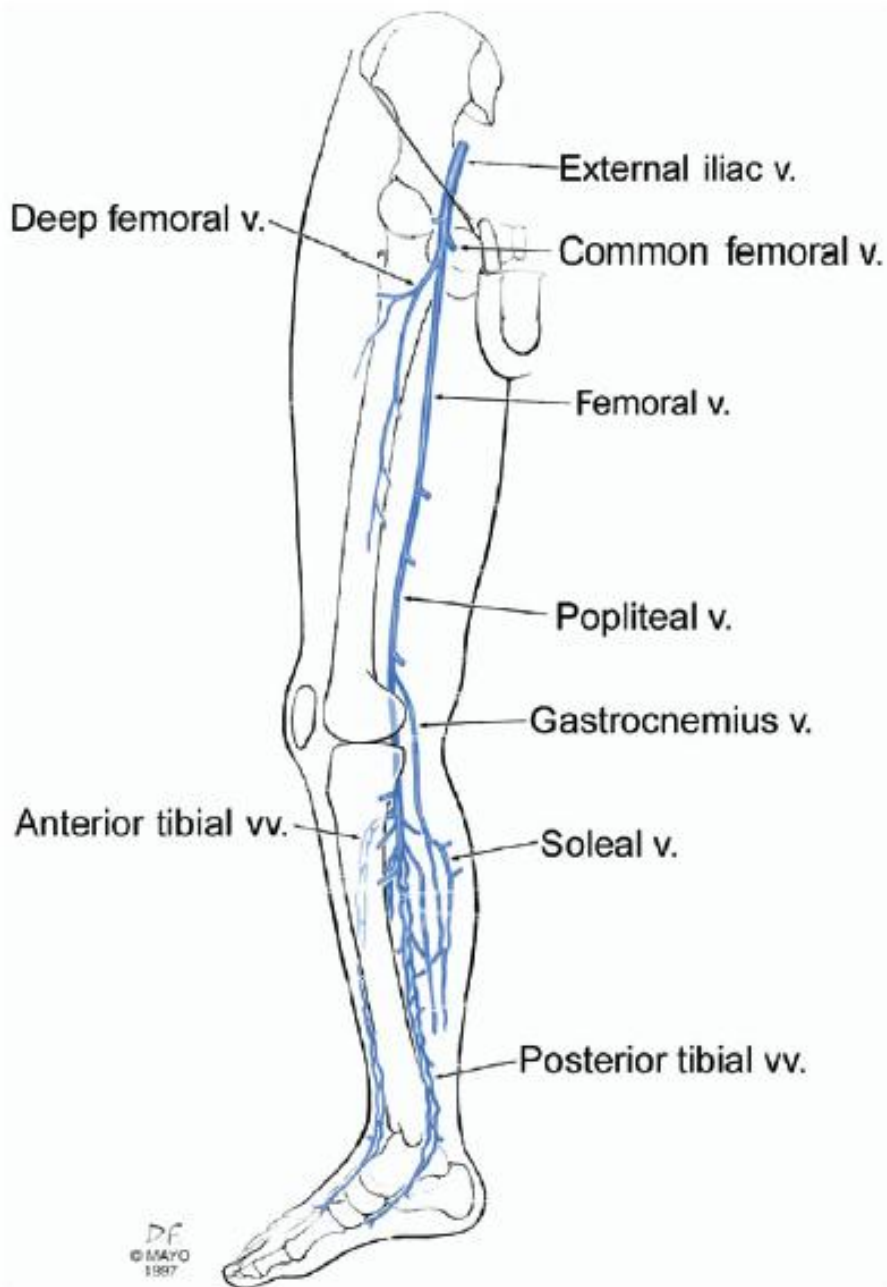


Figure 3: Veins in the Deep Venous System (image from [46]).

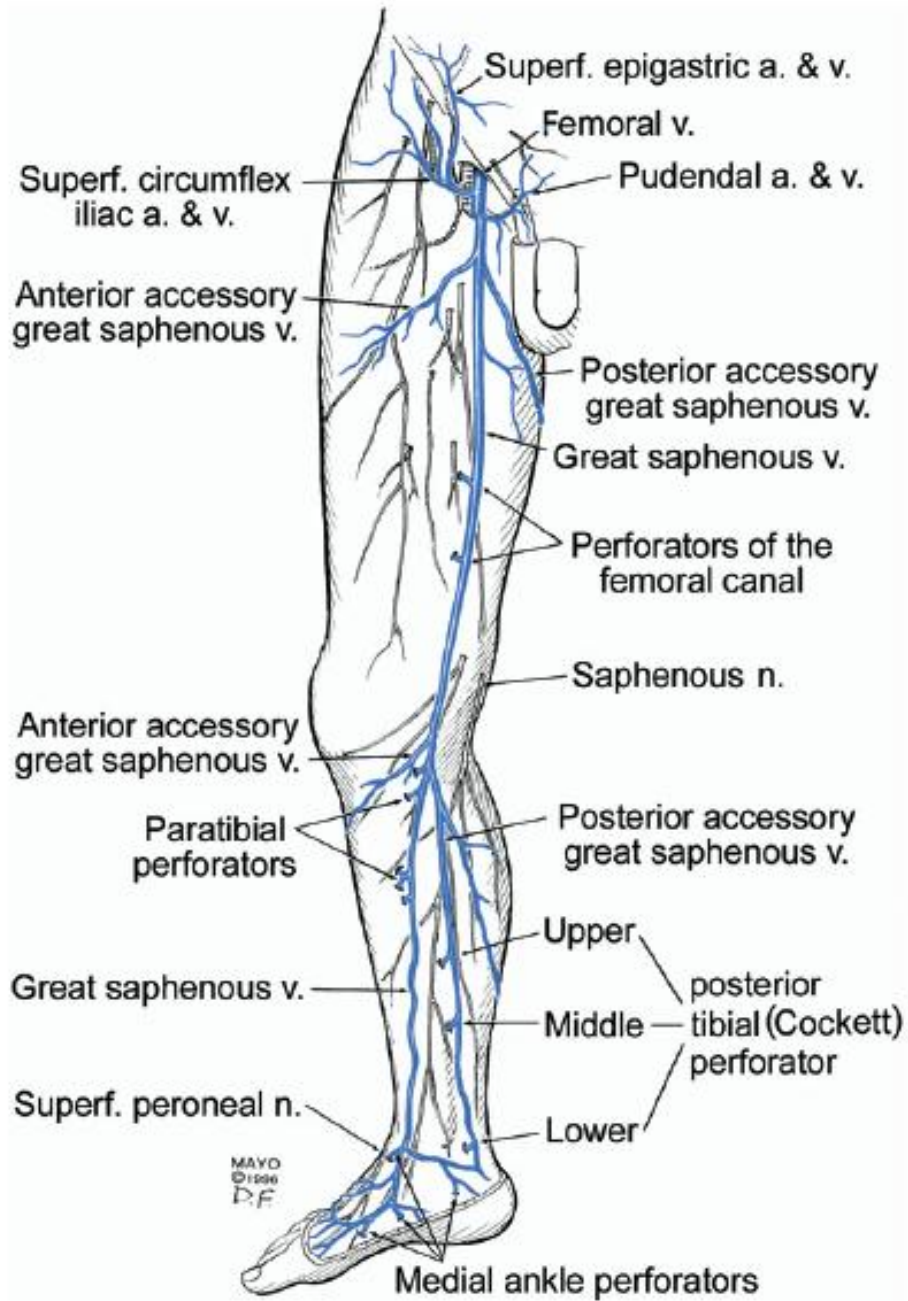


Figure 4: Veins in the superficial and perforating venous systems (image from [46]).

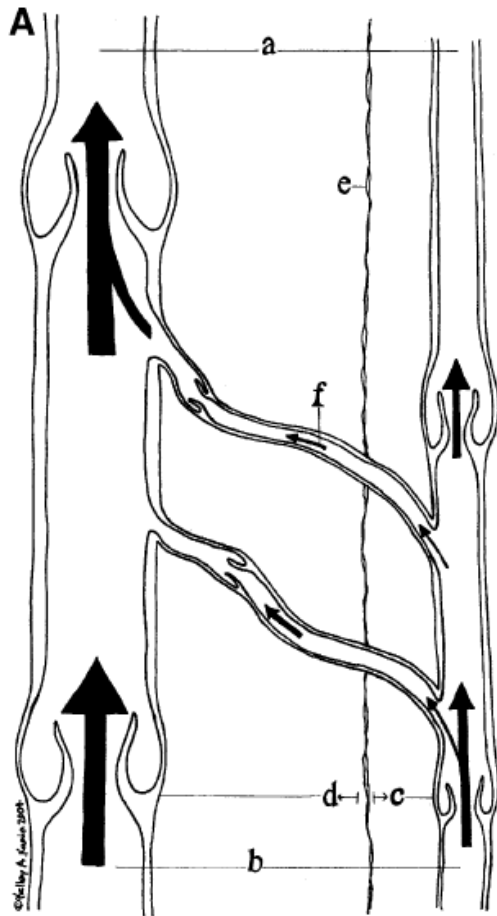


Figure 5: Normal venous flow paths with unidirectional venous valves. Blood flows from the feet (b) towards the heart (a). Perforating veins (f) connect superficial and deep venous systems (image from [9]).

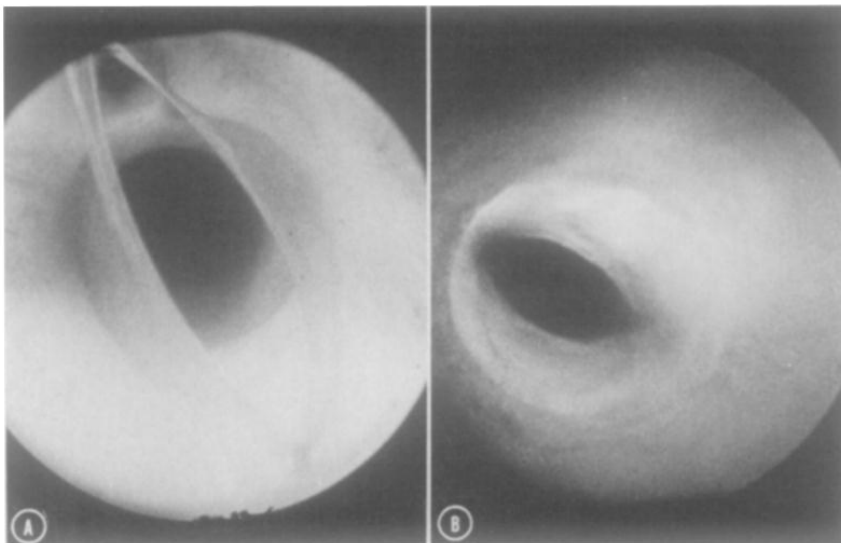


Figure 6: Proximal (left) and distal (right) views of an open saphenous venous valve (image from [19]).

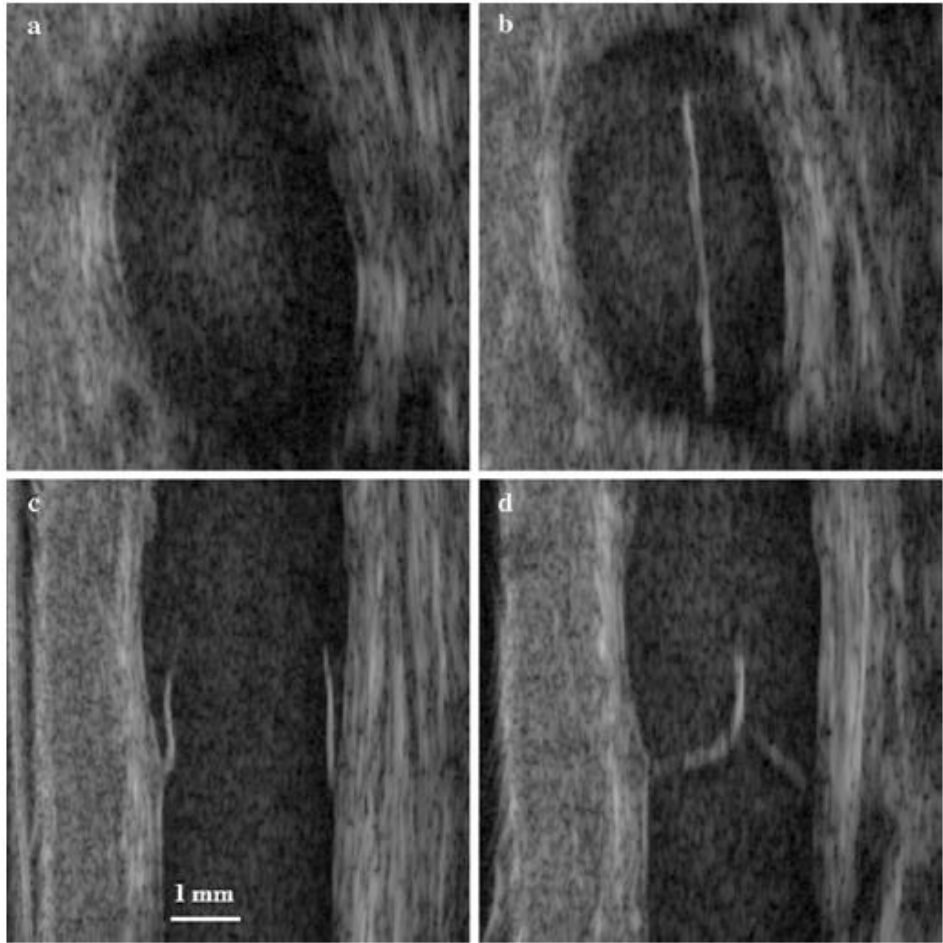


Figure 7: Ultrasound images of a venous valve in the great saphenous vein at the ankle. Distal (a, b) and side (c, d) views of valve leaflets when open (left) and closed (right) (image from [47]).

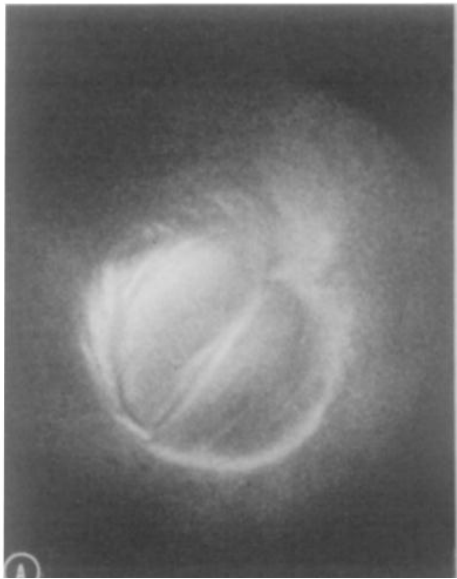


Figure 8: View of a closed venous valve (image from [19]).

Outflow Obstruction

Venous outflow obstruction makes it difficult for blood to leave the lower limbs, thus contributing to the development of venous hypertension and CVI (see Figure 1). Obstruction is typically caused by DVT when there is insufficient recanalization [1, 48]. Other causes of the obstruction can be from extramural venous compression, congenital agenesis, or hypoplasia of the vein [1]. Venous obstruction is present in 14-42% of symptomatic limbs [26, 28, 29]. Patients with venous reflux and outflow obstruction typically have a greater AVP and higher rates of ulceration than individuals with only one factor present [18, 27].

Calf Muscle Pump Dysfunction

In healthy legs, the calf muscle pump ejects blood out of the lower limbs which helps to prevent the development of venous hypertension [3]. A reduction in the efficiency of the calf muscle pump to eject blood out of the limb will also contribute to the development of venous hypertension and CVI [29, 36, 49]. While the efficiency of the calf muscle pump is decreased by outflow obstruction and venous reflux, calf muscle pump dysfunction, such as a reduction in pump compliance, will also reduce the efficiency [29, 36, 49, 50]. The efficiency of the calf muscle pump can be quantified by measuring the fraction of blood ejected (EF) during a single contraction using PG [29, 36, 49]. Lower EF measurements have been correlated with higher AVP measurements and incidents of ulceration with symptomatic limbs having an EF less than 60% [29, 36, 38, 39, 49, 50]. Approximately 44% of limbs with CVI have reduced calf muscle pump compliance [29].

Quantifying Symptom Severity

The Clinical-Etiology-Anatomy-Pathophysiology (CEAP) system is commonly used to classify patients according to symptoms (see Figure 9) [51]. This classification system attempts to capture the progression of CVI symptoms from low to high severity: telangiectases, varicose veins, edema, skin changes, and ulceration (see Table 1). However, CEAP was not designed to measure improvements in a patient's symptoms in response to treatment and is a relatively static measurement [2, 52, 53].

The Venous Clinical Severity Scoring System (VCS) is a tool available to measure the symptom severity of individuals with CVI [4, 54, 55]. The VCS rates pain, varicose veins, venous edema, skin pigmentation, inflammation, induration, active ulcer number, active ulcer duration, active ulcer size, and use of compression therapy for each subject on an objective scale from 0 to 3, with a maximum score of 30 (see Figure 10) [4, 54]. A strong correlation exists between CEAP class and VSC score (see Table 2) [55, 56]. The VCS score has been used in several studies to evaluate the response of a patient's symptoms for a given treatment [52, 53, 57-66]. Patient VCS scores have been shown to change in response to treatment within 3 days, suggesting that this score quickly captures changes in symptoms [52].

Class	Definition	Comments
C ₀	No visible or palpable signs of venous disease	
C ₁	Telangiectases, reticular veins, malleolar flare	Telangiectases defined by dilated intradermal venules <1 mm diameter Reticular veins defined by dilated, nonpalpable, subdermal veins ≤3 mm in diameter
C ₂	Varicose veins	Dilated, palpable, subcutaneous veins generally >3 mm in diameter
C ₃	Edema without skin changes	
C ₄	Skin changes ascribed to venous disease	
C _{4A}		Pigmentation, venous eczema, or both
C _{4B}		Lipodermatosclerosis, atrophie blanche, or both
C ₅	Skin changes with healed ulceration	
C ₆	Skin changes with active ulceration	

Figure 9: CEAP classification system (image from [51]).

Table 1: Examples of CEAP classes C1, C2, C4, and C6 (recreated from [51]).

<u>C1</u> Telangiectases	<u>C2</u> Varicose Veins	<u>C4</u> Pigmentation	<u>C6</u> Active Ulceration
			

Clinical descriptor	Absent (0)	Mild (1)	Moderate (2)	Severe (3)
Pain	None	Occasional	Daily not limiting	Daily limiting
Varicose veins	None	Few	Calf or thigh	Calf and thigh
Venous edema	None	Foot and ankle	Below knee	Knee and above
Skin pigmentation	None	Limited perimalleolar	Diffuse lower 1/3 calf	Wider above lower 1/3 calf
Inflammation	None	Limited perimalleolar	Diffuse lower 1/3 calf	Wider above lower 1/3 calf
Induration	None	Limited perimalleolar	Diffuse lower 1/3 calf	Wider above lower 1/3 calf
No. active ulcers	None	1	2	3 or more
Ulcer duration	None	<3 mo	3-12 mo	>1 y
Active ulcer size	None	<2 cm	2-6 cm	>6 cm
Compression therapy	None	Intermittent	Most days	Fully comply

Figure 10: Revised Venous Clinical Severity Score (image from [4]).

Table 2: Relationship between CEAP class and VCS score (combined data from [55] and [56]).

CEAP Class	95% Confidence Interval for mean VCS scores
C1	1.0-2.4
C2	4.5-5.8
C3	5.5-8.0
C4	8.5-10.1
C5	9.3-11.7
C6	11.0-29.0

Approaches to Treatment

Treatments for CVI include exercise, compression, medication, vein disabling, venous stenting, surgical correction, and valve replacement. Thus far these treatments have demonstrated varying levels of efficacy in reducing the symptom severity. In practice the most conservative treatment is applied first, typically compression stockings, with more invasive procedures being pursued when symptoms do not significantly improve [67]. The appropriateness of each treatment is further determined by the functionality of the calf muscle pump as well as the presence and location of venous reflux and obstruction (see Figure 11) [68].

The time spent by an individual caring for an ulcer has been found to be highly correlated with feelings of resentment and anger [11]. Therefore, in addition to symptom relief, the time required of an individual for a given treatment must be considered when evaluating its efficacy.

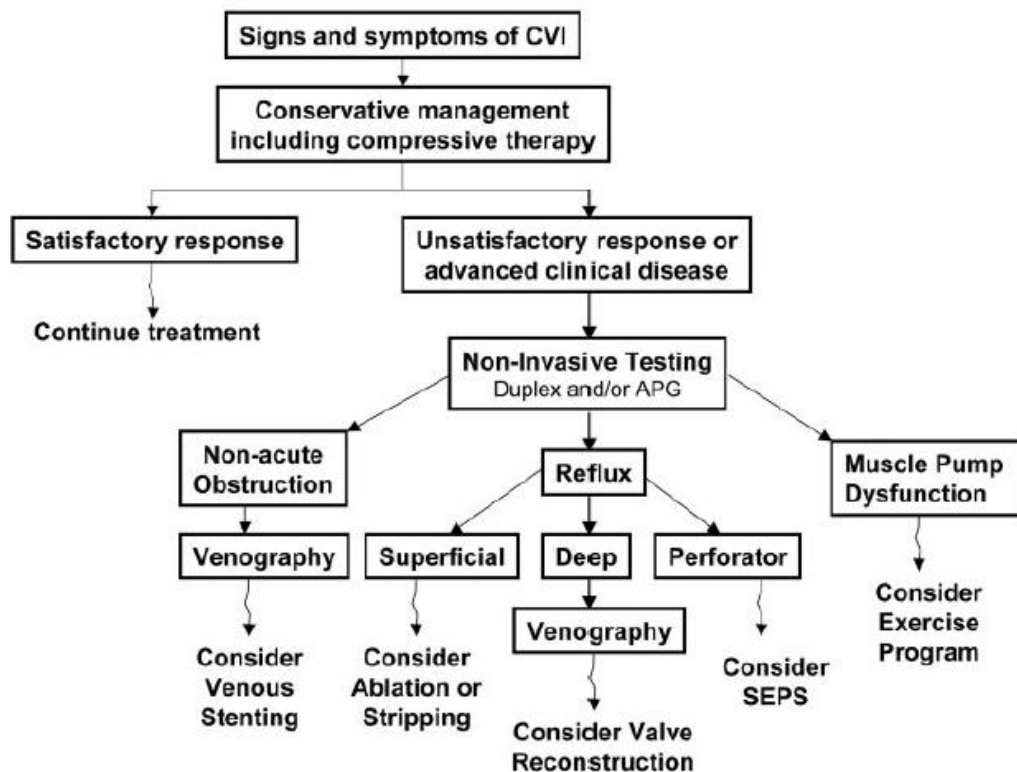


Figure 11: A simplified overview for the diagnosis and treatment of CVI (image from [68]).

Exercise

Exercise has been proposed as a treatment to improve calf muscle pump function [65]. Padberg performed a randomized study of 28 individuals with CEAP classifications C4-6, with 15 individuals undergoing an exercise regimen to strengthen their calf muscles [65]. After 6 months the mean EF in the experimental group increased by 12% and was statistically significant compared to the control group. The mean VCS score decreased from 9.4 to 8.7 for the experimental group, which was not statistically significant. VFI increased by 5% for the control group, which was not statistically significant.

Compression

Compression of the symptomatic limb using elastic stockings is the most common treatment for CVI. Elastic stockings may provide uniform or graduated compression to a limb with pressures ranging from 15 to 60 mmHg, varying from ankle to thigh length [67, 69]. Stockings may vary from ankle to thigh length [69]. Compression of the limb reduces the cross-sectional area of the veins which promotes coaptation of venous valve leaflets which reduces venous reflux [70]. Additionally, reduction of the cross-sectional area of the vein increases the flow velocity and discourages the formation of outflow obstructions from stagnant blood [70]. Reduction of the cross-sectional area of the veins also promotes coaptation of venous valve leaflets which reduces venous reflux [70].

The use of compressive stockings has been shown to moderately improve AVP, VFI, and EF for individuals with both superficial and deep venous reflux (see Table 3) [38]. Cesarone reported that the average VCS score in 31 individuals with CVI decreased from 8.4 to 5.7 after eight weeks when treated with compression therapy, which corresponds to a mild reduction in symptom severity [61].

Approximately 50% of patients are unable to wear compression stockings because of physical limitations, such as frailty or obesity, or simultaneous arterial insufficiency [71]. Even in the presence of severe symptoms, individuals who can wear compressive stockings have a noncompliance rate up to 68% [72, 73]. Patients have questioned the benefits of wearing compressive stockings and expressed concerns that they are uncomfortable to wear [72, 74]. Other patients have reported that the appropriate type of compressive stockings could not be acquired because of high cost and inadequate insurance reimbursement [75].

Table 3: Mean percent change in hemodynamic parameters from elastic compression use; all values are statistically significant ($p < 0.01$) (recreated from [38]).

	Mean Percent Change	
	Limbs with superficial venous incompetence (n = 22)	Limbs with deep venous incompetence (n = 22)
Ambulatory Venous Pressure	-48	-18
Venous Filling Index	-25	-28
Ejection Fraction	19	49

Medication

Several pharmacological agents have been tested in clinical trials to treat individuals with CVI [68, 76-78]. Venoactive medications are intended to increase venous tone and capillary permeability and have shown to reduce pain, edema, itching, heaviness, swelling, and cramping, trophic skin changes, active ulceration [77-79].

However, few studies have measured the change in a subject's VCS score in response to medication. Cesarone reported that the average VCS score in 31 individuals with CVI decreased from 8.4 to 5.7 after eight weeks when treated with the pharmacological agent Pycnogenol® alone, and to 4.0 when combined with compression therapy [61].

Vein Disabling

Various methods, many being minimally invasive, have been used to disable problematic veins in the superficial and perforator venous systems and compel blood to use an alternate route to the heart. These methods include ligation, radiofrequency ablation, endovenous laser ablation, sclerotherapy, SEPS, PAPS, and Cyanoacrylate (super glue) [67, 68, 79, 80]. The baseline and mean VCS scores for several vein disabling procedures are shown in Table 4

Table 4. Complications include bruising, pigmentation, nerve injury, infection, and deep venous thrombosis, and occur in 5-20% of subjects [66, 67, 79, 81]. The long term efficacy of these procedures is mixed, as 7-71% of varicose veins return after a vein disabling procedure due to the recurrence of reflux [81-86].

Table 4: Baseline and follow-up mean VCS scores for various vein disabling procedures.

Procedure	Mean VCS Score		Time of last follow-up
	Baseline	Last follow-up	
Venous Stripping [57]	10.1	1.45	~ 16 months
Radiofrequency Ablation [52]	8.8	2.7	6 months
Sclerotherapy [58]	8	2	~ 20 months
Laser ablation [59]	4	0	12 weeks

Venous Stenting

Venous stenting has been used to treat outflow obstruction in deep veins [87-92]. One study of venous stenting of 982 patients reported that after 5 years, 62% of limbs were free of pain, 32% had no swelling, and 52% had their ulcers heal [89]. Another study reported the mean patient VCS score decreasing from 8.5 to 2 after approximately 27 months [63]. However, venous stenting alone has not demonstrated a statistically significant improvement in AVP, EF, and VFI [89-92].

Surgical Correction

Surgical correction of deep venous incompetence includes valvuloplasty, banding, femoral transposition, valve transplantation, and neovalve construction [93]. Valvuloplasty is the surgical repair of an existing incompetent venous valve and has an ulcer recurrence rate of 21-

50% and a competency rate of 42-91% [93]. Banding is a technique which promotes valve competence by placing a sleeve or cuff around a vein to reduce its diameter and has an ulcer recurrence rate of 20-27% and a competency rate of 70-100% [93]. Femoral transposition is the surgical connection of an incompetent femoral vein to another vein which is competent (see Figure 12). Femoral transposition has an ulcer recurrence rate of 25-56% and a competency rate of 40-77% [93]. Transplantation is the surgical insertion of a vein segment with a competent valve and has an ulcer recurrence rate of 6-67% and a competency rate of 25-90% [93]. However, up to 40% of valves become incompetent after being transplanted [94]. Cryopreserved valves have been explored as an option for surgical transplantation with poor results [95, 96]. In one study, 74% of valves were incompetent after thawing, only 27% of valves implanted into human subjects were still competent and patent after 2 years, and ulcer recurrence was 50% after 3 years [95]. Neovalve construction is accomplished by manipulating the native venous tissue to create a leaflet and has an ulcer recurrence rate of 0-17% and a competency rate of 68-100% [93].

Each of the aforementioned surgical procedures is highly invasive and requires an open surgery. Additionally, transposition and transplantation procedures are not always possible for patients with adverse anatomy or for which a suitable donor valve cannot be found [43, 97-99]. Surgical procedures to correct deep venous reflux are not common as many surgeons doubt their efficacy [100].

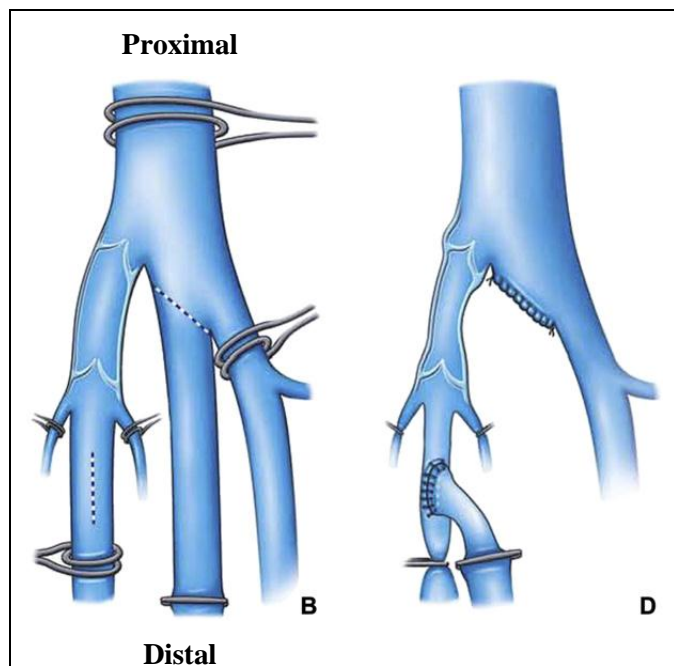


Figure 12: Before (left) and after (right) the transposition of an incompetent femoral vein into a competent great saphenous vein (image from [93]).

Prosthetic Venous Valves

A prosthetic venous valve has the potential to correct reflux in the deep, superficial, and perforating venous systems. While alternative minimally invasive treatments have the potential to stop reflux in the superficial and perforating venous systems, currently only invasive treatments exist for the correction of deep venous reflux. As deep venous incompetence is present in approximately 49-88% of individuals with venous ulcers, a minimally invasive treatment for deep venous reflux could treat up to 2.2 million of the 2.5 million individuals in the United States suffering from venous ulceration [11, 25, 40, 42, 43]. With up to 3 billion dollars spent annually in the United States to treat venous ulcers, the potential market for a minimally invasive treatment of deep venous reflux could be more than 2.6 billion dollars [25].

Dotter was the first to suggest the concept of a transcatheter venous valve [101]. Such a valve would meet the need for a minimally invasive treatment for deep venous reflux. Three

types of replacement valves have been developed by various researchers: mechanical, bioprosthetic, and polymer.

Mechanical

Taheri et al. developed a bicuspid valve made of platinum or pyrolyte carbon-covered titanium (see Figure 13) [12, 102-104]. The valves had inner diameters of 5-10mm. Under a pressure head of 100 mmHg the valve had 145 mL/min of reflux and a forward flow rate of 300 mL/min. The outflow resistance of the valve and the system was 333 mmHg*min/L. After 5 months of fatigue testing one valve incurred a small crack which was suspected to have occurred during manufacturing. Ten valves were implanted into nine dogs via transverse venotomies. Two dogs were sacrificed after 3 months because of valve migration and displacement. The remaining 7 dogs were sacrificed after two years. One valve was still patent but all were rendered functionless by neointimal hyperplasia.



Figure 13: Taheri valve (image from[12]).

Bioprosthesis

McLachlin harvested vein segments containing valves from dogs [105]. 30 segments were implanted into the dogs they were harvested from, with 24 being patent and 16 remaining competent at 4 weeks. 14 segments were implanted into dogs that were different from the donors, with 1 remaining patent and none being competent at 4 weeks.

Gerlock created bioprosthesis venous valves using cardiac valves and implanted them into the inferior vena cava of four dogs [106]. Two valves were checked in two dogs and found to be patent at 6 months. The remaining valves were checked at 8 months and found to be patent.

Hill created a bicuspid valve design by placing glutaraldehyde-fixed human umbilical cord segments over a bicuspid shaped aluminum rod (see Figure 14) [107]. Ten umbilical valves were surgically implanted into dogs. Valves were supported in place by quarter inch stainless steel cylinders which were surrounded by the vein to prevent blood contact. All valves occluded by 8 days. When the valves were harvested and examined red clot was prominent.

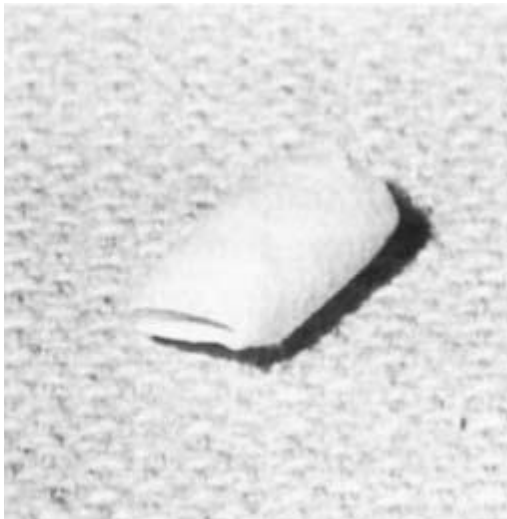


Figure 14: Umbilical valve created by Hill (image from Hill 1985 [107]).

Dalsing transplanted a jugular vein valve incorporating a 6-8mm diameter Z-stent into 5 dogs using a 16 French sheath [108]. Barbs were used to prevent valve migration for some valves. One valve was patent when the dogs were sacrificed at 1-4 weeks. One valve without barbs migrated to the lung. Barbs were observed to cause heavy scarring. Clotting was observed inside the valves and at the distal and proximal ends where the stent interfaced with the vein. The valve that remained patent did not have barbs, was slightly oversized for the vein, and "was placed in a relatively high-flow system" [108].

Ofenloch harvested external jugular vein segments containing valves from goats and sutured them to 10mm Wallstents (see Figure 15) [94]. These valves were then transplanted into the opposing external jugular veins of the goats used for the initial harvest using a 12 French catheter. Five goats were sacrificed after 1 week and all valves were patent and competent. Thrombus had formed on the stent on the downstream end for all valves. At 6 weeks six goats were sacrificed and all valves were patent while 5 were competent. Recanalization had obliterated the incompetent valve.

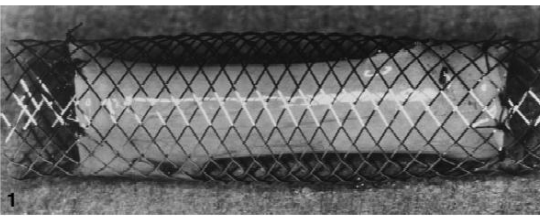


Figure 15: Replacement valve made by Ofenloch (image from [94]).

Gomez-Jorge sutured a portion of a glutaraldehyde-fixed bovine external jugular-vein containing a native valve to self-expanding nitinol Symphony stents, 8.9-14mm in diameter (see Figure 16) [109]. Eleven of these valves were deployed into 11 pigs using 12-24 French catheters. Of seven acute procedures, five valves were competent at implantation. Of the four

survival procedures, one pig died by one week, presumed to be from exsanguination, and had its leaflets entrapped by postmortem thrombus. The other three were sacrificed at 1-2 weeks and had valves that were still patent and competent. All four valves had pronounced inflammatory foreign body reactions.



Figure 16: Replacement valve made by Gomez-Jorge (image from [110]).

Thorpe, et al, fabricated a bicuspid vein valve by combining porcine small intestinal submucosa to a Z-stent. Valves were delivered into pigs using a 16-Fr catheter and demonstrated short term patency [111].

Hasaniya constructed replacement venous valves from bovine external jugular vein segments containing valves [112]. Ten valves were tested in-vitro, with eight being considered to be competent up to 260 mmHg.

Pavcnik developed three incremental stented valve designs, BVV1 (see Figure 17), BVV2 (see Figure 18), and BVV3 (see Figure 19), with leaflets made from SIS, a biomaterial derived from the submucosal layer of the porcine small intestine [110, 113-120]. The SIS leaflets are intended to act as temporary scaffolding for host cells to ultimately cover and replace the SIS. An 11 French catheter was used to deliver 25 BVV1 valves into 12 sheep with 4/5 being patent at 1 month, 10/10 patent at 3 months, and 10/10 patent at 6 months. The valve that occluded was tilted during implantation. Tilting was a factor in decreasing the function of three valves, with one these valves developing thrombus and occluding. The leaflets thickened at the

base and increased in rigidity resulting in moderate reflux at 3 months. An inflammatory response was observed around the valve. The BVV1 was implanted into 3 human subjects. At 1 year, all valves were still patent with 2 valves being competent. Symptoms improved in the two subjects in which the valves remained competent.

The BVV2 valve design modified the stent geometry of the BVV1 to reduce the risk of misalignment [117, 120]. A 10 French sheath was used to implant 48 valves into the jugular veins of 14 sheep. After 6 weeks all valves were patent and 44 were competent. All valves were free of thrombus.

The BVV3 valve was designed to bring the leaflets closer together and prevent them from contacting the vein wall and to increase the size of the sinus region [110, 118, 119]. A 10 French catheter was used to deliver 12 of these valves into the jugular veins of 6 sheep. All valves were patent and one valve was incompetent at 5 weeks. BVV3 valves were implanted into 15 patients with a 12 French catheter. One valve was incompetent at implantation. Four valves occluded, 3 in less than 2 weeks and one at 7 months. At 3 months only 2 valves remained competent. At 12 months none of the valves had migrated and none were competent.



Figure 17: BVV1 (image from [110]).

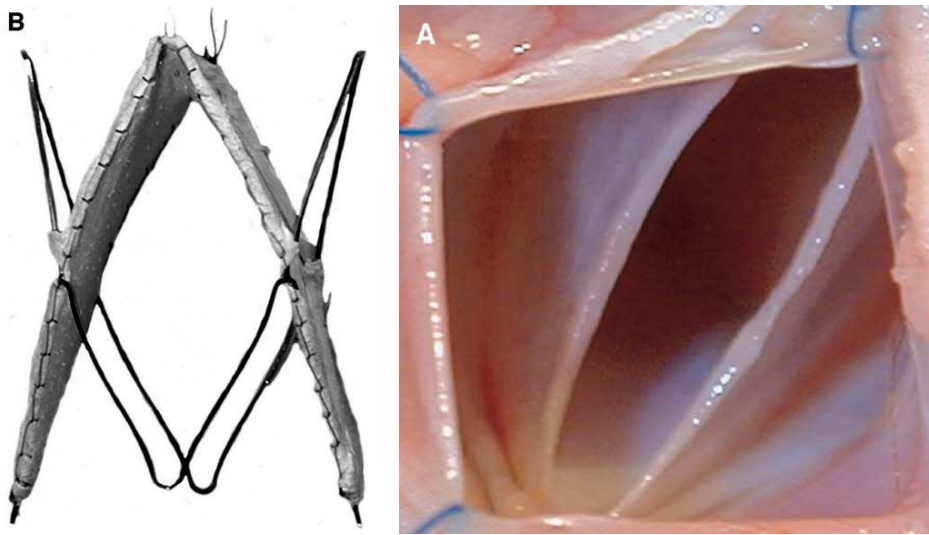


Figure 18: BVV2 before (left) and after (right) implantation cellularization (images from [117]).

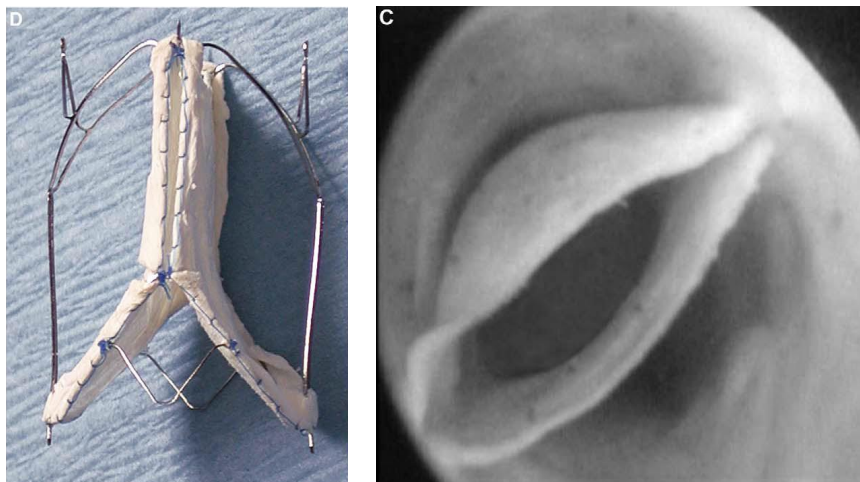


Figure 19: BVV3 before (left) and after (right) implantation and cellularization (images from [110]).

Pavcnik also created a percutaneous autogenous venous valve (PAVV) by suturing native sheep valves to 13-15mm diameter stents (see Figure 20) [121]. Nine valves were implanted into 9 sheep using a 13-Fr catheter and were secured by barbs. The PAVV leaflets were oriented in the same direction as the sheep's native valve. One valve was damaged during insertion and was

rendered incompetent. After 3 months the remaining 8 valves were incorporated into the vein wall, competent, and free of thrombus. Chronic inflammation and foreign body type giant cells were present around sutures and stent wires near the vein wall.

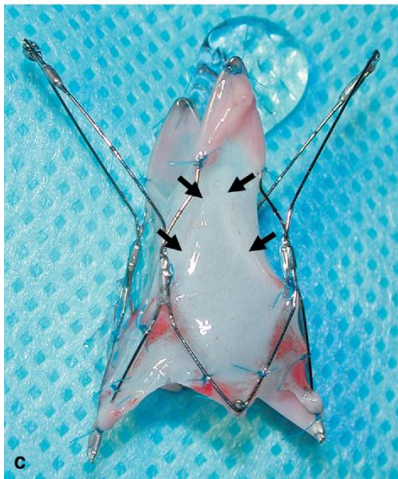


Figure 20: PAVV valve developed by Pavcnik (image from [121]).

Venpro developed the PVVB valve, a glutaraldehyde preserved bovine external jugular-vein segment containing a native valve sutured to nitinol Symphony stents, 10-14mm in diameter (see Figure 21) [122-126]. *In vitro* testing found valve reflux under a 287 mmHg pressure head to be 120 mL/min in valves made from fresh specimens and 40 L/min in fixed tissue valves. The pressure drop across the valve was 2.9 mmHg with a flow rate of 1200 mL/min, resulting in a combined resistance of the flow system and the valve of 322 mmHg*min/L. Valves were constrained in place by oversizing the diameter by 2mm. 18 valves were deployed into 10 pigs using a 16 French catheter. All valves were deemed patent and competent after insertion. 5 pigs received vitamin K for anticoagulation, developed bleeding complications and were sacrificed at 2 weeks; of the 8 valves implanted in this group, 7 were patent and 3 were competent. 5 pigs received aspirin for anticoagulation and were sacrificed at 4 weeks; of the 10 valves implanted in

this group, 5 were patent, 3 were competent, and 5 valves experienced thrombosis. One valve migrated and was suspected to have been undersized. A fibrous layer between the stent and vein and a fibrous capsule around the stent developed for all valves. Some stents were found to have not fully expanded. The PVVB was also implanted into 5 human subjects. One valve remained patent and competent at 16 months, the remaining four valves occluded. One valve migrated into the pulmonary artery. Ultimately this valve was deemed unfit for further use in venous implantation [110].



Figure 21: PVVB developed by Venpro (image from [125]).

Kucher encased 8mm Symphony stents inside external jugular vein segments containing valves harvested from dogs and compared their performance to end-to-end anastomosis grafts in seven dogs [127]. Seven valves were delivered using 11 French catheters and expanded a little larger than the vein diameter to prevent migration. One dog had both grafts occlude in less than 2 weeks after surgery while the remaining valves and grafts were still patent after 120 days.

Minimal to moderate stenosis was present at the suture lines which raised concerns that thrombosis may be caused from the sutures themselves.

Teebken fabricated 12 tissue engineered venous valve grafts by repopulating decellularised allogeneic ovine veins with the future recipient's myofibroblasts and endothelial cells [128, 129]. The burst strength of these valves was an average of 2085 mmHg. These grafts were implanted into the external jugular veins of 12 sheep. Anticoagulants were not dispersed after surgery. Valves with reflux lasting more than 1.5 seconds were deemed incompetent. Four sheep were sacrificed at 1 week and all valves were patent and competent; thrombus had formed at the suture site and in the sinus in two valves. Four sheep were sacrificed at 6 weeks and all valves were patent and competent; thrombus had formed at the suture site and in the sinus in all four valves. The remaining four valves were harvested at 12 weeks where 3 were patent and 2 were competent. A control group of 8 sheep with implanted autografts was also studied. These grafts remained patent and competent for the 6 weeks they were studied.

Wei combined endothelial progenitor cells (EPC) with allogenic decellularized valved venous stents and implanted 12 of these valves into 12 dogs [130]. A control group of 12 dogs which had autogenous valves implanted was also studied. The EPC valves had a reflux velocity of 1.4 ± 0.3 cm/s while the autogenous valves had no reflux. The maximum forward flow velocity was 18.2 ± 3.3 cm/s for the EPC valves and 21.3 ± 2.1 cm/s for the autogenous valves. After valve closure the sinus region expanded from 7.1 to 8.4 mm (116.8%) for the EPC valves and from 7.0 to 8.2mm (118.5%) for the autogenous valves.

Dijkstra endovenously transferred a stented venous valve into the internal jugular veins of 16 sheep (see Figure 22) [131]. Thrombosis, tilting, endoleak, or migration of valves was not observed in any of the sheep after six months. Six valves have been implanted into four human

subjects with leg ulcers. After insertion, 2 ulcers healed, 1 increased in severity, and 1 remained the same. One of these valves had a type 1 venous endoleak.

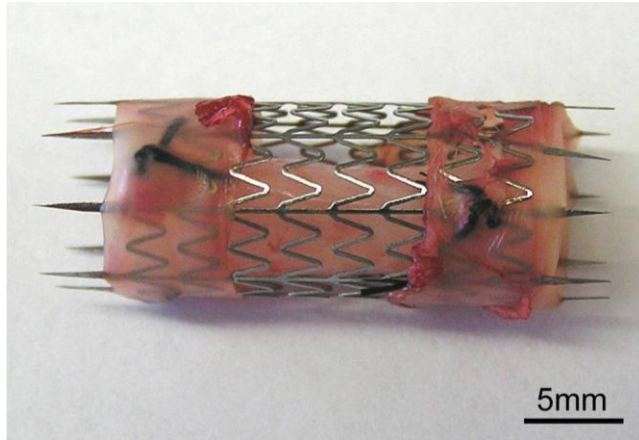


Figure 22: Stented valve made by Dijkstra (image from [131]).

Liu created a porous tissue engineered a vein valve by seeding scaffolds made of Poly(lactic-co-glycolic acid) (PLGA) with cells (see Figure 23). The scaffold had an inner diameter of 9mm and a wall thickness of 0.9 mm. Valves were studied *in vitro* using PBS as the working fluid. The valves had an opening pressure of 3.8 ± 0.7 mmHg. Reflux rates for the valves decreased from approximately 16 to 12 mL/min as the pressure head increased from 100 mmHg to 200 mmHg (see Figure 24).

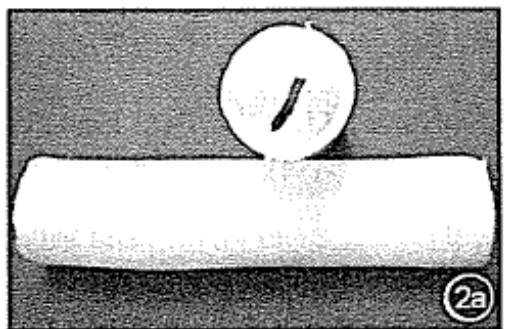


Figure 23: Tissue engineered vein containing valve scaffolds made by Liu (image from [132]).

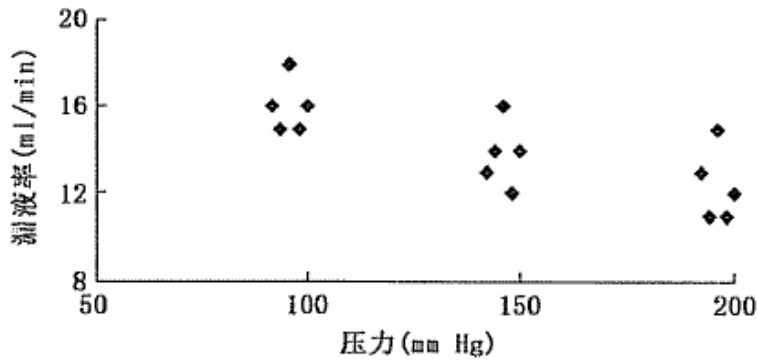


Figure 24: Reflux flow rate of tissue engineered venous valve developed by Liu at various pressures. The vertical axis is reflux (mL/min) and the horizontal axis is pressure (mmHg) (image from [132]).

Wen fabricated tissue engineered vein valves using two types of bone marrow derived progenitor cells obtained from canine multipotent adult progenitor cells (MAPC) and endothelial progenitor cells (EPC) (see Figure 25) [133].



Figure 25: Tissue engineered vein containing venous valve made by Wen (image from [133]).

Polymer

Hill created a bicuspid valve by dip coating a mandrel in liquid Pellethane and cutting open the orifice (see Figure 26) [107]. This valve had an opening pressure of 4.5mmHg. After 47 days of fatigue-cycles at 120/80 mmHg pressures at 60 bpm the valve showed no signs of material weakening. Ten Pellethane valves were surgically implanted into dogs. Valves were supported in place by quarter inch stainless steel cylinders which were surrounded by the vein to

prevent blood contact. All valves occluded by 8 days. When the valves were harvested and examined, red clot was prominent.

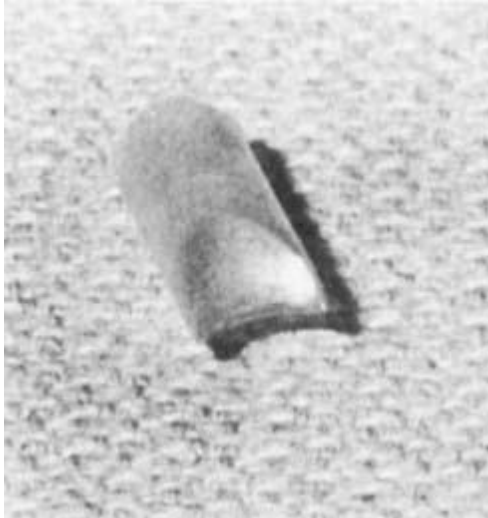


Figure 26: Pellethane valve developed by Hill (image from [107]).

Uflacker developed a monocusp venous valve composed of a polyether urethane leaflet attached to a Z-stent (see Figure 27) [110, 134]. The valves were inserted into pigs using a 10-Fr sheath into the inferior vena cava. After 1 week, thrombus was found inside the valve's cusp.



Figure 27: Uflacker monocusp valve (image from [110]).

Nadzeyka developed a tri-leaflet valve with a self expanding nitinol stent and leaflets made of Polyurethane (see Figure 28) [135]. A 10mm valve of this design is able to compress into a 10-Fr catheter.

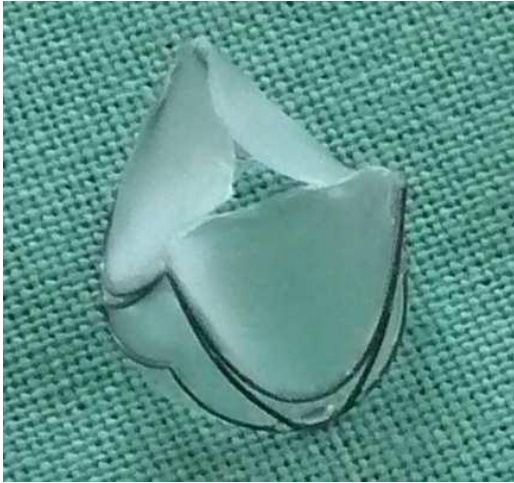


Figure 28: Nadzeyka valve (image from [135]).

De Borst developed the sail valve (see Figure 29) [136]. This valve is secured by 2 stents and was designed to allow some reflux. To avoid inadvertently sticking to the vein wall, the valve's leaflet never fully opens or closes. This valve is currently undergoing animal testing.



Figure 29: Sail valve (image from [136]).

Researchers from the University of Akron have reported three generations of prosthetic venous valve development [137-140]. Experimental testing for the second and third generation valves used a 3.45% dextran solution. Experimental testing applied forward flow rates up to 1600 mL/min, corresponding to flexing the ankle while standing, to calculate the outflow resistance of each valve. A backpressure of approximately 40 mmHg was applied with a column of solution 55 cm above the valves to induce reflux. The first generation design underwent seven iterations which focused on improving leaflet closure while preventing unwanted leaflet buckling (see Figure 30). The second generation design was composed of a rigid frame with a BioSpan® (polyether urethane) leaflet that was naturally open (see Figure 31). A 2:1 scale prototype valve took 1.38 seconds to close. 1:1 scale valves had a mean reflux volume of 5.83 mL over approximately 4 seconds, which corresponds to an average reflux flow rate of 87.45 mL/min, and increased the outflow resistance by 1.15-4.66 mmHg*min/L [137]. A computation fluid dynamics (CFD) simulation of blood flowing through this valve inside a 12.5774 mm vein with an inlet flow rate of 700 mL/min calculated the maximum shear rate to be approximately 7600 s^{-1} [139]. Concerns with the high residence time of fluid behind the leaflets in the CFD simulations of the second generation design prompted the development of the third generation valve design (see Figure 32). The third generation design had bowl shaped leaflets which were naturally closed and allowed forward flow by separating from the vein walls and moving towards the center of the vein. Valves of this design had a mean reflux volume of 0.95 mL over approximately 4 seconds, which corresponds to an average reflux flow rate of 14.25 mL/min, and increased the outflow resistance by 1.15-4.66 mmHg*min/L [140].



Figure 30: First generation prosthetic venous valve prototype developed by researchers from the University of Akron (image from [140]).



Figure 31: Second generation prosthetic valve developed by researchers from the University of Akron (image from [138]).

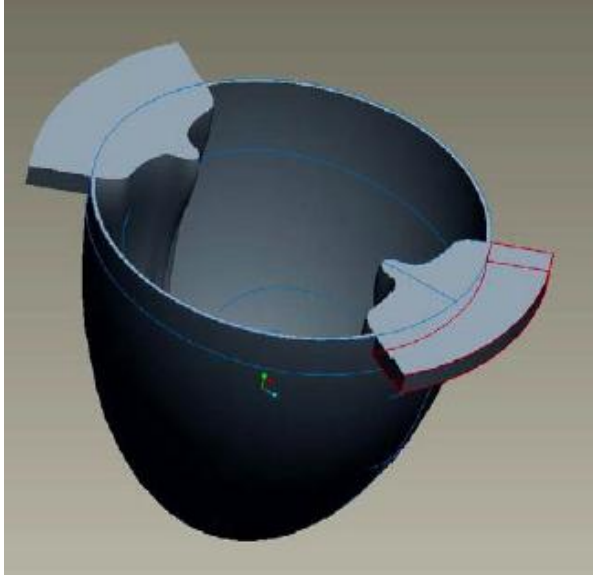


Figure 32: Third generation prosthetic venous valve developed by researchers from the University of Akron (image from [140]).

The third generation design from researchers from the University of Akron is similar in function to a prototype replacement venous valve made by Sathe which was not further pursued because of the high rate of reflux and opening pressure, 1-30 mL/min (over a 25-250 mmHg pressure range) and 26.4 mmHg respectively (see Figure 33) [141].



Figure 33: Parabolic shaped valve developed by Sathe (image from [141]).

Moriyama developed two prosthetic valves made by electrospinning polyurethane fibers onto a stent (see Figure 34) [142]. The valves tested at pressures ranging from 30-150 mmHg using a 50 wt% glycerin solution. The first design, named bPVV, had a reflux rate of 0.034 mL/s (2.04 mL/min) and increased the outflow resistance of the system by 744.4 mmHg*min/L. The second design, named oPVV, had a reflux rate of 0.514 mL/s (30.84 mL/min) and increased the outflow resistance of the system by 91.3 mmHg*min/L. The bPVV was selected as the better performing valve because it had a smaller stagnation zone and because its distal pressure rose more gradually during a pressure change simulating standing ankle flexion.

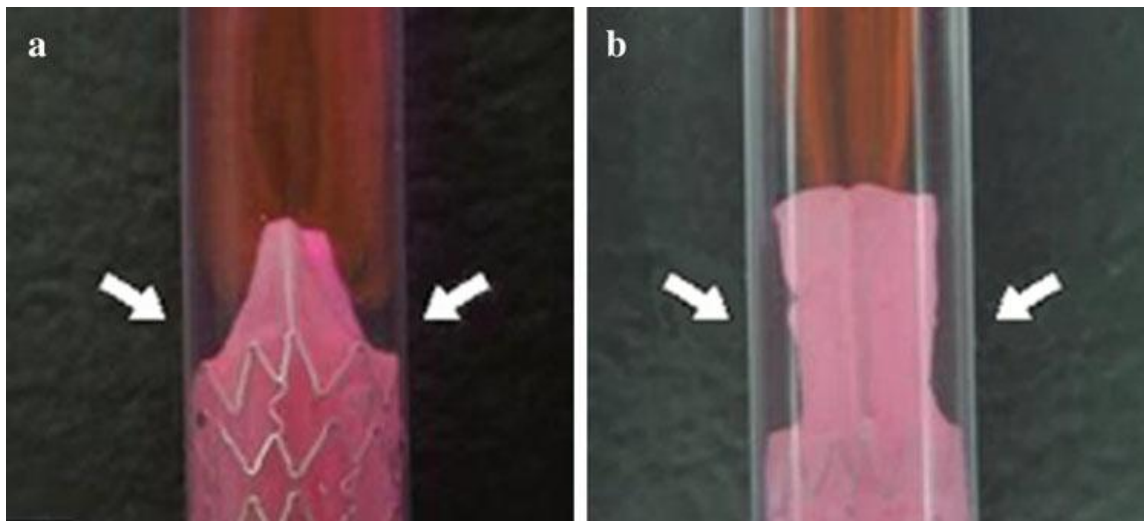


Figure 34: Forward flow of rhodamine solution through the Moriyama valves: bPVV (left) and oPVV (right) (image from [142]).

Sathe designed a naturally closed prosthetic venous valve composed of Poly(vinyl-alcohol) (PVA) cryogel (see Figure 35) [141, 143-145]. This valve had a reflux flow rate less than 0.3 mL/min under an applied backpressure ranging from 0-300 mmHg before and after 500,000 cycles. The valve increased the outflow resistance by 324.6 mmHg*min/L. A CFD simulation of the open configuration of this valve in a 10 mm vein with an average inlet flow

velocity of 0.27 m/s, corresponding to an inlet flow rate of approximately 1300 mL/min, revealed shear rates to exceed $10,000 \text{ s}^{-1}$. The valve occluded in an *in vitro* porcine blood flow loop in less than 20 minutes with a 470 mL/min forward flow induced by a roller pump. Two valves were implanted into a sheep and were not patent when examined at 5 weeks. It was hypothesized that thrombus had formed in response to elevated shear rates from the valve's narrow orifice.

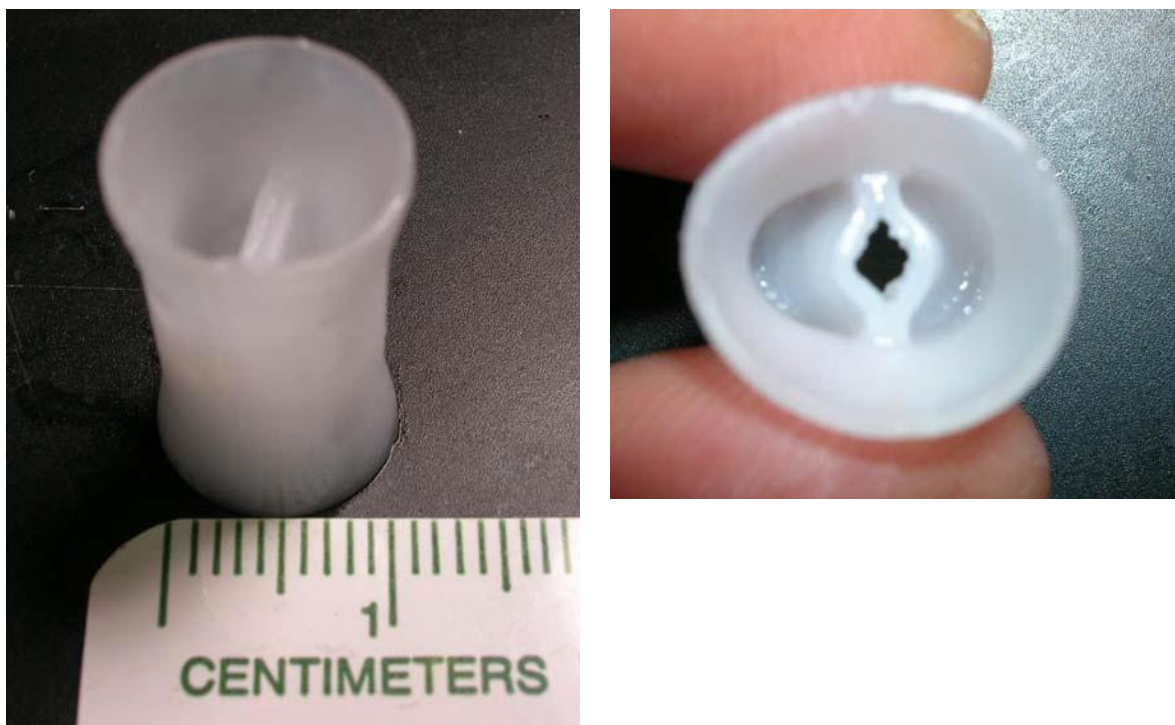


Figure 35: Sathé valve when closed (left) and open (right) (images from [141]).

Midha developed a naturally open prosthetic venous valve with a lemon shaped orifice made with PVA (see Figure 36) [145]. This valve had a mean reflux flow rate of 30.8 and 41.1 mL/min under an applied backpressure of 75 mmHg before and after 500,000 cycles respectively. Small gaps remained after leaflet closure at the corners where the two leaflets joined which allowed this amount of reflux. The valve increased the outflow resistance by 7.3

mmHg*min/L. A CFD simulation of this valve in a 10 mm vein with an average inlet flow velocity of 0.27 m/s, corresponding to an inlet flow rate of approximately 1300 mL/min, predicted shear rates up to $3,000 \text{ s}^{-1}$. Dye placed behind the leaflets was completely washed out under a forward pressure gradient of 75 mmHg. The valve did not occlude in an *in vitro* porcine blood flow loop after 3 hours with a 470 mL/min forward flow induced by a roller pump. Four valves were implanted into the external jugular veins of sheep. One valve remained patent at 6 weeks with the other three valves occluding by week 4. It was hypothesized that thrombus had formed in response to elevated shear rates induced by radial buckling of the valves. The base of valve had a propensity to radially buckle because of the ovular shape of the shoulder. Further experimental testing of the valve revealed the tendency of the valve's leaflets to prolapse under retrograde pressure. The Midha valve is the predecessor to the valve presented in this work.

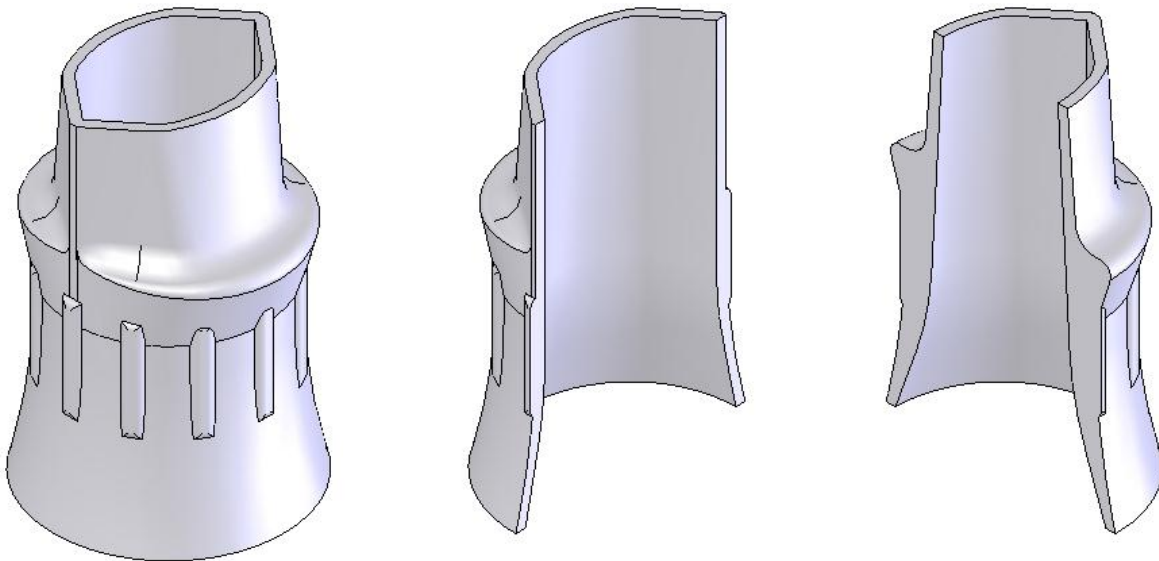


Figure 36: Midha valve (left) with views of the valve cut along the major (middle) and minor (right) axes (image from [145]).

Remaining Issues

While a transcatheter prosthetic venous valve has the potential of being an effective minimally invasive solution to venous reflux, particularly in the deep venous system, an adequate valve has yet to be developed. While venous reflux and outflow obstruction are major contributors to the development of CVI, none of the previous valves that have undergone experimental testing have been demonstrated to reduce reflux below that seen in individuals with venous reflux while also not increasing outflow resistance to venous obstruction levels. Of the few valves which have been tested in humans, only one has reported to have remained both patent and competent inside an individual for more than a year, but this valve was deemed unfit to further use for venous implantation [110]. Thus far prosthetic valves tested in animals or humans have commonly reported concerns with:

- Thrombogenicity
- Biocompatibility
- Correct sizing, and subsequent fixation and functionality of the valve

For a prosthetic venous valve to be developed which is effective in treating individuals with CVI, design specifications (design inputs) must first be determined. The Code of Federal Regulations (CFR) Title 21 Part 820.30 states that design inputs “ensure that the design requirements relating to a device are appropriate and address the intended use of the device, including the needs of the user and patient” [146]. Protocols to measure “design outputs in terms that allow an adequate evaluation of conformance to design input requirements” are to be established [146]. CFR Title 21 Part 820.30 also states, “Design verification shall confirm that the design output meets the design input requirements. The results of the design verification,

including identification of the design, method(s), the date, and the individual(s) performing the verification, shall be documented in the [Design History File]” [146].

With a foundation of relevant design specifications and verification testing, a prosthetic venous valve can be developed which has low thrombogenicity, is biocompatible, is sized correctly, is sufficiently competent, does not significantly obstruct forward flow, can function in a distensible vein, and so forth. The goals of this work, which are outlined in the following chapters, are the following:

1. Specify design specifications which are necessary for a prosthetic venous valve to effectively treat individuals with venous reflux.
2. Design a prosthetic venous valve capable of meeting all design specifications.
3. Perform finite element and computational fluid dynamic simulations to analyze the valve.
4. Create and conduct verification tests that will determine if the proposed valve meets the required design specifications.
5. Propose validation tests for the proposed valve in animals and humans.
Determine where the valve should be placed and specify valve sizes which will fit these locations.

CHAPTER 2: DESIGN SPECIFICATIONS

Competency

The primary function of a prosthetic venous valve is to reduce retrograde flow. Greater reflux flow rates have been correlated with increases in symptom severity [32, 147]. Neglén measured the time average reflux flow rate for incompetent CFV (n=47), femoral (n=87), and popliteal (n=103) deep veins to be 3-3357 mL/min [32]. A competent prosthetic venous valve should have a time average reflux flow rate below 3 mL/min to ensure reflux is reduced below pathologic levels.

A valve must remain competent under all of the potential retrograde pressures it may encounter in a vein when an individual is standing. Retrograde pressure in veins is caused primarily by the hydrostatic pressure from the column of blood above it which can range from 30 to 100mmHg [2, 148, 149]. The Valsalva maneuver can increase backpressure up to an additional 30mmHg [150]. Thus a venous valve could experience retrograde pressures ranging from 30 to 130 mmHg. Applying a safety factor of 1.25 to the maximum pressure, a competent prosthetic valve will have a reflux flow rate less than 3 mL/min under backpressure ranging from 30 to 160mmHg.

A vein may not be fully distended when the valve is required to close, such as when a Valsalva maneuver is performed in the supine position. The diameter of the average CFV at rest in the supine position is approximately 17% smaller than during a Valsalva maneuver in the 15% reverse Trendelenburg position [151]. Assuming that a valve is sized to fit into a vein when it is fully distended, it will need to remain competent when the vein's diameter is 17% smaller. A valve intended to be inserted in a 10mm vein would need to remain competent when its leaflets

were constrained inside a 8.5mm tube or smaller. As a lower retrograde pressure will be less likely to force a valve closed, this test should be performed under a 30 mmHg pressure head. Determining the smallest diameter in which a prosthetic valve can remain competent will also be helpful to direct surgeons in inserting an appropriately sized valve into a vein.

Fatigue Life

A prosthetic venous valve must remain competent after undergoing extensive cyclical loading. It has been predicted that a prosthetic valve would undergo 9 million cycles over the course of 10 years in a subject, with valves cycling at a rate of 0.67 Hz during walking [143]. It is assumed that a valve produced under good manufacturing practices will have a longer fatigue life than a valve produced in laboratory conditions. Thus if a prototype valve manufactured in a laboratory can function properly after 5% of the expected number of cycles (500,000), then it can be assumed that it would still function after 9 million cycles when produced with good manufacturing practices [143]. Thus a competent and fatigue resistant valve would have a reflux flow rate less than 3 mL/min under 30 and 160 mmHg of retrograde pressure before and after 500,000 cycles.

Closing Time

Healthy native venous valves typically close in less than 0.5 seconds under retrograde pressure, with valves with longer closure times typically being deemed incompetent in clinical practice [30-34]. Thus, in addition to restricting retrograde flow, a prosthetic venous valve should close in less than 0.5 seconds to be deemed competent.

Distal Pressure Rise

Contraction of the calf muscle pumps blood out of veins which decreases venous pressure. Pressure returns to the original level as the vein refills from arterial inflow and valvular reflux. This pressure rise is captured by recording the 90% venous refill time (VFT90), which is measured by recording the time it takes for venous pressure to rise back to 90% of the initial pressure after calf flexion. Individuals with CVI have a VFT90 of less than 30 seconds, while normal individuals have a VFT90 greater than 30 seconds [2, 36, 37]. Lower VFT90 measurements have been correlated with increased symptom severity [18, 37]. Assuming that reflux from a healthy venous valve is responsible for 10% or less of the pressure rise, a prosthetic valve should see its distal pressure rise to 10% or less of the original pressure 30 seconds after a simulated calf flexion.

Outflow Resistance

A prosthetic venous valve should not significantly impede venous return to the heart.

Flow resistance is calculated by:

$$R = \frac{\Delta p}{Q} \quad (1)$$

Where Δp is the pressure difference and Q is the flow rate.

Because veins are distensible, their resistance changes with pressure. Therefore, it is important to compare venous resistance at similar pressures. At a forward pressure difference of 15 mmHg, the average venous resistance in a normal individual calculated by Equation (1) is 10 mmHg*min/L [48]. Four grades of obstruction, each resulting in an increase in venous resistance, have been specified [48]. The lowest grade of obstruction has been reported to

increase the average venous resistance by 5 mmHg*min/L at a forward pressure gradient of 15 mmHg [48]. A prosthetic venous valve should not increase venous resistance as much as venous obstruction grade levels do. Thus a prosthetic venous valve should add less than 5 mmHg*min/L to the outflow resistance under a forward pressure difference of 15 mmHg.

Thrombogenicity

A prosthetic venous valve should have low thrombogenicity. While there is no standard method to quantify the degree of a device's thrombogenicity, items that have been shown to promote thrombus formation should be systematically reviewed. Virchow's Triad proposes that thrombus formation in the veins can occur in the presence of stagnant blood, endothelial injury, and blood hypercoagulability [152]. Of these three factors of the triad, a prosthetic venous valve may contribute to the formation of stagnant blood which could result in thrombus formation. In contrast, regions with high shear rates and the material used can increase the risk of thrombus formation. Ultimately, the formation of thrombus when the valve is placed in blood will determine if it is thrombogenic.

Stagnation Zones

Virchow found that stagnant blood increases the risk of thrombosis [152]. Blood behind the leaflets of a prosthetic venous valve has the highest risk of being stagnant and clotting. Stagnation zones behind the leaflets are unlikely to exist while the leaflets are cycling, such as when standing, sitting, or walking. However, when a person is in the supine position, there is typically only prograde pressure, so the leaflets may remain open and motionless for long periods of time [20]. Venous flow rates of an individual resting in the supine position are between 400 to 600 mL/min, which are lower than when standing, further increasing the risk of

stagnation zones in this position [137, 153, 154]. To predict if blood behind the leaflets of a prosthetic venous valve will clot in the supine position, all of the fluid behind its leaflets should wash out under a forward flow rate of 400 mL/min.

Radial buckling of a valve could create stagnant zones and result in clotting. The valve developed by Midha is suspected to have thrombosed for this reason [145]. The average CFV diameter at rest in the supine position is approximately 17% smaller than its diameter during a Valsalva maneuver [151]. Assuming that a valve is sized to fit into a vein when it is fully distended, it must not radially buckle when the vein is at rest and the diameter is smaller. Thus a valve should not radially buckle when placed in a tube with a diameter that is 17% smaller than the diameter size it is designed to fit in. Thus, a valve intended to fit inside a 10mm vein should not radially buckle in a 8.5mm tube.

Regions of High Shear

High wall shear rates have been shown to increase platelet activation and binding, ultimately leading to thrombus formation and growth [155-157]. High shear rates also lead to increased platelet transport and deposition rates [158-160]. The maximum thrombus growth rate in human blood occurs at a wall shear rate of roughly $10,000 \text{ s}^{-1}$ [161, 162]. Physiologic shear rates are generally considered to be below 3500 s^{-1} [163]. The highest shear rate in the valve will occur when flow through it is the highest. The peak flow rate through the femoral vein can be up to 1600 mL/min, which can occur during ankle flexion while standing or after a Valsalva maneuver [137, 151]. To avoid shear induced thrombosis and to have shear rates at physiologic levels, the maximum shear rate of the blood flowing through a prosthetic venous valve at a rate of 1600 mL/min is required to be below $3,500 \text{ s}^{-1}$.

Material Biocompatibility

A valve should be composed of a material that has been shown to be biocompatible and have low thrombogenicity. The selected material must demonstrate its biocompatibility by not eliciting inflammation or a foreign body reaction, manifesting as fibrous encapsulation, when placed in the bloodstream, as well as passing the biocompatibility tests specified by ISO and USFDA [164, 165]. While there is no standard method to quantify the degree of a material's thrombogenicity, a material that requires at least as much time for thrombus to form on it when exposed to blood as a material currently used in FDA cleared blood contacting devices, such as Dacron™, is assumed to have low thrombogenicity.

Blood Flow Loop

One way to predict the short term patency and relative thrombogenicity of a valve is to place it in an *in vitro* blood flow loop. Porcine blood has a non-Newtonian flow behavior and viscoelasticity similar to human blood [166-168]. Porcine blood will thrombose at low and high shear rates, similar to human blood [157, 166, 169]. In addition to similarity, porcine blood has been found to thrombose faster than human blood [169]. For these reasons, porcine blood can be used to accurately predict a device's performance in human blood and is advantageous to use in a short term test.

Midha demonstrated that his valve was less thrombogenic than Sathe's by placing it in a flow loop with heparinized (3.5 mL/L) porcine blood flowing at a rate of 470 mL/min: the Sathe valve occluded in 18 minutes while the Midha valve was still patent after three hours [145]. A prosthetic venous valve should demonstrate that its short term patency in heparinized (3.5 mL/L) porcine blood is no worse than the Midha valve under a similar flow rate. Flow rates of this

magnitude can occur when an individual is in the supine position, so a valve should be oriented in the horizontal direction when verifying this specification for the gravitational force to be in the correct direction [137, 153, 154].

Deliverability

The demand by patients and surgeons for a prosthetic venous valve that can be percutaneously delivered by a catheter is much greater than one that requires an open surgery. Catheters sized 16 Fr (5.3mm) and smaller are commonly used by surgeons and have shown better results when used in abdominal aortic aneurysm repair [170]. Thus a prosthetic valve should fit inside a 16 Fr catheter or smaller.

A valve will not function properly if it is placed inside a vein in an incorrect orientation. To promote a stable orientation, the length of the portion of the valve in contact with the vein wall should be at least 1.5 times the diameter. Hence a valve designed to fit inside a 10mm vein should have a 15mm long section in contact with the wall.

Summary

The design specifications for a prosthetic venous valve are summarized in Table 5.

Table 5: Summary of design specifications for a prosthetic venous valve.

	Metric	Units	Specification
1	Reflux rate under a 30 mmHg pressure head	mL/min	≤ 8
2	Reflux rate under a 160 mmHg pressure head	mL/min	≤ 8
3	Smallest diameter in which the valve remains competent	mm	≤ 8.5
4	Reflux rate under a 30 mmHg pressure head after 500,000 cycles	mL/min	≤ 8
5	Reflux rate under a 160 mmHg pressure head after 500,000 cycles	mL/min	≤ 8
6	Leaflet closing time	s	< 0.5
7	Distal pressure rise 30 seconds after a simulated calf flexion	%	≤ 10
8	Outflow resistance added by the valve under a 15 mmHg pressure head	mmHg*min/L	< 5
9	Fluid behind leaflets washes out under 400 mL/min	Binary	1
10	Smallest diameter in which a valve does not buckle	mm	≤ 8.5
11	Maximum shear rate on the valve walls with an inlet flow rate of 1600 mL/min	s^{-1}	< 3500
12	Material does not elicit inflammatory response or foreign body reaction when placed in the bloodstream	Binary	1
13	Material passes biocompatibility tests specified by ISO and USFDA	Binary	1
14	Material is less thrombogenic than Dacron	Binary	1
15	Time to occlusion when running heparinized (3.5 mL/L) porcine blood in a flow loop	Hours	> 3
16	Minimum catheter size the valve can fit in	Fr	≤ 16
17	Ratio of the valve length that contacts the vein wall to the vein diameter	NA	≥ 1.5

CHAPTER 3: PROPOSED VALVE DESIGN AND FABRICATION

Material Selection

Prosthetic venous valves are typically mechanical, bioprosthetic, or polymer valves. A polymer valve is desirable because a mechanical valve may not be able to function in a distensible vein, and a bioprosthetic valve would be difficult to manufacture in large quantities.

Poly(vinyl-alcohol) cryogel (PVA) was chosen as the primary material for the proposed prosthetic venous valve. PVA is a relatively new and promising biomaterial developed by researchers at Georgia Tech [171, 172]. PVA is prepared by combining Poly(vinyl-alcohol) pellets with water to obtain a desired wt%, heating in an autoclave at 120 °C until the pellets have dissolved. At this point the PVA is in a viscous state and can be used to coat solid objects, such as stents, or be injected molded and assume the shape of a desired geometry [141, 145, 173]. The liquid PVA is then solidified by cross-linking which occurs during freeze-thaw cycling.

PVA meets the requirement of being biocompatible. PVA passed the biocompatibility tests specified by ISO and USFDA [165]. When placed in the bloodstream of sheep and rats, inflammatory responses and fibrin encapsulation have not occurred [145, 173, 174]. Furthermore, medical devices containing PVA have been implanted in humans for over ten years without any negative reports [173].

PVA meets the requirement of having low thrombogenicity. PVA has been shown to be less thrombogenic than DacronTM when perfused with porcine blood [144, 175]. The thrombogenicity of PVA can be reduced further by its ability to incorporate and elute anti-

coagulation drugs, such as citrate [145]. Additionally, it is difficult for cells to attach to PVA because the proteins necessary for adhesion do not easily absorb into it [176].

The mechanical properties of PVA can be altered by modifying the solution's wt% and the thermo cycling process [177-188]. Increasing the PVA wt% from 10 to 20 percent has been found to increase the ultimate tensile strength and Young's modulus by up to 192% and 250% respectively [177]. The ultimate tensile strength and Young's modulus have been found to increase for each freeze-thaw cycle, with diminishing increases per cycle after the fourth cycle [179, 180, 185-187]. For example, Fromageau reported that the mean Young's modulus for a 10 wt% PVA solution increased by 77-104 kPa (57-320%) for cycles 1 through 4 and by 16-20 kPa (6-7%) for cycles 5 and 6 [179]. Decreasing the rate of freezing and thawing has been found to increase the stiffness by up to 340% for the same wt% [178, 179]. One study found the Young's Modulus of PVA having undergone 4 freeze-thaw cycles to remain stable for a period of 7 months without significant variation, suggesting that the valve leaflets will remain flexible in the long-term [183].

In the present application, the PVA needs to be flexible enough to close under low pressures, yet stiff enough to resist prolapse under backpressure. To accomplish these goals, prototype valves were made out of 20% PVA and underwent four freeze-thaw cycles. For each cycle valves were frozen at -20 °C for at least three hours. The rate of thawing was decreased by placing valves in a 4 °C refrigerator instead of at room temperature for at least three hours.

Geometry

A prosthetic venous valve was designed to fit a 10mm vein and meet the aforementioned design specifications. The valve's geometry is shown in Figure 37 and Figure 38. The valve has

two general regions: the base, which includes the valve's entry region and shoulder, and the leaflets.

The base of the valve is circular and has an outer diameter slightly smaller than the average diameter of the human femoral vein, which decreases the overall bulk of the valve. The circularity allows a stent to be placed inside the base of the valve during manufacturing. The stent can cause the valve base to expand inside of a vein and provide the necessary radial pressure to fix its position. This expansion decreases the risk of radial buckling and potential clotting at the inlet while enabling the valve to fit perfectly into a large range of vein sizes. The wall thickness at the base is thick enough to expand with the stent without tearing while keeping the overall bulk of the valve low. The base is 15mm long, which ensures that there is only one stable orientation for the valve when it is inserted in a vein. The valve shoulder is 0.5 mm wide and encourages washout of blood behind the leaflets. The top of the stent is coincident with the shoulder which supports the base of the leaflets and reduces the risk of prolapse without interfering with leaflet function. Thus the shoulder also helps the stent to be placed correctly inside of the valve mold during manufacturing. The circular orifice at the entrance of the base transitions into an ellipse to allow the base to support the leaflets. This transition happens in a nonlinear manner that keeps the volume of the valve low while not raising the shear rate to critical levels with abrupt changes. The orifice of the valve in its unexpanded state is 29 mm^2 at its most constricted point, which occurs at the level of the shoulder, which is 36% of the area of a 10 mm circular vein.

The valve's leaflets are naturally open and are designed to close under retrograde flow. The pressure difference between the fluid on the inside and outside of the leaflets during retrograde flow causes the leaflets to move inward and close. The leaflets remain closed because

of the hydrostatic pressure provided by the column of blood above them. Forward flow causes the leaflets to open again.

Several features were incorporated into the leaflet geometry with the intent to enable them to seal during closure while keeping shear rates low when they were open. The elliptical orifice at the top of the valve's base linearly transitions into a lemon shaped orifice by the time it reaches half the height of the leaflets after which it remains lemon shaped. The linear transition helps keep the shear rate low while decreasing the risk of prolapse. The lemon shaped orifice with a 120 degree angle encourages the valve to close properly. The tips of the leaflets are 0.5 mm thick which allows the ends of the leaflets to be more flexible and seal better while decreasing the risk of tearing during removal from the mold during manufacturing. The 128 degree angle at the outside corner of the leaflets ensures that the smallest thickness of the leaflets is no less than 0.5 mm to avoid tearing during mold removal. Various design iterations revealed that a decrease in the leaflet diameter along the minor axis of the orifice strongly correlated with a decrease in the amount of reflux in a valve. Thus this valve was designed to have this dimension as small as possible to decrease reflux while keeping the shear rates at levels below those that would increase the risk of platelet activation. The length of the orifice along the inner length was set as large as possible to decrease the maximum shear rate.

To further improve the sealing of the valve, 0.1mm wide and 2.25 mm high slits are present at the top of the leaflets at the corners of orifice. These slits enable the leaflets to seal better by eliminating any gaps that would otherwise exist at the corners of the leaflets during closure. The slits were not made wider or longer because doing so could result in the leaflets not lining up correctly during closure. By including these slits in the original geometry, there is no need to later create the slits by cutting which could result in a crack at the bottom of the slit that

would likely propagate during cycling. The leaflets along the major axis of the orifice flare out to ensure that the slits do not lie in the path of high velocity fluid flow, even when the valve base is expanded by the stent, which would otherwise result in a spike in the shear rate and increase the risk of platelet activation.

Additional features were incorporated into the leaflet geometry to reduce the risk of prolapse. The bottoms of the leaflets along the minor axis of the orifice are the thickest portion of the geometry and resist over bending. The leaflets are 10 mm long which is intended to provide a friction force great enough to prevent the leaflets from sliding down each other. The internal leaflets along the minor axis of the orifice are vertical which was found to help the leaflets seal better and be less likely to prolapse than when angled.

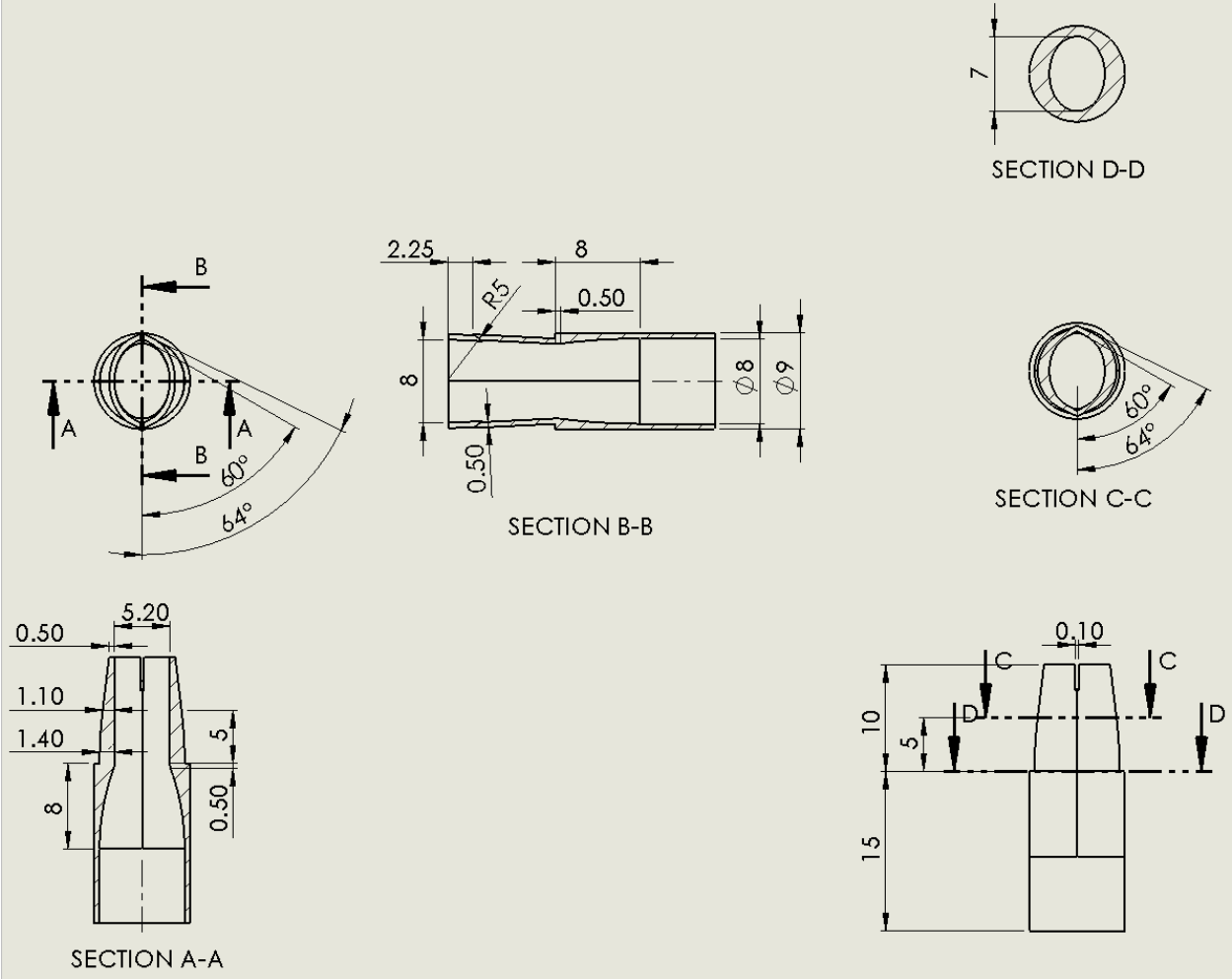


Figure 37: Drawings and dimensions of proposed valve.

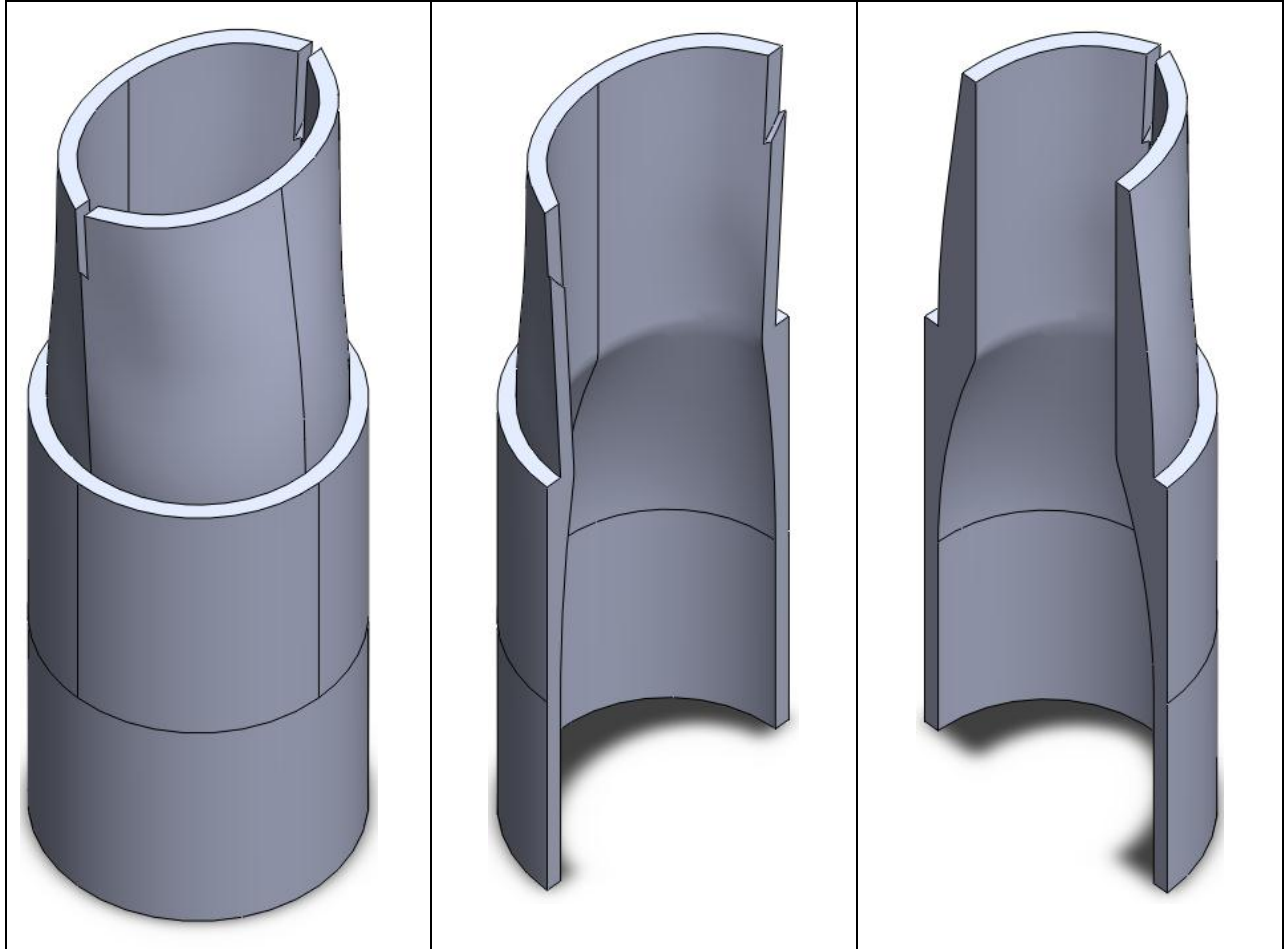


Figure 38: Isometric views of the proposed valve geometry (left) and halved along the major (middle) and minor (right) axes.

Manufacturing

Physical valve prototypes of the proposed valve design with and without stents were fabricated by injecting 20 wt% PVA into a two-part mold and then temperature cycling for four cycles. For valves combined with a stent, the stents were prepared and inserted into the mold prior to PVA injection. Details of the mold creation, stent preparation, and subsequent valve fabrication are as follows.

Mold Creation

The proposed valve's geometry was modeled using SolidWorks® v 2012 CAD software (Dassault Systèmes Solidworks Corporation, Waltham, MA). The cylindrical base of the valve was extruded an additional 5mm which would later assist in the manufacturing process without changing the length of the valve. Rigid rapid prototypes of the modified geometry composed of FullCure®720 were created using an Objet Eden250™ 3D printer (Stratasys Ltd., Edina, MN). The prototypes were then placed in a container of the desired mold size and shape, with the cylindrical base of each prototype flush against the base of the container. A steel shim measuring 10mm in diameter and 0.1 mm thick was placed in the leaflet slits of each prototype (see Figure 39). The steel shims would later ensure the dimensional accuracy of each valve's slits during manufacturing.

A two part mold was chosen to make the valves to ensure that the valves could be removed from the molds without tearing or deflection of the stent. At this point in mold creation, four to six toothpicks were placed in the container which would later help align the two mold halves during valve fabrication (see Figure 40).

Polydimethylsiloxane (PDMS) was chosen as the material for the mold primarily for its ability to accurately capture the small features of the proposed valve design. After curing, PDMS retains its shape in the presence of water and has a high melting point, allowing it to be in contact with PVA or cleaned in an autoclave without deforming [189]. PDMS is transparent which allows visual detection of unwanted air bubbles during PVA injection. PVA does not adhere to PDMS, enabling fabricated valves to be easily removed from the mold [141, 145].

PDMS was made from mixing a 10:1 ratio of parts A and B of Sylgard 184® (Dow Corning, Midland, Michigan) and then poured into the container around the outside of the rapid

prototypes until the bottom 10-15mm was filled. The container was then degassed in a vacuum chamber until all bubbles had been expelled from the PDMS. The container was then placed in an oven at 45 °C for at least two hours, allowing the top surface of the PDMS to solidify. A thin layer of Evercoat 105685 mold release (Evercoat, Cincinnati, Ohio) was poured on top of the PDMS around the outside of the rapid prototypes and allowed to dry at room temperature for at least 6 hours. The inside of the rapid prototypes and the remainder of the container were then filled with PDMS and degassed in a vacuum chamber until all bubbles had been removed. The container was then placed in an oven at 45 °C for at least four hours, allowing all of the PDMS to fully cure.

The solidified mold was then removed from the container. Water was used as a lubricant as the two halves of the mold were gently pulled away from each other and separated along the parting line. The toothpicks were cut at the level of the parting line and removed from the mold, allowing the two mold halves to be separated; the rapid prototypes remaining lodged inside the top mold half. The top half of the mold was then placed in a beaker of water at 100 °C. The hot water served to soften the rapid prototypes allowing them to be removed from the mold using forceps without tearing the PDMS. Flutes for the leaflets were created by poking holes through the PDMS using a blunt needle. The final valve mold halves are shown in Figure 40.

5 mm tall cylindrical spacers having the same dimensions as the valve's base made of FullCure®720 were created using an Objet Eden250™ 3D printer (Stratasys Ltd., Edina, MN). During valve fabrication, spacers were placed in the bottom of each valve cavity to help the cylindrical mold geometries be concentric (see Figure 41). This also eliminated the presence of a parting line inside of the valves, decreasing the risk of clotting inside of the valves due to coagulation of blood caught in this region or a jump in the shear rate due to the sharp change in

geometry. During valve fabrication, toothpicks were reinserted to help align the two mold halves correctly.

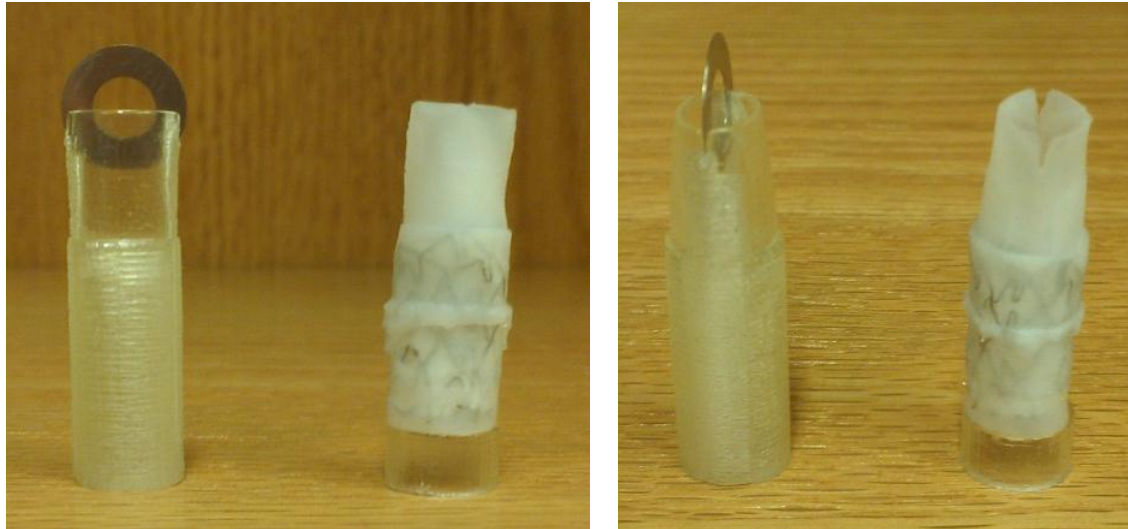


Figure 39: Views of rapid prototype with steel shim and PVA valve on top of cylindrical spacer from the front (top) and side (bottom).



Figure 40: Venous valve mold (left). Individual mold halves (right).

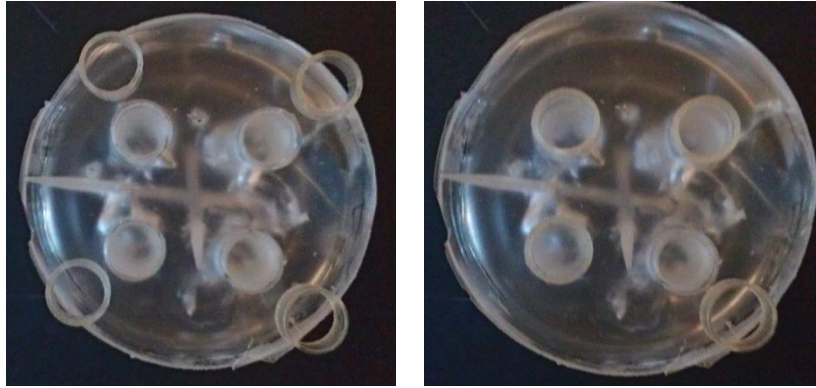


Figure 41: Bottom of mold prior to spacers being inserted (Left). Bottom of valve mold with three of the four spacers inserted into the mold (Right).

Stent Preparation

When the proposed valve is implanted in an animal or human it will be fixed in place by a stent. The risk of material related thrombosis increases if the metal stent is in direct contact with the blood. Weaver proposed coating a stent with PVA as a way to reduce the risk of material related thrombosis [173]. To ensure that each valve's stent was completely covered by PVA, stents were coated with PVA prior to mold insertion by following Weaver's method [173]. A 20 wt% PVA solution was prepared and autoclaved at 120 °C for 25 minutes. Stents were expanded with a balloon to 8.5 mm and then dip coated in 20 wt% PVA. Excess PVA inside each stent was manually removed using a wire. The stents were then placed in the freezer at -20 °C and thawed in the fridge at 4 °C three times to solidify the PVA.

Valve Fabrication

Prototype valves of the proposed design were fabricated as follows. For valves with a stent inside, the stent was first placed inside the mold with its top edge aligned with the future valve's shoulder. Toothpicks were then inserted to constrain the mold halves in the correct aligned position. 20 wt% PVA was prepared and injected into the mold through the leaflet flutes

and the cylindrical base until all air bubbles had been removed. If present, the stent was inspected to make sure it was still aligned with the valve's shoulder. The spacers were then inserted into the base of the mold to constrain the internal cylindrical portions of the mold at their bases. The mold then underwent four thermo cycles in a -20 °C freezer and a 4 °C refrigerator for at least three hours at each temperature. To avoid dehydration, the valves were kept in the molds until after they were finished cycling. The valves were then removed and placed in water in preparation for testing.

A stented valve is shown in Figure 39. Views of the valve when open and closed are shown in Figure 42.



Figure 42: Proximal views of the prototype valve when open (left) and closed (right).

Intended Use

The intended use of the proposed valve is to correct venous reflux in individuals with chronic venous insufficiency.

CHAPTER 4: COMPUTATIONAL ANALYSIS

Finite Element Model

A finite element model was created to obtain the geometry of the proposed valve after being expanded by a stent into a 10mm vein. The deformed geometry was then used in the computational fluid dynamics simulation.

Material Properties

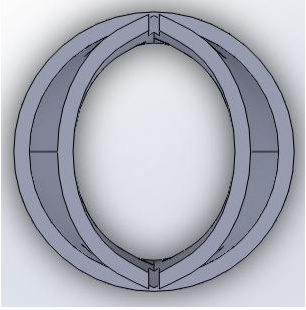
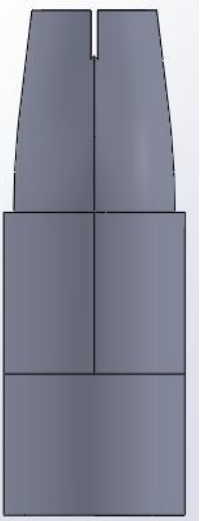

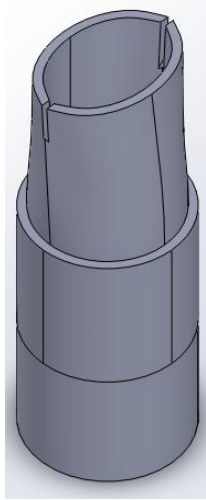
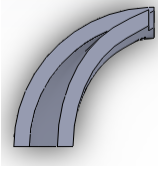
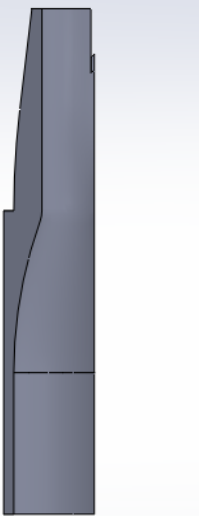

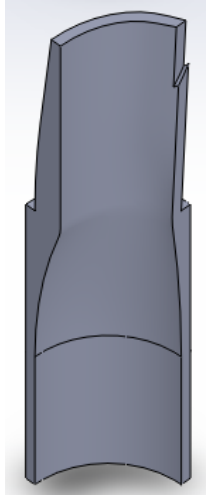
As the strain in a PVA valve during its expansion by a stent is expected to be small, the material of the valve in this model was assumed to be linearly elastic and isotropic. The Young's modulus of the PVA can be estimated from its manufacturing conditions. Fromageau reported that 10 wt% PVA undergoing four freeze-thaw cycles with slow temperature transitions had a mean Young's modulus of 286 kPa [179]. Weaver reported that increasing from a 10 to 20 wt% solution can increase the Young's modulus by 250%, suggesting that the stiffness of the PVA used in this application to be approximately 1000 kPa [177]. PVA is nearly incompressible, having a Poisson's ratio between 0.42 and 0.499 [178, 179]. The Poisson's ratio used for this simulation was 0.45. It was assumed that the influences of the stent could be accounted for by the boundary conditions so the simulation assumed the material to be homogenous.

Model Creation

The original geometry of the proposed valve was halved along its two planes of symmetry to reduce the geometry to a quarter of the original (see Table 6). This symmetry was later utilized in the finite element simulation to reduce the computational burden without losing

accuracy. The modified geometry was then exported into COMSOL and used in the finite element simulation.

Table 6: Views of the original and finite element model geometry.

	Top	Side 1	Side 2	Isometric
Original Geometry				
Finite Element Model Geometry				

Boundary Conditions

The following boundary conditions were applied to the model to simulate a stent expanding the base of the valve to fit inside a circular vein with a 10 mm inner diameter. The

outer wall of the valve's base was constrained to displace 0.5 mm in the direction normal to its surface. The bottom of the valve's base was also constrained to not move vertically. Symmetry was enforced by constraining the portions of the valve on the planes of symmetry to not displace in the normal direction.

Mesh Refinement and Convergence

Eight meshes for the quarter model were created using COMSOL Multiphysics® v 4.2a with characteristics listed in Table 7. The smallest dimension on the vein valve is 0.5 mm so the smallest element size for the initial mesh was 0.5 mm. Additional meshes with element densities 2 to 8 times greater than the first mesh were also created. Each mesh used a moderate element growth rate of 1.5, a high resolution of curvature of 0.2, and a high resolution of narrow regions of 1. The convergence criteria for the iterative solver was $10E-6$.

The simulation was performed and the resulting maximum total displacement magnitude was recorded for each mesh (see Figure 43). The mesh with elements size six times as dense as the original mesh had the same total displacement as higher density meshes, indicating that this mesh was sufficiently refined. The mesh selected for this simulation is shown in Figure 44.

Table 7: Element characteristics of meshes constructed during mesh refinement for the finite element model.

Relative Mesh Density	Max Element Size (mm)	Min Element Size (mm)
1	2.5	0.5
2	1.25	0.25
3	0.833	0.167
4	0.625	0.125
5	0.5	0.1
6	0.417	0.083
7	0.357	0.071
8	0.313	0.063

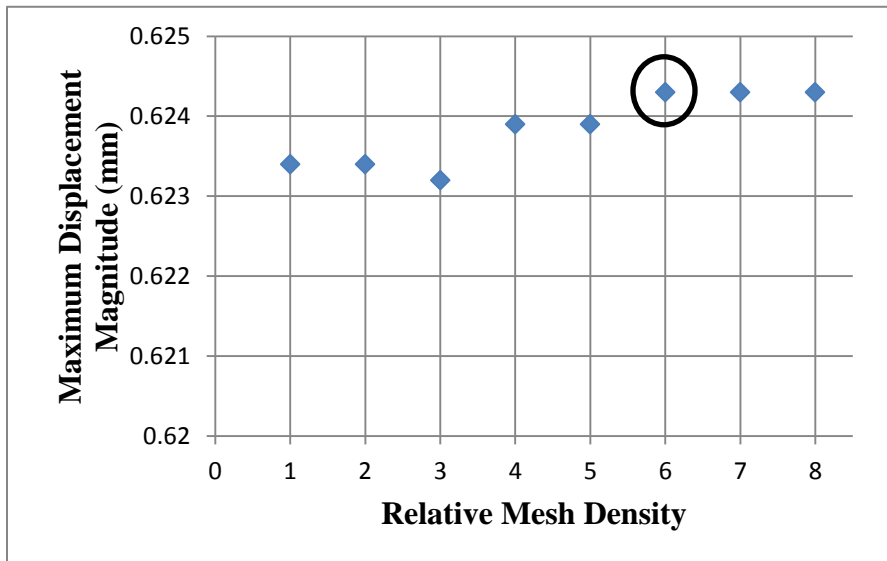


Figure 43: Mesh Convergence for the finite element model. The circled mesh was selected for the finite element model.

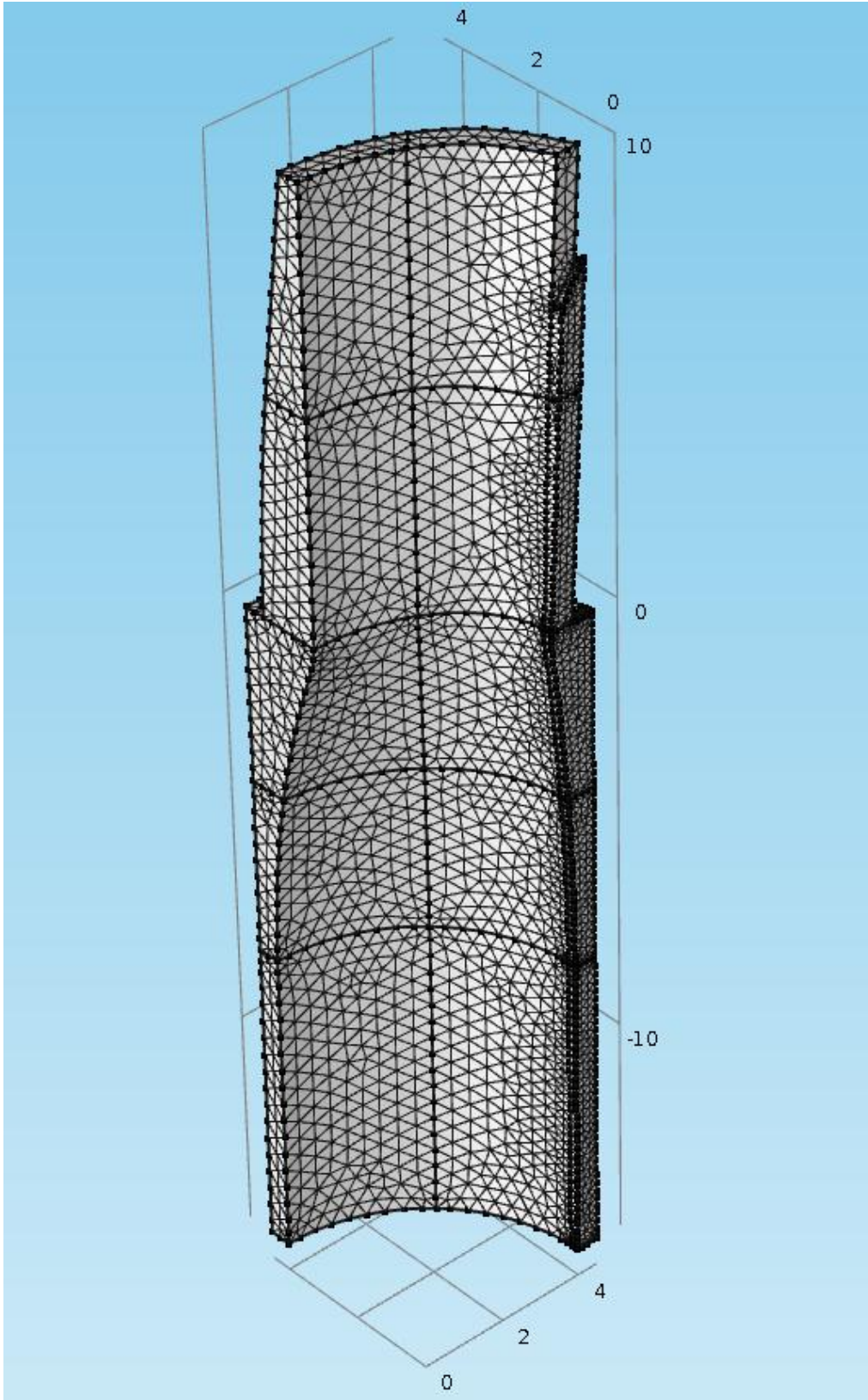


Figure 44: Selected mesh for the finite element simulation.

Results

The deformed geometry of the finite element model with the valve's base displaced in the normal direction by 0.5 mm, simulating the expansion of the valve by a stent into a 10mm vein, is shown in Figure 45 and Figure 46. The maximum principle strain in the valve was 0.473, suggesting that the original assumption of a linear elastic modulus was valid for this simulation. The leaflets expanded with the shoulder at their base and gradually transitioned back to their original geometry 4 mm above the shoulder (see Table 8). After expanding, the minimum orifice area of the valve remained approximately 28.4 mm², which is 36.1% of the cross-sectional area of the vein. This is within the stenosis range of 30-70% caused by native valves [19, 22].

Table 8: Orifice area of the original and deformed valve geometries at specified distances above the shoulder.

Distance Above Shoulder (mm)	Original Geometry: Orifice Area (mm²)	Deformed Geometry: Orifice Area (mm²)	% Increase
0	28.6	36.9	29.0
1	28.7	32.2	12.1
2	28.6	29.8	4.2
3	28.5	28.8	0.9
4	28.4	28.4	0.0

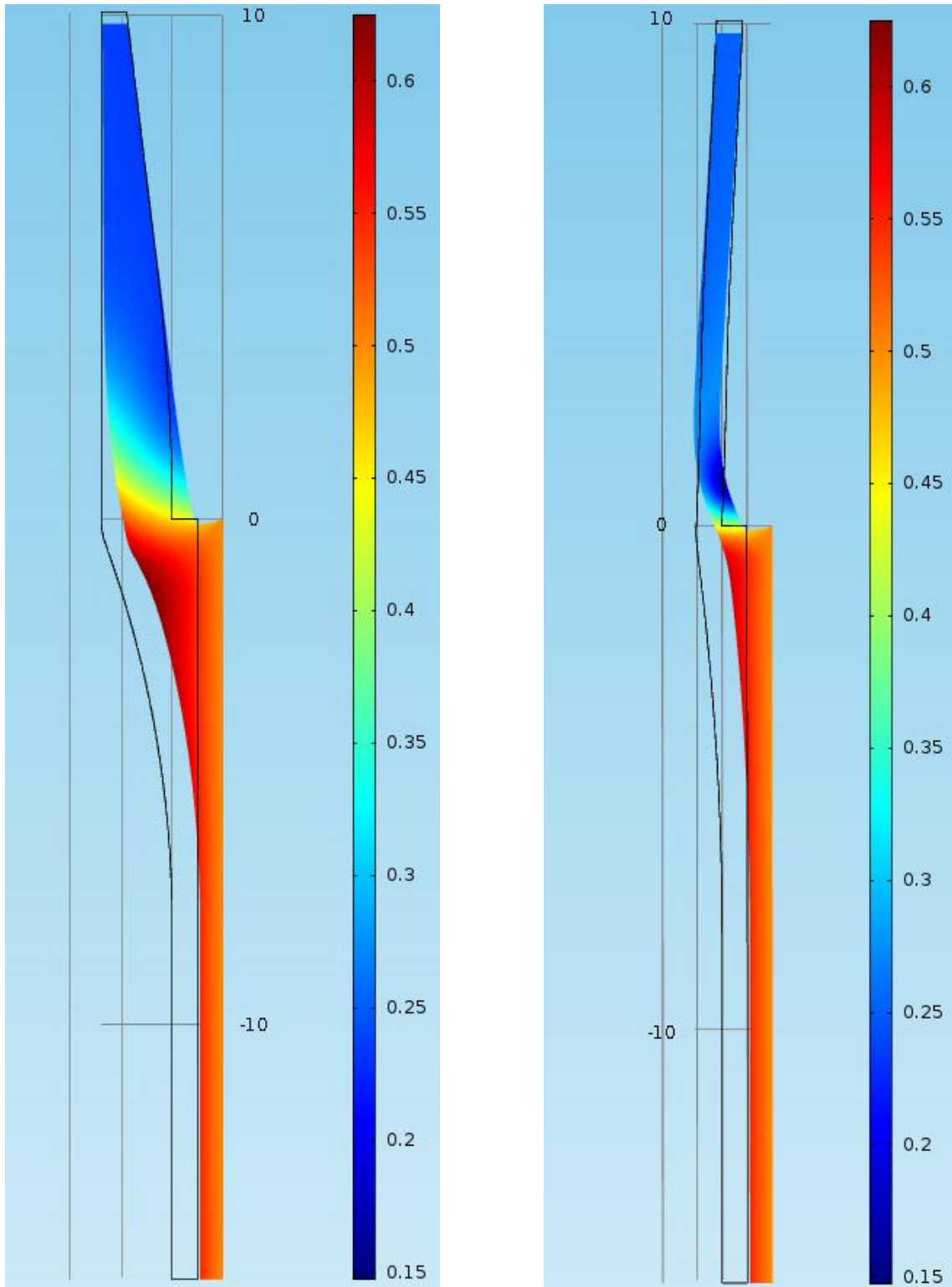


Figure 45: 2D plots of total displacement magnitude on the first (left) and second (right) planes of symmetry of the finite element model with the valve's base displaced in the normal direction by 0.5 mm. Black wireframe lines indicate the original geometry.

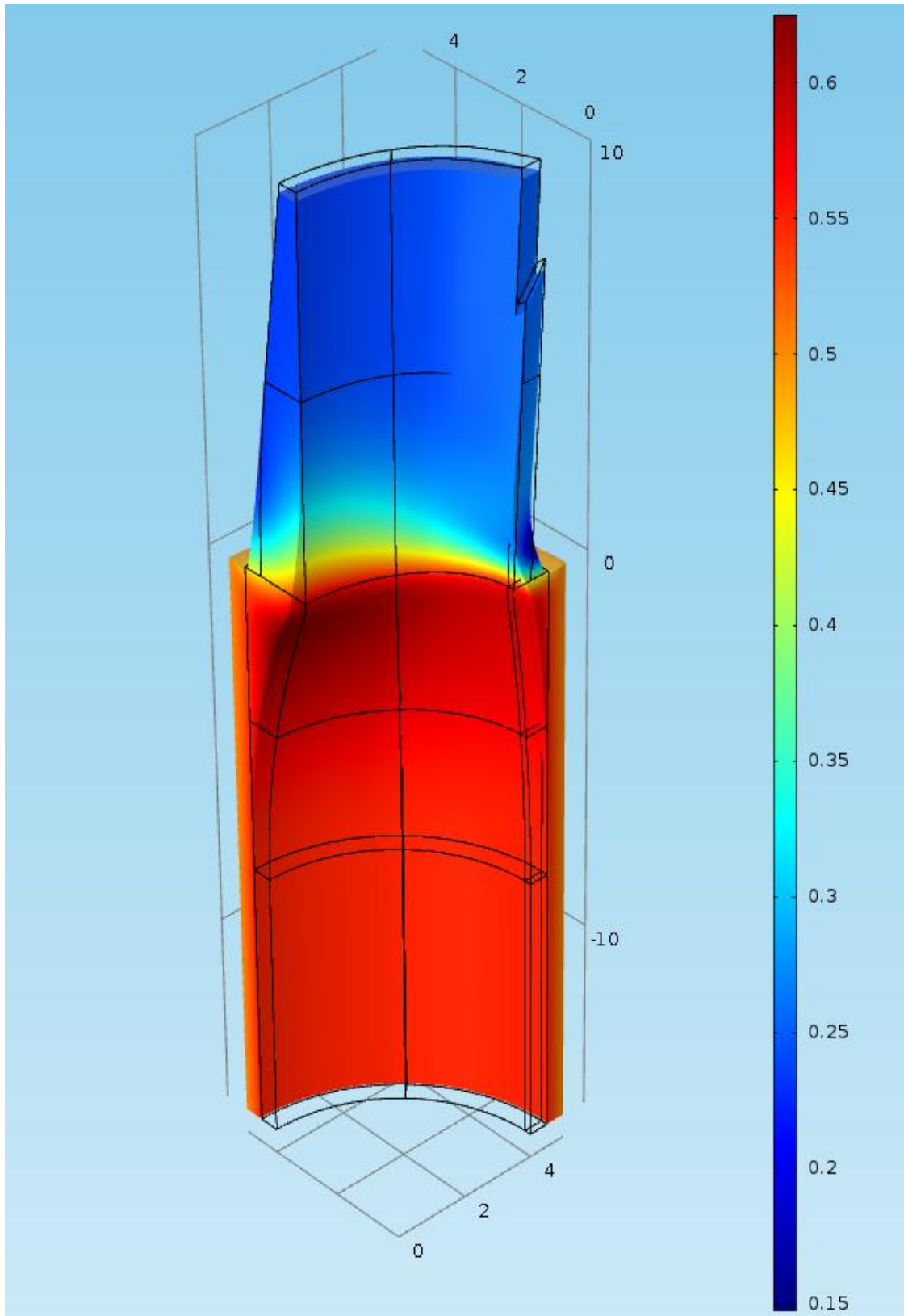


Figure 46: 3D plot of total displacement magnitude in of the finite element model with the valve's base displaced in the normal direction by 0.5 mm. Black wireframe lines indicate the original geometry.

Computational Fluid Dynamics Model

A steady state computational fluid dynamics (CFD) model was created to quantify the maximum shear rate of blood flowing through the proposed valve when expanded into a 10mm vein at a rate of 1600 mL/min ($2.67E-5 \text{ m}^3/\text{s}$) [137, 151]. The maximum shear rate is required to be less than $3,500 \text{ s}^{-1}$ with this forward flow rate for the valve to meet the design specification and reduce the risk of shear induced thrombosis.

Material Properties

The working fluid in the simulation was blood, which was assumed to be homogenous and incompressible. While blood is inherently non-Newtonian, its viscosity becomes nearly constant above a shear rate of 100 s^{-1} [190-192]. As the shear rates encountered in veins in this simulation are expected to be above 100 s^{-1} , blood was modeled as a Newtonian fluid with a viscosity of $0.00345 \text{ Pa}\cdot\text{s}$ and density of $1056 \text{ kg}/\text{m}^3$ [193].

The deformed geometry of the valve was assumed to be rigid because the deflection of the leaflets with forward flowing fluid observed during experimental testing was small. The vein wall was also assumed to be perfectly rigid. Both of these assumptions served to decrease the computational burden of the model while still obtaining meaningful results.

Model Creation

The 3D locations necessary to create a wireframe of the surface of the expanded valve were extracted from the deformed geometry of the finite element simulation (see Figure 47). SolidWorks® v 2012 was used to create surfaces from these points which were then lofted together by guide curves. The CAD model of the expanded valve is shown in Figure 47.

A CAD model of the fluid domain of a circular 10 mm vein was created by modeling a 10 mm diameter cylinder 80 mm long. Two planes of symmetry were used to reduce this cylinder to a quarter of the original geometry. The fluid domain of a vein with the expanded valve inside of it was created by subtracting the geometry of the expanded valve from the quarter cylinder geometry (see Figure 48). As flow through the inlet was programmed to be fully developed, the entry region was 5 mm. The exit region was 5 diameters (50 mm) to prevent any flow abnormalities at the outlet from influencing the flow through the valve.

Boundary Conditions

A no-slip condition was imposed on the valve and vein walls. Symmetry was enforced by constraining the velocity of the fluid on the planes of symmetry to be 0 m/s in the normal direction.

The Reynolds number is defined as:

$$Re = \frac{\rho \bar{u} D}{\mu} \quad (2)$$

Where Re is the Reynold's number, ρ is the density of blood (1056 kg/m^3), D is the vein diameter (0.01 m), μ is the viscosity of blood ($0.00345 \text{ Pa}\cdot\text{s}$), and \bar{u} is the average velocity which can be stated in terms of the inlet flow rate:

$$\bar{u} = \frac{Q}{A} \quad (3)$$

Where Q is the inlet flow rate ($2.67\text{E-}5 \text{ m}^3/\text{s}$), and A is the cross sectional area of the vein ($7.85\text{E-}5 \text{ m}^2$). Equation (3) evaluates to 0.34 m/s, which is the average velocity at the inlet. By combining Equations (2) and (3), the Reynolds number at the inlet was found to be 1040, signifying that the flow will be laminar [194].

Poiseuille flow was assumed with a velocity profile in a circular tube of [194]:

$$u = \frac{r^2 - R^2}{4\mu} \frac{dp}{dx} \quad (4)$$

Where u is the fluid velocity, r is the radial distance from the centerline, and R is the radius of the vein (5 mm), and $\frac{dp}{dx}$ is the pressure drop. Poiseuille flow through a rigid circular tube can be described as [194]:

$$Q = -\frac{\pi R^4}{8\mu} \frac{dp}{dx} \quad (5)$$

Equations (4) and (5) can be combined to find the velocity profile in terms of the flow rate:

$$u = \frac{2Q(R^2 - r^2)}{\pi R^4} \quad (6)$$

Equation (6) was used to impose Poiseuille flow on the inlet of a 10 mm diameter vein with a 1600 mL/min flow rate (see Figure 48). A pressure of 0 Pa was imposed on the outlet (see Figure 48).

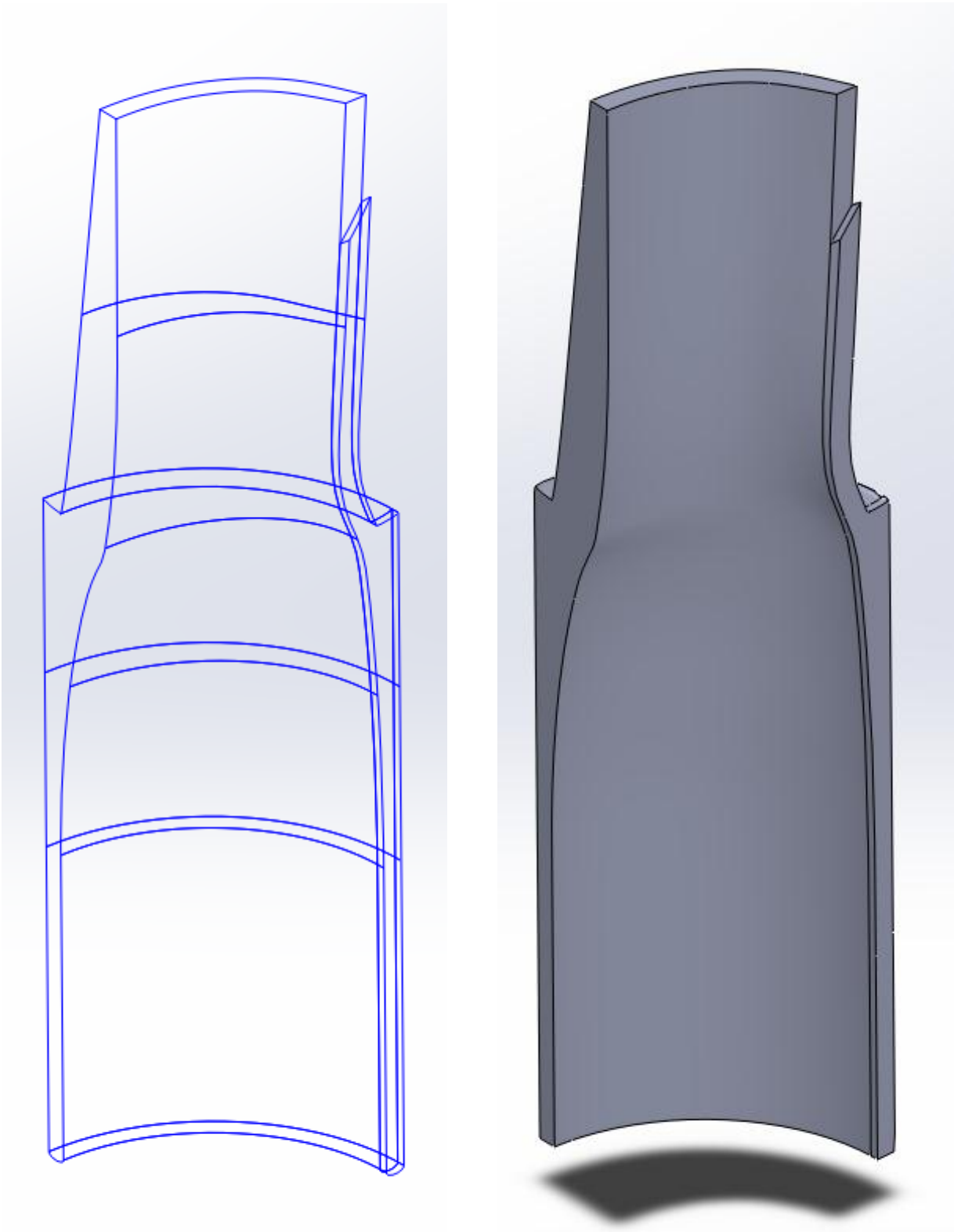


Figure 47: 3D plot of points extracted from the deformed finite element simulation (left). CAD model of the expanded valve created from the extracted points (right).

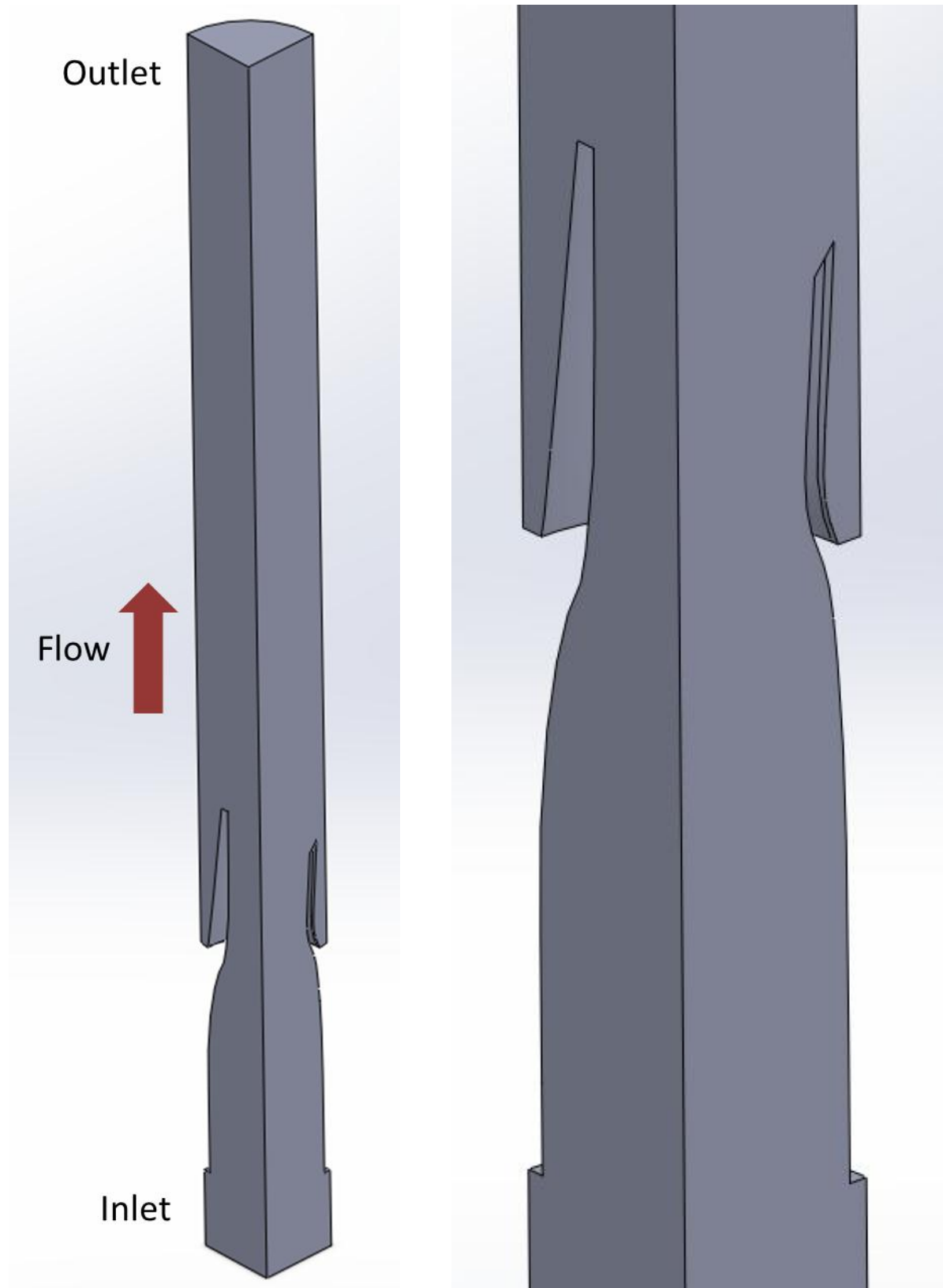


Figure 48: View of entire fluid domain used in the CFD simulation (left). Zoomed in view of the portion of the fluid domain inside the deformed valve (right).

Mesh Refinement and Convergence

Six meshes for the fluid domain of the expanded valve were created using COMSOL Multiphysics® v 4.2a with characteristics listed in Table 9. A similar approach used in meshing the finite element model was used, with the exception that the smallest element sizes were no smaller than those used in the finite element mesh. Each mesh used a moderate element growth rate of 1.5, a low resolution of curvature of 1, and a moderate resolution of narrow regions of 0.5. The convergence criteria for the iterative solver was $10E-6$.

The simulation was performed and the resulting maximum velocity magnitude was recorded for each mesh (see Figure 49). The mesh with elements five times as dense as the least refined mesh had a velocity magnitude within 3% of the highest density mesh, suggesting that this mesh was sufficiently refined. The mesh selected for this simulation is shown in Figure 50.

Table 9: Element characteristics of meshes constructed during mesh refinement for the CFD simulation.

Relative Mesh Density	Max Element Size (mm)	Min Element Size (mm)
1	2.5	0.5
2	1.25	0.25
3	0.833	0.167
4	0.625	0.125
5	0.5	0.1
6	0.417	0.083

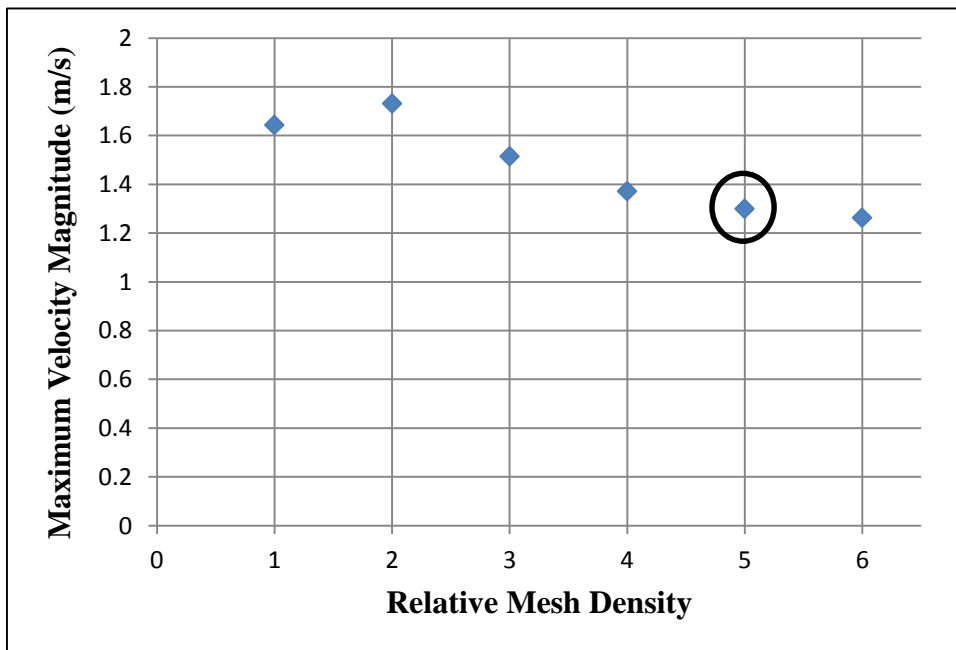


Figure 49: Mesh Convergence for the CFD simulation. The circled mesh was selected for the CFD simulation.

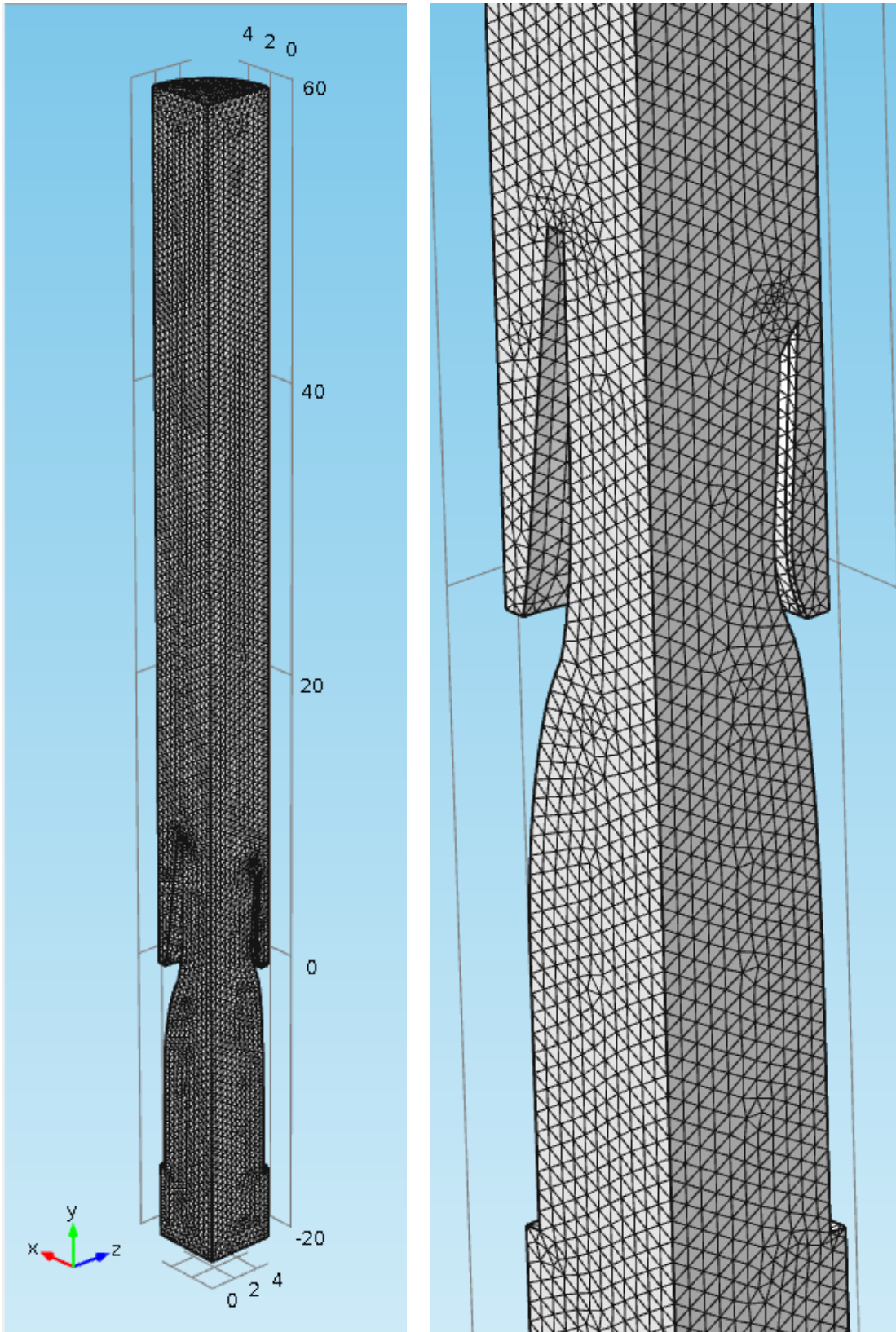


Figure 50: View of entire selected mesh for the CFD simulation (left). Zoomed in view of the portion of the mesh near the deformed valve (right).

Results

Fully developed flow entered the inlet of the valve and transitioned into a jet inside the leaflets (see Figure 51). The centerline velocity increased from 0.679 to 1.299 m/s inside the valve. Reversed flow up to -0.08 m/s was observed behind the thicker leaflet (see Figure 52 and Figure 53). Streamlines revealed that flow was circulating behind the leaflets (see Figure 54).

The maximum shear rate inside the proposed valve was 2300 s^{-1} , which was located on the internal wall of the leaflets (see Figure 55). This meets the design specification of having a maximum shear rate less than 3500 s^{-1} .

Regions of shear rates below 50 s^{-1} were found behind both leaflets (see Figure 56). It is assumed that the shear rate behind the leaflets will increase upon leaflet closure, but experimental testing is needed to see if blood will wash out or clot in this region. High and low shear rates were not observed in or adjacent to the leaflet's slit, suggesting that this design feature may not increase the device's thrombogenicity (see Figure 55 and Figure 56).

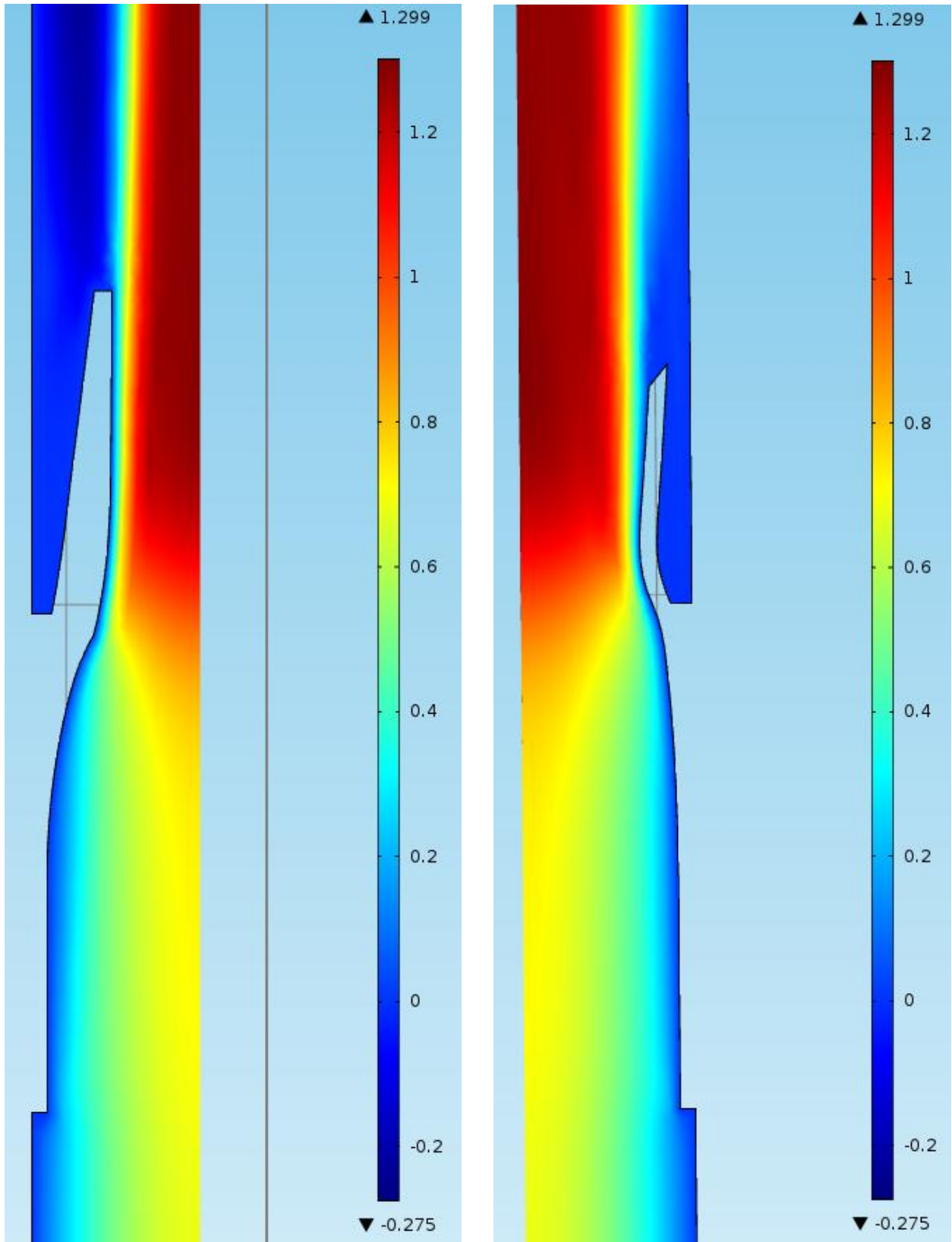


Figure 51: 2D Contour plots of y velocity on the first (left) and second (right) planes of symmetry.

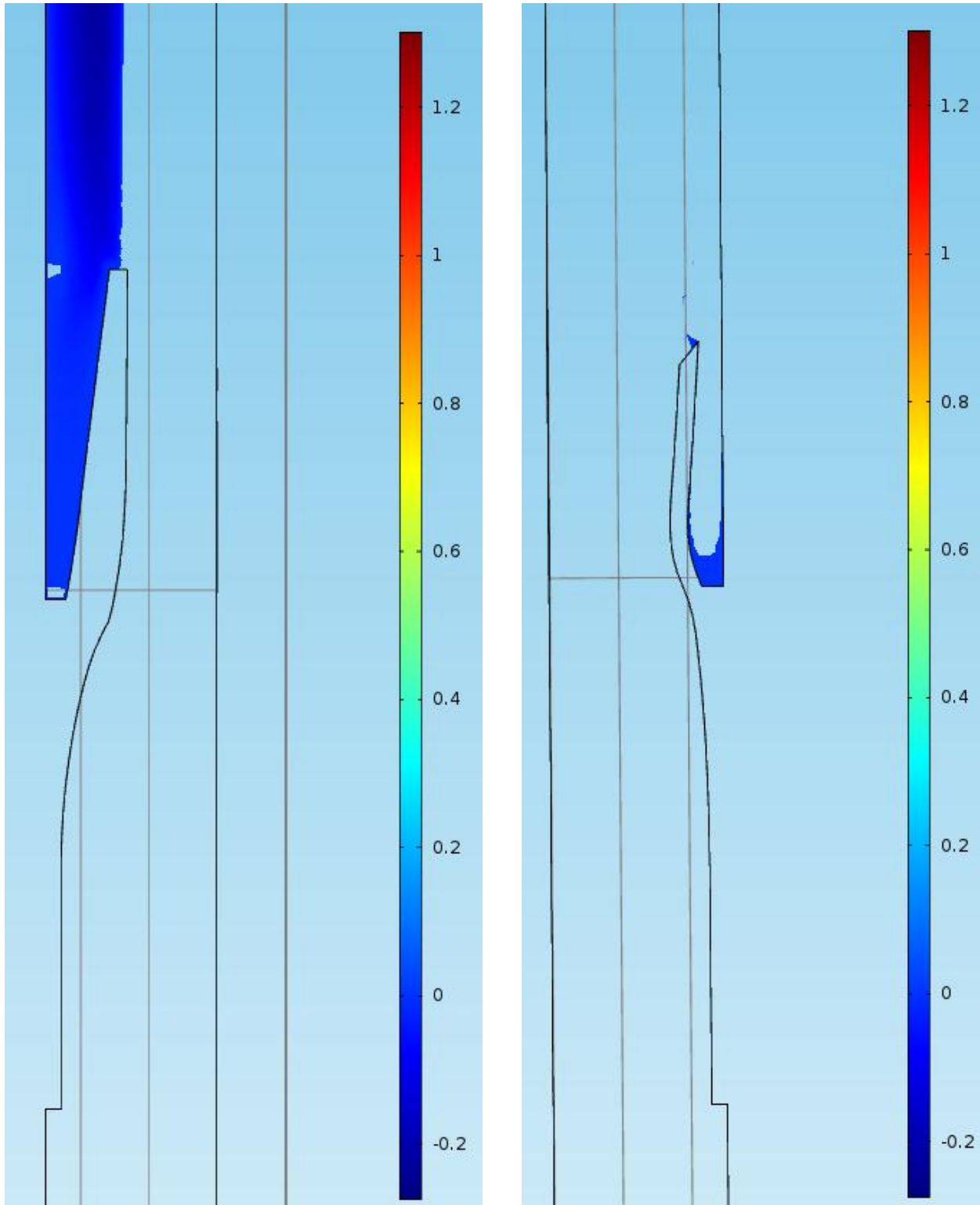


Figure 52: 2D Contour plots of y velocity on the first (left) and second (right) planes of symmetry. Only regions of reverse flow are shown.

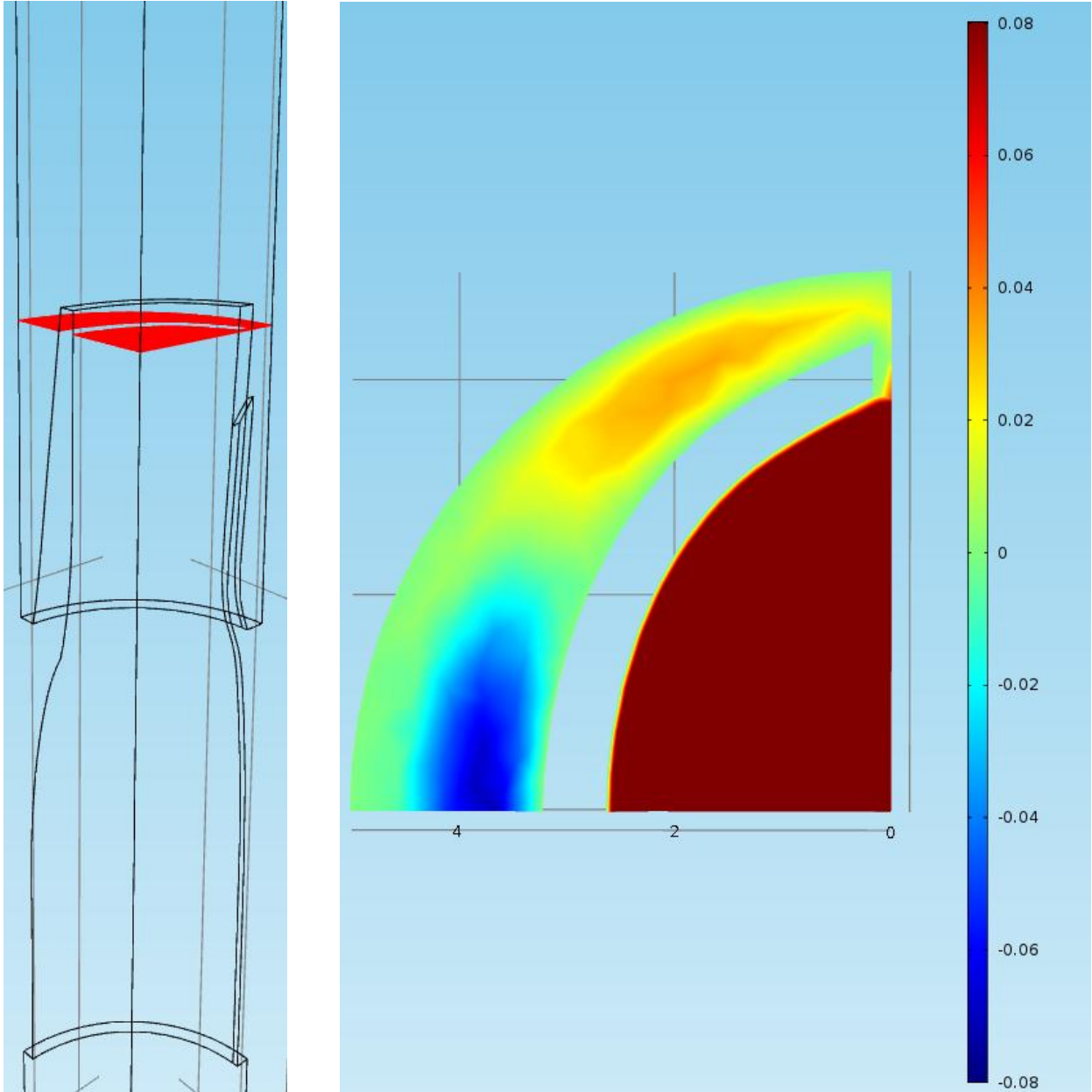


Figure 53: Wireframe view of fluid domain with a horizontal plane, marked in red, intersecting the domain 9 mm above the valve's shoulder (left). 2D contour plot of y velocity on this plane (right); reversed flow, indicated by shades of blue, is into the page.

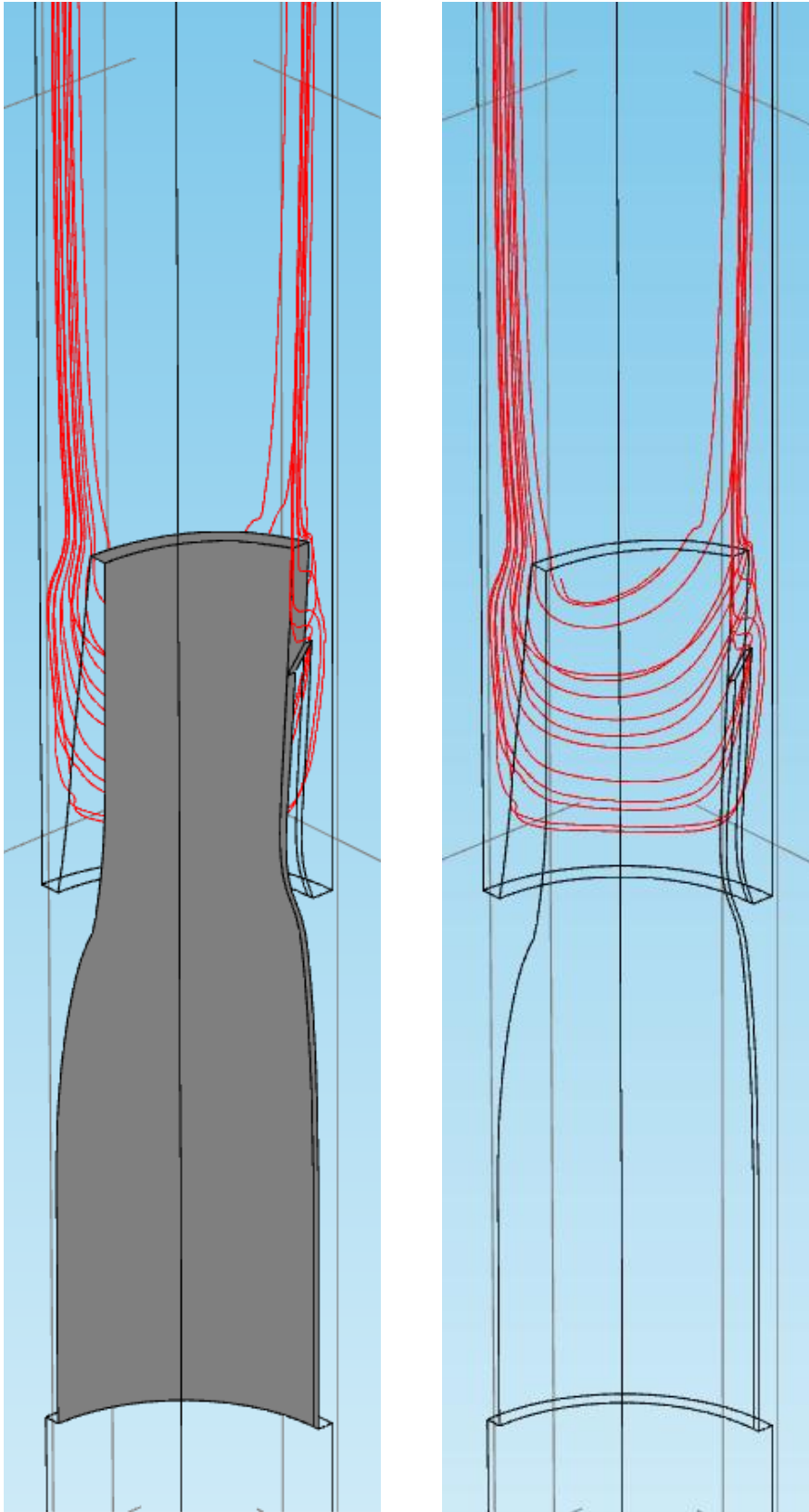


Figure 54: 3D plot of streamlines behind the valve's leaflets with (left) and without (right) the valve's internal orifice wall and leaflet slit shaded gray. Streamlines indicate that flow is circulating behind the leaflets.

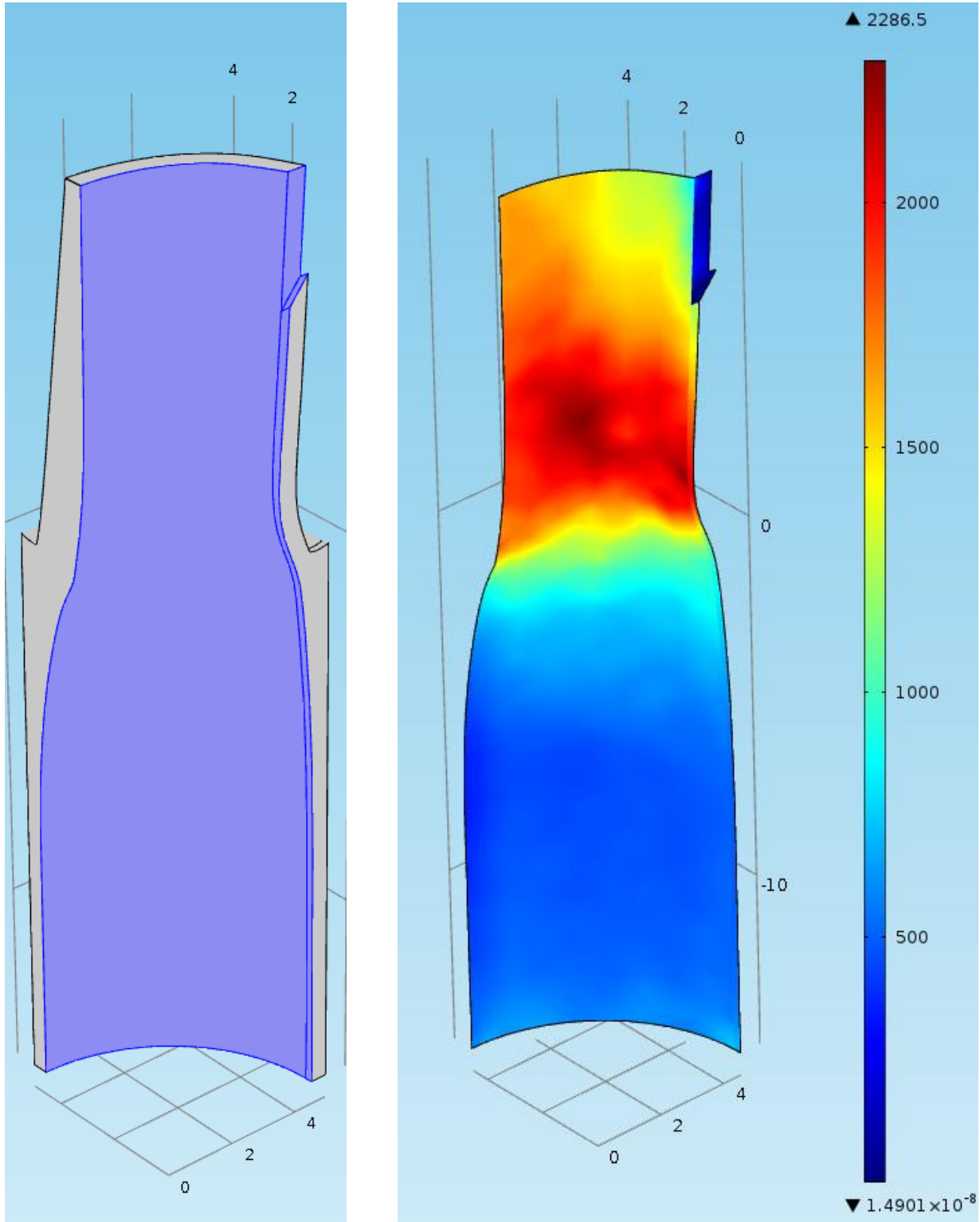


Figure 55: 3D view of deformed valve's geometry with the inner walls and leaflet slit highlighted in purple (left). 3D contour plot of shear rate on the valve's inner walls and leaflet slit (right).

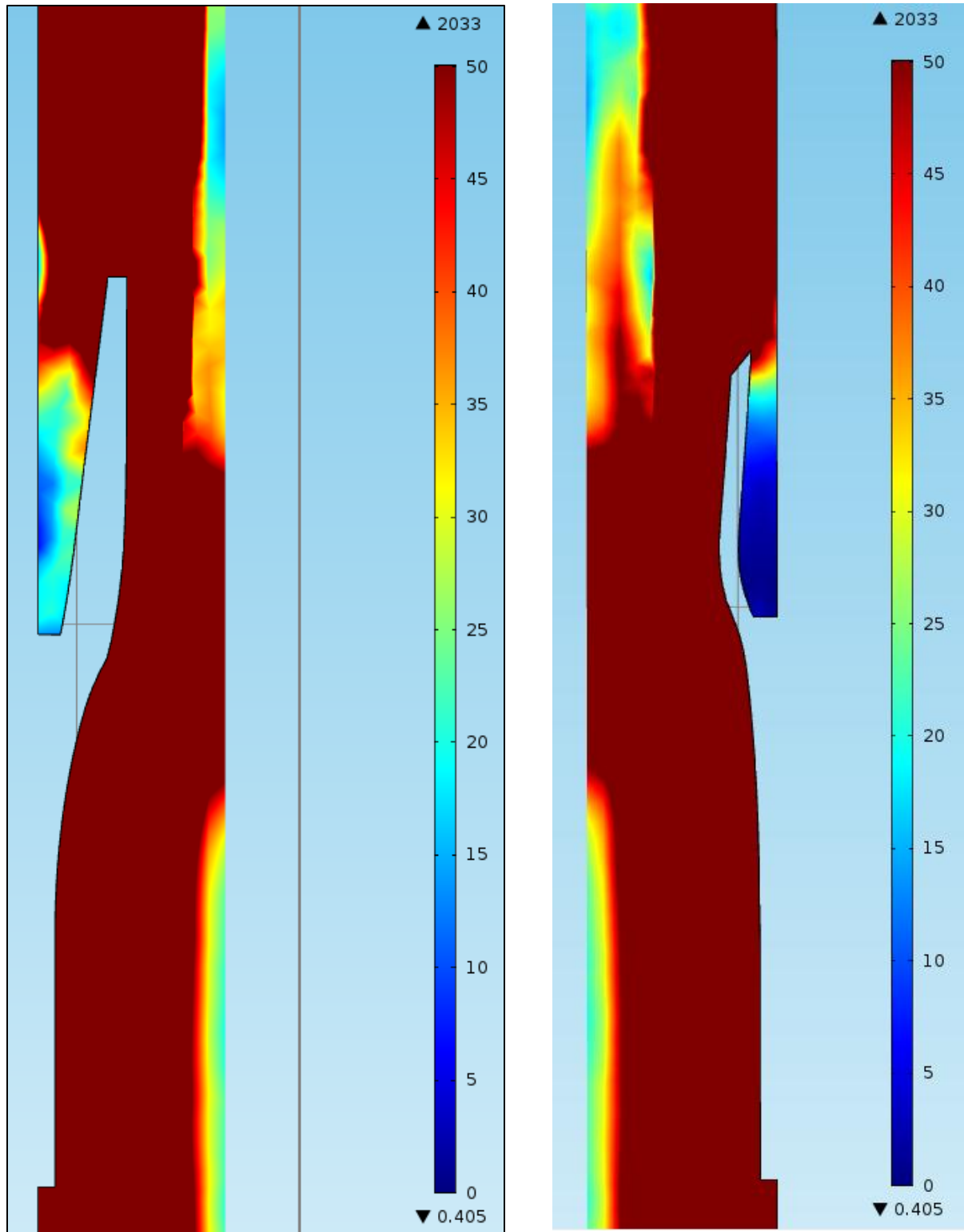


Figure 56: 2D contour plots of shear rate on the first (left) and second (right) planes of symmetry emphasizing regions of low shear. Shear rates higher than 50 s^{-1} are dark red.

CHAPTER 5: VERIFICATION TESTING

Preparation

PVA Tube Fabrication and Valve Fixation

15% PVA tubes, similar to those used by Sathe, were fabricated to simulate veins during the reflux flow rate, smallest competent diameter, distal pressure rise, and outflow resistance tests (see Figure 57) [141]. These tubes were 7mm long, 1mm thick and had 10 mm inner diameters. Like veins, these tubes distend under pressure and mimic the expansion seen in the sinus region of a native valve when the valve inside of them is closed [143].

The PVA tubes were created by injecting 15 wt% PVA in a mold made of two cylinders held concentric by two end caps (see Figure 57). The mold then underwent three thermo cycles in a -20 °C freezer and a 20 °C room for at least three hours at each temperature. The tubes were removed from the molds after they were done cycling.

Valves without stents were then placed inside PVA tubes and fixed with Loctite liquid super glue (Düsseldorf, Germany) to simulate a valve being fixed inside a vein. After the glue had dried, the tubes with valves joined inside were then placed in water in preparation for testing.

Glycerol Solution Preparation and Properties

A 40 wt% glycerol solution was prepared to mimic the viscosity of human blood. The viscosity of the glycerol solution was measured to be 0.00349 Pa-s by a viscometer. This is within 1% of the generally accepted Newtonian viscosity of blood, 0.00345 Pa-s [195]. The density of the solution was measured to be 1088 kg/m³ using a 100 micropipette and a scale. This

solution was used to enhance the accuracy of the reflux flow rate, smallest competent diameter, distal pressure rise, outflow resistance, and washout tests.

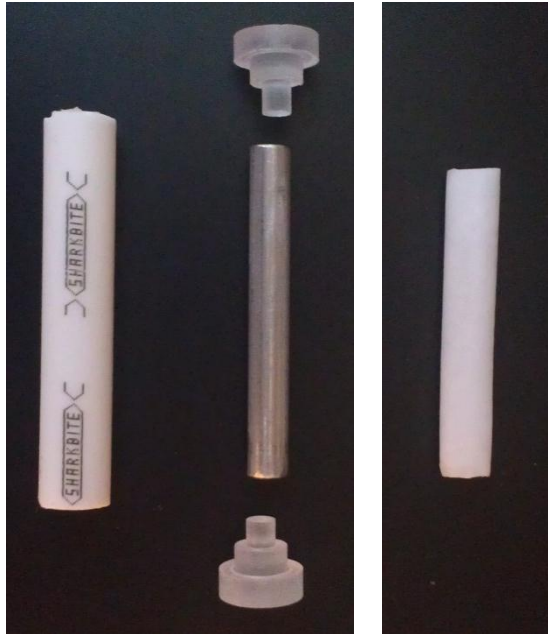


Figure 57: Mold components (left) used to fabricate PVA tubes (right).

Reflux Flow Rate

Methods

A test was developed to determine the average reflux rate of a prosthetic valve under 30 mmHg and 160 mmHg of retrograde pressure (see Figure 58). The proximal end of a PVA tube with a valve glued inside was tied to 9 mm inner diameter Tygon tubing. The tubing was connected to a reservoir filled with a 40% glycerol solution which was elevated 37 cm above the valve's shoulder to create a retrograde pressure gradient of 30 mmHg. When testing the Midha valve, it was discovered that the rate of pressure increase, caused by variations in the time taken to get the reservoir to its elevated position, influenced the valve's competency, with faster rates

raising the likelihood of leaflet prolapse. To decrease the variation of the pressure application rate, the distal end of the tube was manually squeezed closed after the reservoir was elevated. Entrapped air in the tube was then forced through the valve causing its leaflets to open. The tube was then released and the full pressure head was immediately applied to the leaflets.

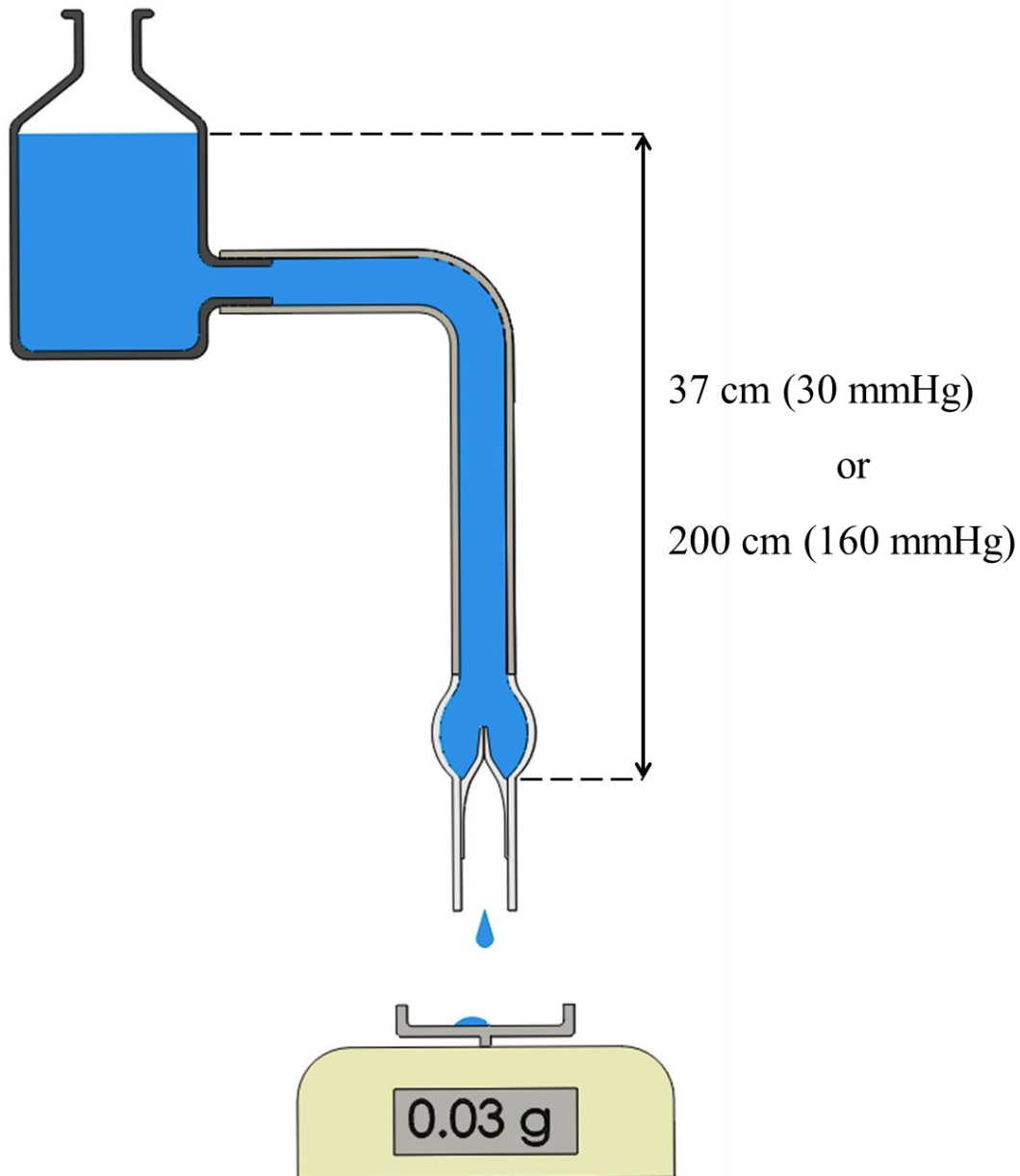


Figure 58: Schematic of reflux flow rate test. A column of glycerol induces a pressure to close the valve. The reflux flow rate is then measured using a scale and a stopwatch.

The average reflux flow rate of the valve over time was then measured using a scale and a stopwatch. The scale weighed the amount of reflux with a resolution of 0.01 g. The density of the glycerol solution was used to convert grams to mL with the following relation:

$$Volume = Mass * 0.92 \frac{mL}{g} \quad (7)$$

The volume calculated using Equation (7) was then divided by the amount of time taken to expel it to find the time average reflux flow rate. Each valve was tested five times to find the mean and standard deviation of its reflux flow rate. Each test lasted for at least 1 minute.

The reservoir was then elevated to 200 cm above the valve's shoulder to create a retrograde pressure gradient of 160 mmHg. The test was repeated as outlined previously, and the mean and standard deviation of the reflux flow rate were found for each valve at this higher pressure head.

Results

The average reflux rate for five valve prototypes was found to be 0.44 ± 0.26 and 0.30 ± 0.27 mL/min under 30 and 160 mmHg pressure heads respectively (see Table 10 and Figure 59). This corresponds to a 99.98-99.99% reduction in the average reflux flow rate compared to that without a valve. This suggests that the average reflux rate of the valve will be from 0.30 to 0.44 mL/min along the entire pressure range of 30-160 mmHg, meeting the design specification of less than 3 mL/min.

Neglen measured the median reflux flow rate of incompetent CFV, femoral, and popliteal venous segments to be 318, 162, and 131 mL/min respectively [32]. Thus the proposed

valve would reduce the reflux flow rate in a typical incompetent CFV, femoral, or popliteal vein segment by more than 99.63% [32].

Table 10: Measured time average reflux flow rates for five valve prototypes at 30 and 160 mmHg.

Time Average Reflux Flow Rate (mL/min) \pm stdev		
Valve	30 mmHg	160 mmHg
None	2390 \pm 70	3950 \pm 270
A	0.19 \pm 0.05	0.09 \pm 0.11
B	0.69 \pm 0.40	0.20 \pm 0.10
C	0.40 \pm 0.32	0.63 \pm 0.07
D	0.72 \pm 0.20	0.52 \pm 0.03
E	0.18 \pm 0.14	0.04 \pm 0.07
Average	0.44 \pm 0.26	0.30 \pm 0.27

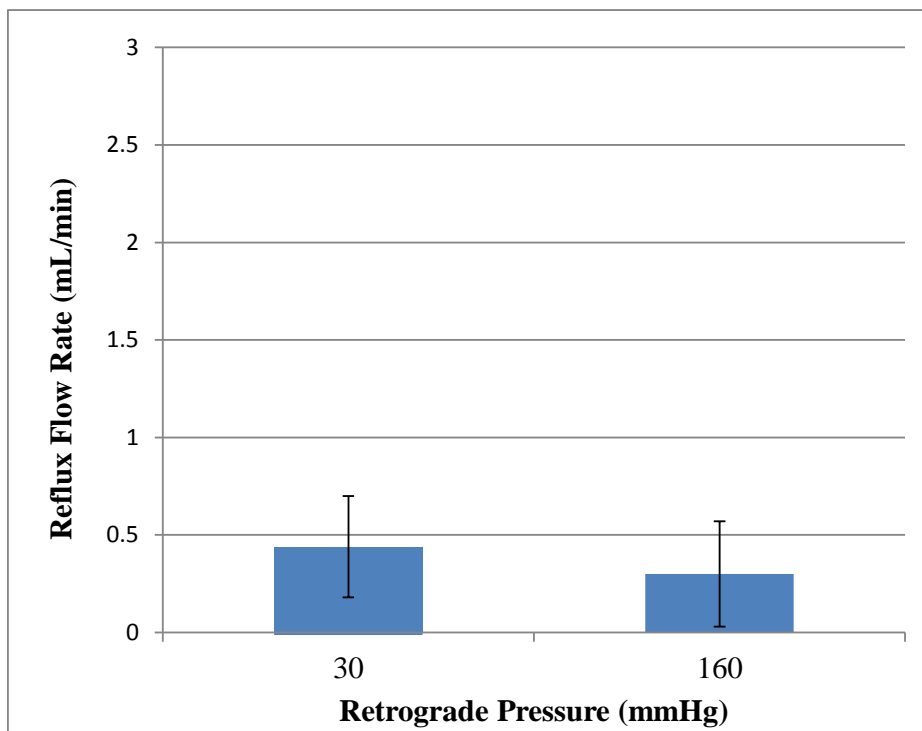


Figure 59: Average reflux flow rate for the proposed valve at low (30 mmHg) and high (160 mmHg) retrograde pressures. The valve meets the specification of having a reflux flow rate of less than 3 mL/min.

Smallest Competent Diameter

Methods

To determine the smallest diameter in which a valve can remain competent, a set of 25 mm long rigid tubes comprised of FullCure®720 were created using an Objet Eden250™ 3D printer (Stratasys Ltd., Edina, MN) with inner diameters ranging from 6.5 to 10.0 mm in increments of 0.5 mm. A rigid tube was placed around the leaflets of a valve glued inside a PVA tube. A 30 mmHg pressure head from the 40% glycerol solution was created using the same setup as the reflux flow rate test. A valve was deemed competent if its leaflets still closed in spite of the constriction of the rigid tube around them. If the valve was still competent, the rigid tube was removed and a smaller diameter replaced it. The largest diameter at which the valve leaflets did not close was recorded and the diameter 0.5 mm larger was assumed to be the smallest diameter in which a valve could remain competent.

Results

The leaflets of the valve did not close when constricted by the 7.5 mm rigid tube. This suggests that the smallest diameter in which the valve will remain competent is 8 mm. This meets the specification of being 8.5 mm or less.

Fatigue

Methods

A flow loop was created to cycle a valve open and closed (see Figure 60). A valve was placed on a connector having a 7 mm inner diameter and 9mm outer diameter at its most

constricted point (see Figure 61). The valve on the connector was then placed inside transparent tubing having an inner diameter of 10mm. This segment of tubing was then connected to the rest of the flow loop. The loop was then filled with water. A column of water 55 cm above the valve provided a 40 mmHg retrograde pressure to close the valve. A roller pump (Cobe 043605-000, Cardiovascular Inc., Avada, CO) caused flow through the inlet of the valve to open the leaflets at a specified frequency. The pump rollers only partially displaced the tubing, allowing retrograde flow to close the valve whenever the rollers were not inducing full forward flow. Any overflow out of the tube above the valve was channeled into a reservoir which had the same elevation as the valve. The reservoir then fed back into the roller pump.

While a venous valve is expected to cycle at approximately 0.67 Hz in an individual when walking, an accelerated fatigue test is desirable to reduce the time required to perform the test [143]. As increasing the cycling frequency of polymers can reduce their elastic modulus and lead to early cycle failure, two accelerated fatigue frequencies were used in this test, 3 Hz and 6 Hz [196].

The time average reflux flow rate of each valve at 30 and 160 mmHg was measured before and after undergoing 500,000 cycles. The protocol for the competency test was followed with the exception of having the valves secured inside transparent 10 mm inner diameter tubing with the connectors mentioned previously instead of PVA tubes. This change was made to allow the valves to be visually inspected during cycling to confirm that they were fully opening and closing.

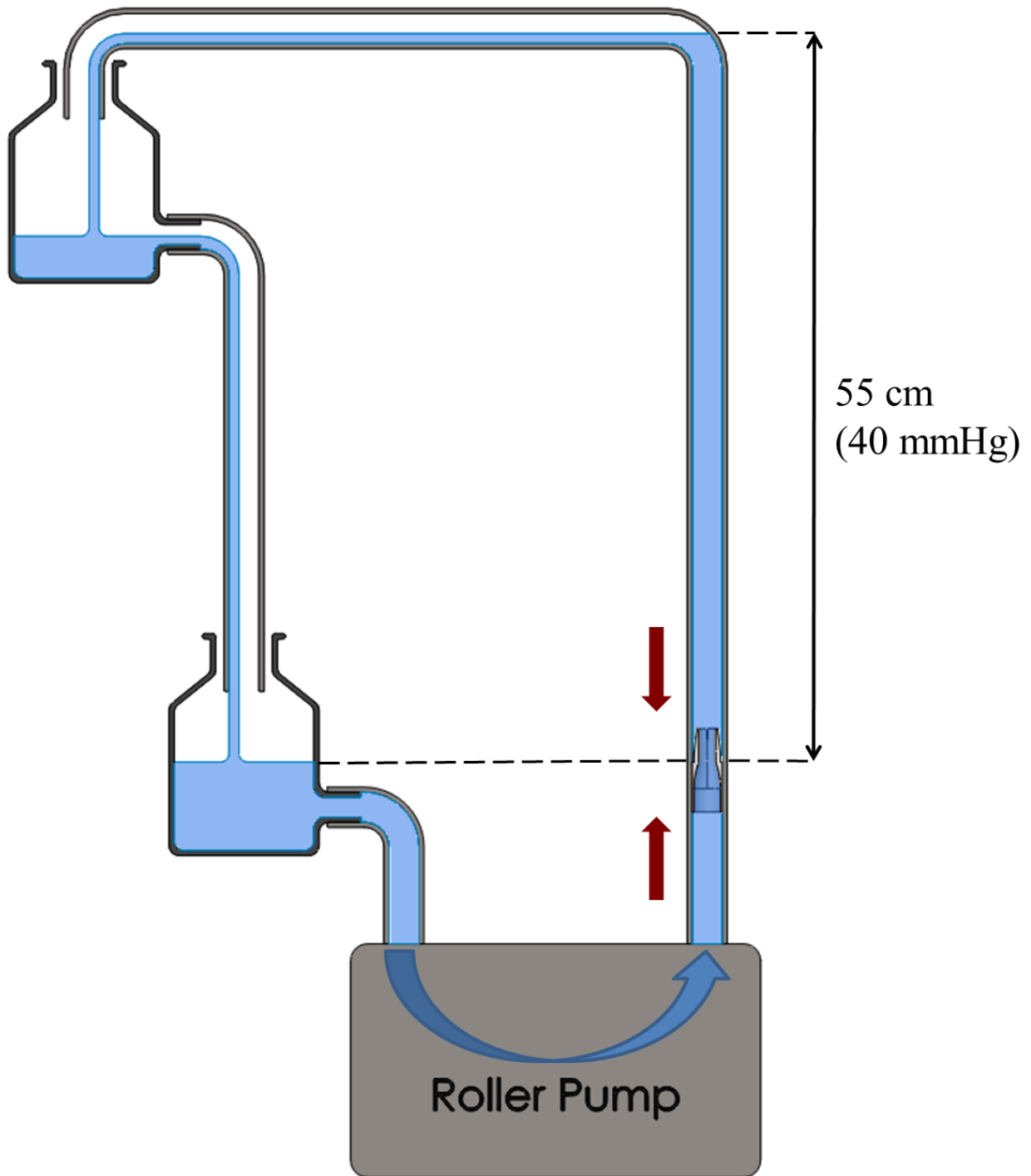


Figure 60: Schematic of fatigue test. Pulsatile flow is created by a column of water creating a 40 mmHg retrograde pressure head which closes the valve and a roller pump which induces forward flow to open the valve. The valve closes whenever the roller pump is not inducing full forward flow.

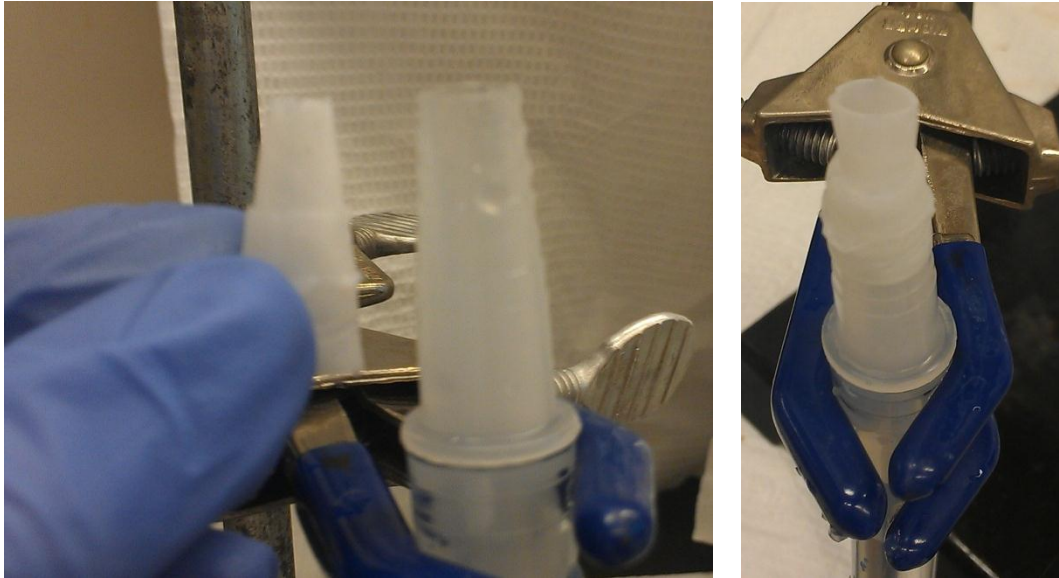


Figure 61: Prototype valve before (left) and after (right) being placed on a connector in preparation for fatigue cycling or washout test.

Results

Two valves without any visible defects were selected for the fatigue test. Their time average reflux flow rates at 30 and 160 mmHg were measured (see Table 11). The first valve was placed in the fatigue flow loop and cycled at 6 Hz for 500,000 cycles. After 500,000 cycles the valve was removed from the flow loop and inspected for defects. A crack had formed at the base of one leaflet slit which had propagated down the entire length of the leaflet (see Figure 62). Reflux testing of this valve revealed that it was no longer competent, having a reflux flow rate greater than 3 mL/min under 30 and 160 mmHg of retrograde pressure (see Table 11).

The cycling frequency was halved for the second valve, which was fatigued at 3 Hz for 500,000 cycles. After 500,000 cycles the valve was removed from the flow loop and no visible fatigue damage was present (see Figure 63). Reflux testing showed that this valve was still

competent, having a reflux flow rate less than 3 mL/min at 30 and 160 mmHg pressure heads (see Table 11).

The difference in outcome between the two valves is likely due to the difference in fatigue frequencies. Hysteretic heating from the elevated cycle speed of the valve fatigued at 6 Hz likely reduced the elastic modulus of the PVA and led it to fail at fewer cycles than if cycled at the rate of the valve in actual use, approximately 0.67 Hz [141, 196]. This also suggests that the valve that underwent accelerated fatigue testing at 3 Hz would have remained competent for more than 500,000 cycles if cycled at the rate of the valve in actual use. While it is encouraging that the valve cycled at 3 Hz remained competent after 500,000 cycles, more extensive fatigue testing is required to determine if this valve design will remain competent for the expected 9 million cycles in a patient.

Table 11: Time average reflux flow rates for valves before and after 500,000 cycles.

Valve (Cycle Speed)	Pressure	Time Average Reflux Flow Rate (mL/min) \pm stdev		Change (mL/min)
		0 Cycles	500,000 Cycles	
A (6 Hz)	30 mmHg	0.73 \pm 0.41	4.61 \pm 1.32	3.88
	160 mmHg	0.40 \pm 0.65	32.17 \pm 7.06	31.77
B (3 Hz)	30 mmHg	0.01 \pm 0.01	0.03 \pm 0.06	0.02
	160 mmHg	0.08 \pm 0.14	0.04 \pm 0.05	-0.04



Figure 62: Valve after undergoing 500,000 cycles at 6 Hz.



Figure 63: Valve before (left) and after (right) undergoing 500,000 cycles at 3 Hz.

Closing Time

Methods

To determine the average closing time of a valve, it was placed in a pulsatile flow loop and video recorded. The valve was constrained in the loop by a tubing connector placed inside of its base just below the shoulder. A column of water above the valve provided 40 mmHg of pressure to close it, as measured by a pressure transducer proximal to the valve's shoulder. A roller pump (Cobe 043605-000, Cardiovascular Inc., Avada, CO) induced forward flow which caused the valve to open at a rate of 3 Hz. A video recording was taken of the valve cycling open and closed at a speed of 30 frames per second, a resolution of 0.033 seconds per frame. The video recording was then reviewed frame by frame. The number of frames the valve took to close was recorded and converted into a closing time. The mean closing time for an individual valve was found by averaging the closing time for three different cycles. To meet the design requirement of closing in less than 0.5 seconds a valve would need to close in less than 15 frames.

Results

The average number of frames three valves took to close and the corresponding closure time are recorded in Table 12. Each valve took 2 frames for the leaflets to close which equates to a closing time of 0.067 seconds (see Figure 64). This suggests that the proposed valve design meets the design requirement of closing in less than 0.5 seconds.

Table 12: Valve closure time results for three valves.

Valve	Number of Frames to Valve Closure \pm stdev	Closing Time (s) \pm stdev
A	2 ± 0	0.067 ± 0
B	2 ± 0	0.067 ± 0
C	2 ± 0	0.067 ± 0
Average	2 ± 0	0.067 ± 0



Figure 64: Example of Frames used to determine valve closure time. Frame 0 (Left). Frame 2 (Right).

Distal Pressure Rise Test

Methods

A test was developed to determine the distal pressure rise of a prosthetic valve after a simulated calf flexion. Both ends of a PVA tube with a valve glued inside were tied to 9 mm inner diameter Tygon tubing (see Figure 65). A pressure transducer was located distal to the

valve. Reservoirs were connected to the Tygon tubing upstream and downstream of the valve. The reservoirs were filled with the 40 wt% glycerol solution and elevated 120 cm above the valve to create an equilibrium pressure of 95 mmHg, which is a typical venous equilibrium pressure near the calf [2]. The pressure transducer was calibrated to read 95 mmHg when the system was in equilibrium.

The ejection of blood out of the calf by contraction of the calf muscle was simulated by lowering the reservoir connected to the proximal end of the valve until the pressure transducer read 0 mmHg. This reservoir was then quickly raised back to its original height. The reading on the pressure transducer was recorded after 30 seconds. As the results of this test will be highly dependent on the diameter of the tubing used, the valve was tested in tubing slightly smaller than the femoral vein to determine the worst case scenario results.



Figure 65: View of valve and pressure transducer in the distal pressure rise test.

Results

The distal pressure rise test was performed with and without a valve present. 30 seconds after the simulated ankle flexion, the system without a valve present had returned to the equilibrium pressure of 95 mmHg. This showed that the system could mimic the quick rise in distal pressure seen in individuals with incompetent valves.

A valve was then tested in this system three times. The average distal pressure rise 30 seconds after the simulated ankle flexion was 7 ± 1 mmHg, which was approximately 7% of the equilibrium pressure, which satisfies the specification of rising 10% or less.

Outflow Resistance

Methods

A test was created to measure a valve's outflow resistance (see Figure 66). The distal end of a PVA tube with a valve glued inside was tied to 9 mm inner diameter tubing. The tubing was connected to a reservoir filled with 40% glycerol which was quickly elevated 19 cm above the valve's shoulder to create a forward pressure gradient of 15 mmHg. A stopwatch and a graduated cylinder were used to measure the average forward flow rate through the valve. The amount of fluid dispelled through the valve into the graduated cylinder was determined visually, as the 2 second response time of a scale was too slow to provide an accurate measurement.

The total outflow resistance was calculated by dividing the pressure gradient by the measured flow rate. This test was performed without a valve to determine the resistance inherent in the system. The resistance added by the valve was calculated by subtracting the resistance inherent in the system from the total outflow resistance.

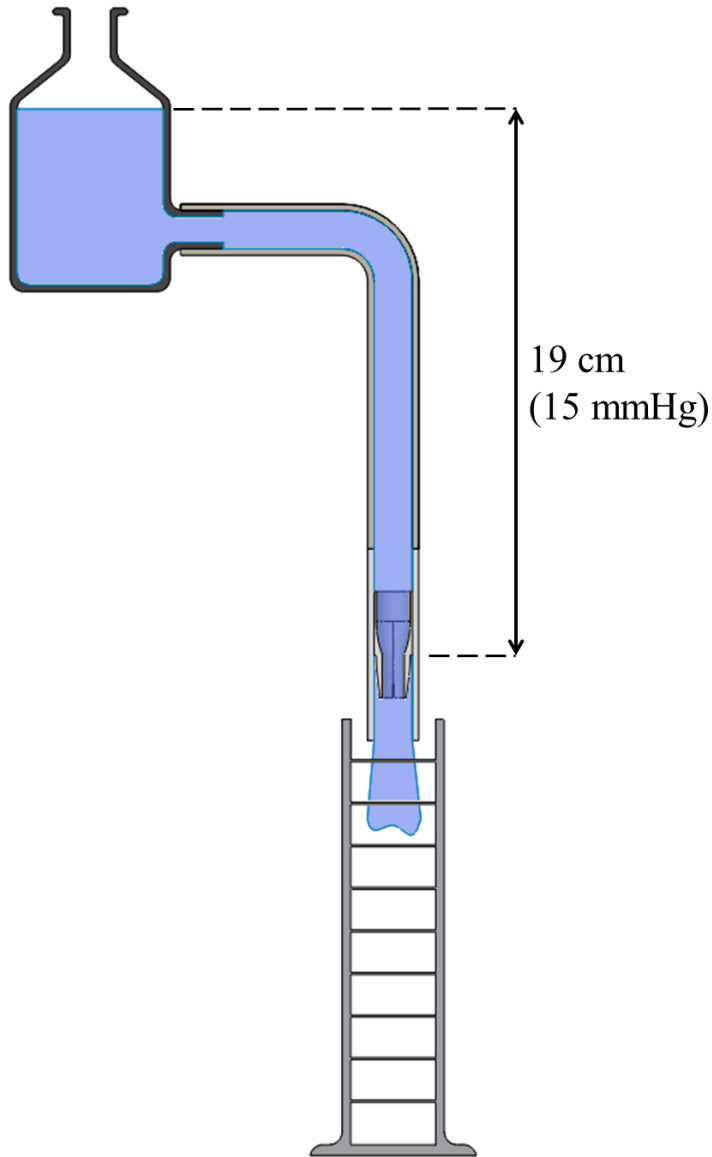


Figure 66: Schematic of outflow resistance test. A 15 mmHg pressure head is induced by a column of glycerol solution 19 cm above the valve's shoulder. Flow rate is measured visually using a graduated cylinder and a stopwatch.

Results

The measured flow rates, total outflow resistances, and resistance added by the valves were found for five individual valves and are shown in Table 13. The outflow resistance inherent in the system was 9.1 mmHg*min/L, which is similar to the resistance of a healthy vein at this pressure gradient, 10 mmHg*min/L [48]. The average resistance added by the valves was $2.3 \pm$

1.0 mmHg*min/L. This suggests that the valve will not significantly impede blood flow back to the heart and that it meets the design specification of increasing the outflow resistance by less than 5 mmHg*min/L (see Figure 67).

Table 13: Measured average flow rates, total outflow resistances, and resistance added by the valves results.

	Average Flow Rate (mL/min) ± stdev	Total Outflow Resistance (mmHg*min/L) ± stdev	Outflow Resistance Added by Valve (mmHg*min/L) ± stdev
No Valve	1651 ± 76	9.1 ± 0.42	NA
A	1161 ± 65	13.0 ± 0.7	3.9 ± 0.7
B	1426 ± 37	10.5 ± 0.3	1.4 ± 0.3
C	1417 ± 53	10.6 ± 0.4	1.5 ± 0.4
D	1333 ± 46	11.3 ± 0.4	2.2 ± 0.4
E	1281 ± 66	11.7 ± 0.6	2.6 ± 0.6
Average	1323 ± 109	11.4 ± 1.0	2.3 ± 1.0

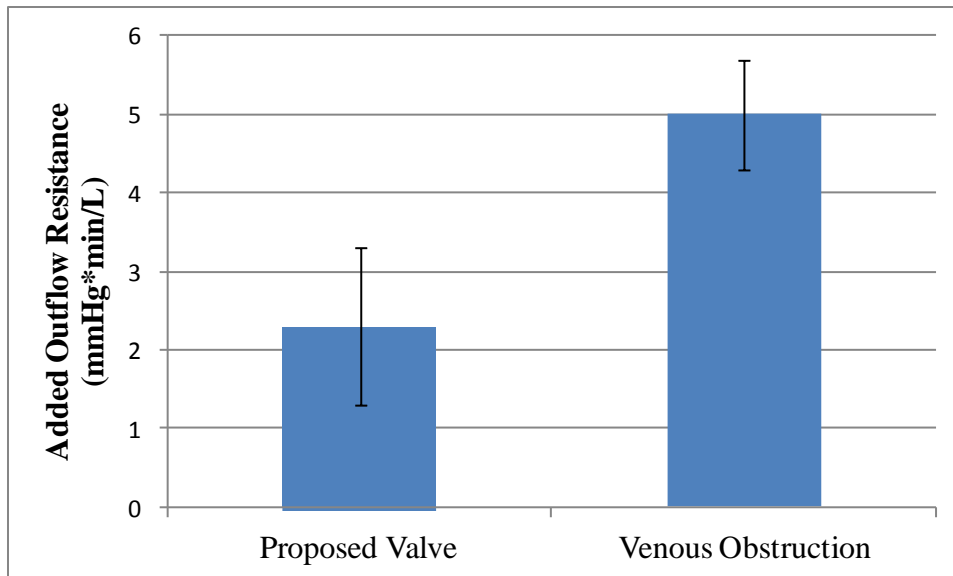


Figure 67: Comparison of outflow resistance added by the valve and venous obstruction Grade 1 at 15 mmHg (obstruction data from [48]).

Washout Test

Methods

A closed flow loop was created to determine if all of the fluid behind the valve's leaflets washes out under a flow rate of 400 mL/min (see Figure 68). A valve was placed on a connector and fixed inside a transparent tube with a 10 mm tube similar to the fatigue test (see Figure 61). This segment of tubing was then connected to the rest of the flow loop. The loop was then filled with a 40% glycerol solution. To visualize the flow of the fluid behind the valve's leaflets, a green hydrophilic dye, McCormick Green Food Color (McCormick & Company, Sparks, MD), was injected behind the valve's leaflets (see Figure 69). A roller pump (Cobe 043605-000, Cardiovascular Inc., Avada, CO) caused an average flow rate of 410 mL/min through the inlet of the valve. The pump rollers displaced the tubing enough to prevent any retrograde flow. The fluid then flowed into a closed reservoir, which fed back into the roller pump. If the dye is completely washed out from behind the leaflets then the valve is considered to have passed this test.

Results

The dye washed out from behind the leaflets in a few seconds when the roller pump was turned on (see Figure 69). This suggests that flow behind the valve leaflets will not become stagnant under the low flow rate encountered in the supine position.

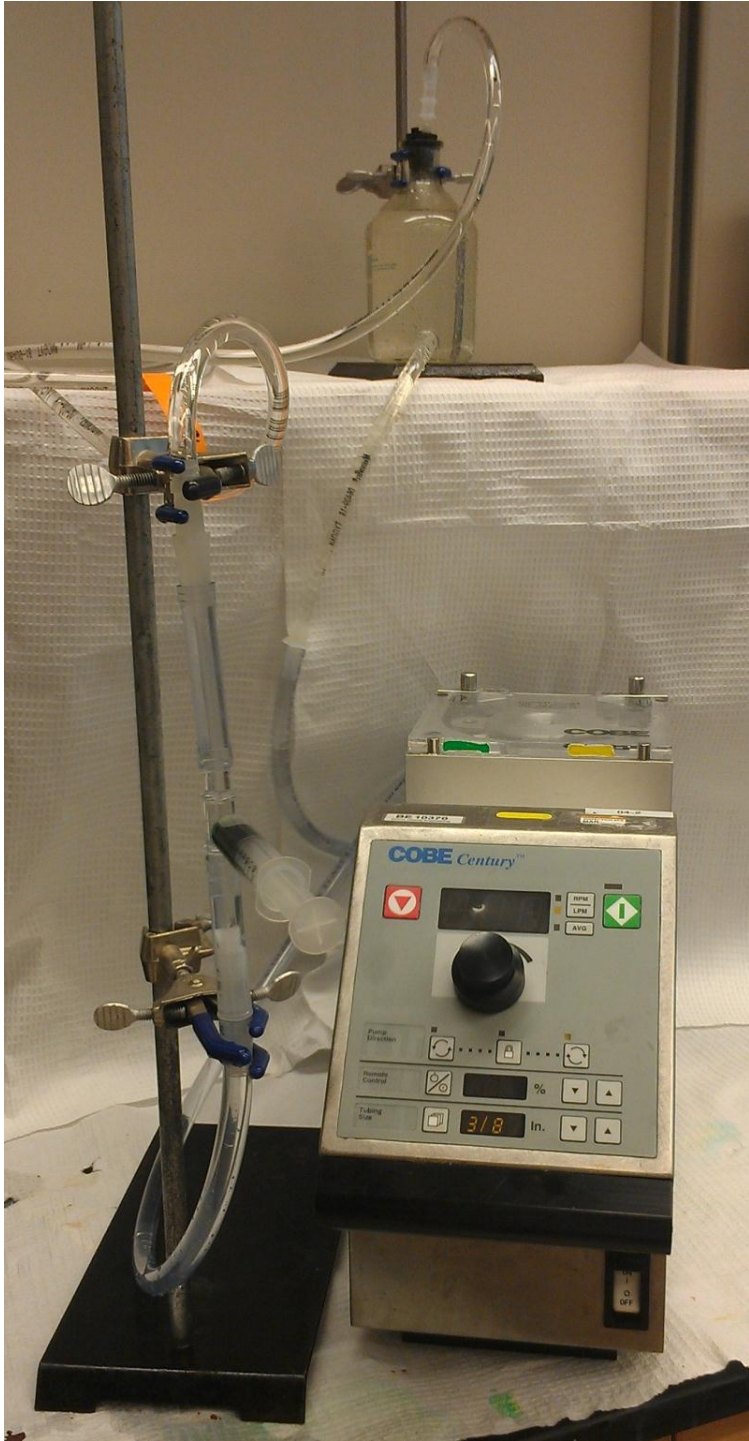


Figure 68: Flow loop used for the washout test.

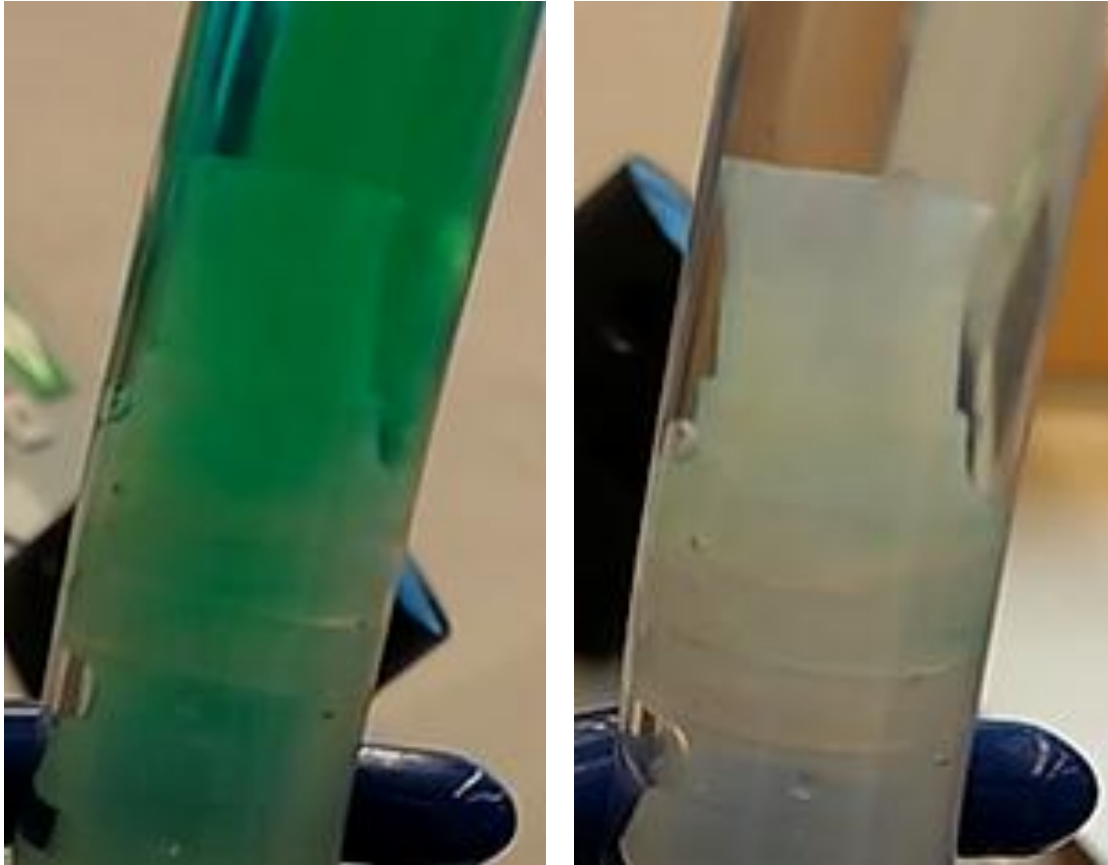


Figure 69: Green hydrophilic dye behind the leaflets (left) completely washes out under a forward flow rate of 400 mL/min (right).

Buckling Test

Methods

25 mm long rigid tubes comprised of FullCure®720 were created using an Objet Eden250™ 3D printer (Stratasys Ltd., Edina, MN) with inner diameters ranging from 6.5 to 10.0 mm in increments of 0.5 mm. These tubes were used to determine the smallest diameter a valve could be inserted into without radially buckling for a prototype valve without a stent. The valve was inserted into a tube using and then expanded with a 10 mm balloon. The balloon was then removed and the base of the valve was visually inspected for radial buckling. The largest

diameter at which the valve buckled was recorded and the diameter 0.5 mm larger was assumed to be the smallest diameter a valve could be in without buckling.

Result

A prototype valve without a stent was able to decrease in diameter from 9 to 7mm (22%) without radially buckling. 7mm was the smallest diameter the valve could be inserted into without buckling as it radially buckled in a 6.5 mm tube (see Figure 70). This is 1.5 mm smaller than the 8.5mm required by the specification. A 10 mm Midha valve was found to radially buckle in a 9.5 mm tube, so it would not have met this specification.

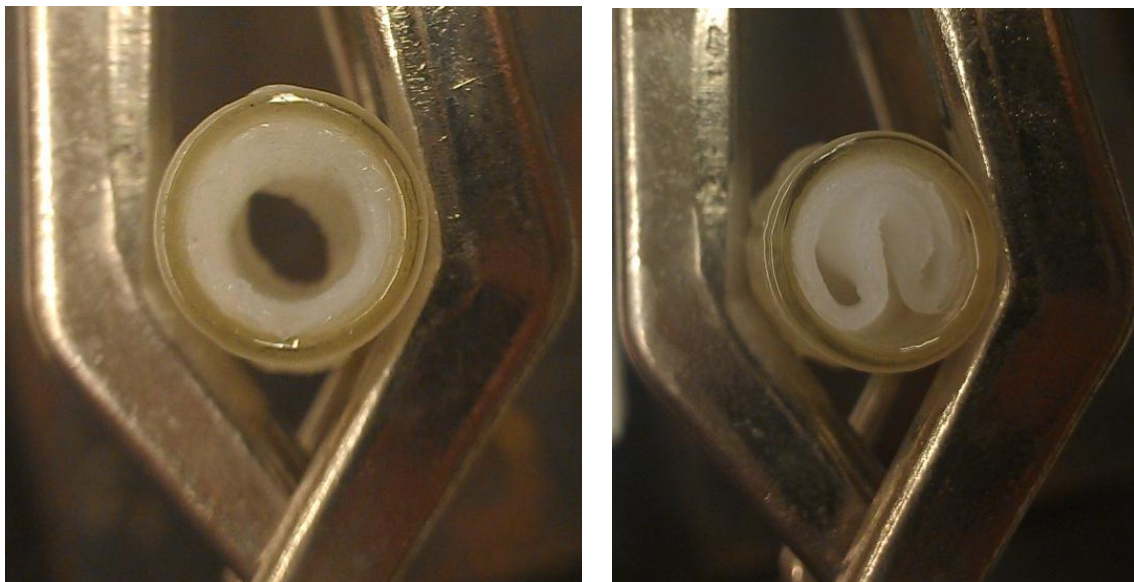


Figure 70: Valve inserted into a 7 mm inner diameter rigid tube does not radially buckle (left) but buckles in a 6.5 mm tube (right).

Blood Flow Loop Test

Methods

A blood flow loop similar to that used by Midha was erected (see Figure 71) [145]. A stented valve was placed inside a section of 10 mm inner diameter transparent tubing. A 10 mm balloon was inflated to expand the stent to fit the tubing. Clamps constrained this section of tubing to ensure that the valve was oriented horizontally. Whole porcine blood was heparinized (3.5 mL/L) and put into the flow loop. A roller pump (Cobe 043605-000, Cardiovascular Inc., Avada, CO) caused the blood to flow through the inlet of the valve at an average of 510 mL/min. The blood then dispensed into an open reservoir which fed into the roller pump. Blood flowed through the loop for three hours. At this point the section of tubing containing the valve was removed and inspected for clots. The cessation of flow from the tubing into the reservoir would indicate that a clot had formed in the flow loop and would signal that the test should be stopped prematurely.

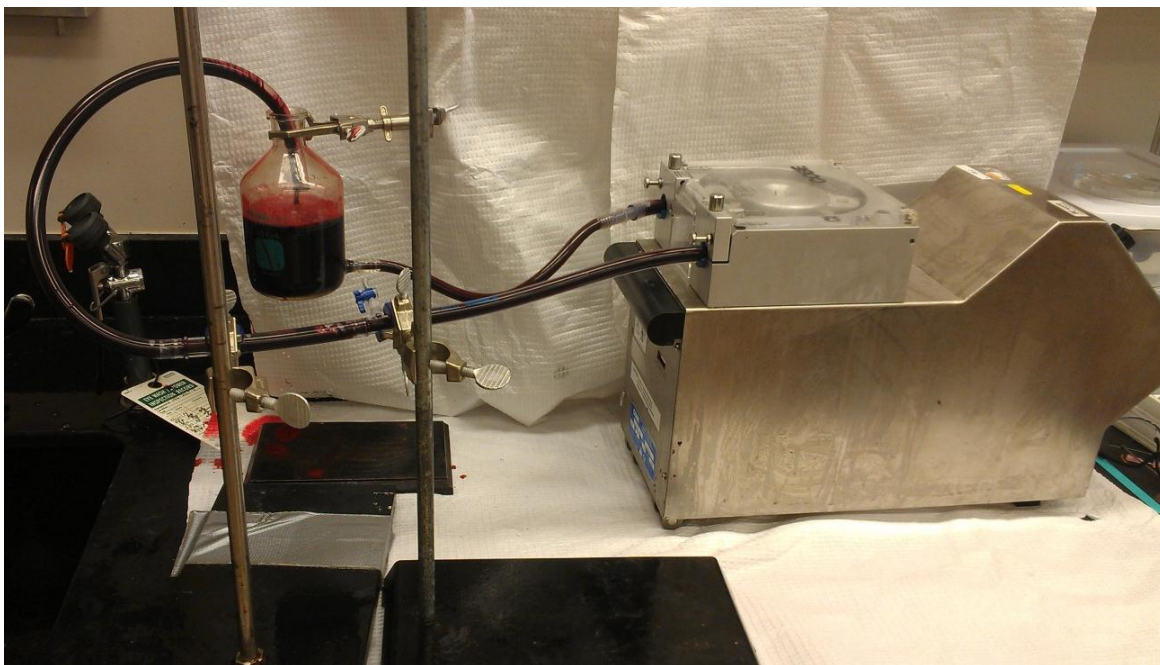


Figure 71: Blood flow loop.

Results

A stented valve was placed in the blood flow loop for three hours. The section of tubing containing the valve was removed and lightly rinsed with water to drain it of blood. No clots were present inside the valve (see Figure 72) or behind its leaflets (see Figure 73). Small clots were beginning to form around the tubing connectors, demonstrating that clot formation was possible in this system with the porcine blood used. This test demonstrated the short term patency of the proposed valve to be at least equivalent to the Midha valve and meets the design specification.

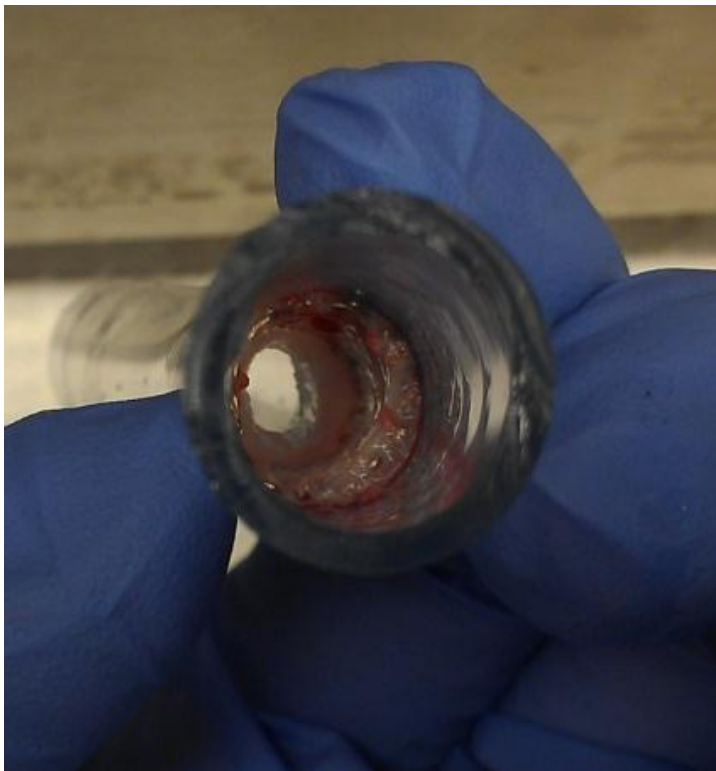


Figure 72: View valve's inlet after being in the blood flow loop for three hours.



Figure 73: Outside view of valve after being in the blood flow loop for three hours.

Deliverability

Methods

The minimum catheter size a valve can fit in can be estimated as follows. If a prosthetic valve is crimped and perfectly fits into a cylindrical catheter without any gaps or lengthening of the valve, the volume of the valve in terms of its crimped radius and length would be:

$$V = \pi r^2 L \quad (8)$$

Where V is the volume of the valve in mm^3 , r is the crimped radius of the valve, and L is the length of the valve. The relationship between French size and the internal radius of a catheter in mm is:

$$F = 3 * (2r) \quad (9)$$

Where F is the French size of the catheter and r is the radius of a catheter in mm.

Equation (9) can be manipulated to find the radius in terms of French gauges:

$$r = \frac{F}{6} \quad (10)$$

As the radius of the catheter is the same as the crimped radius of the valve, Equation (10) can be substituted into Equation (8) to obtain:

$$V = \pi \left(\frac{F}{6}\right)^2 L \quad (11)$$

Equation (11) can be rearranged to find the French size in terms of the volume and length of the valve:

$$F = 6 \sqrt{\frac{V}{\pi L}} \quad (12)$$

Equation (12) can be used to estimate the minimum French size of a catheter that a valve can be placed into. As the direct calculation will likely include a fractional part, a more realistic estimate will be the result rounded up to the next whole number.

To verify that the valve meets the specification of fitting inside of a 16 Fr (5.3 mm) catheter, a 25 mm long rigid tube made of FullCure®720 was created using an Objet Eden250™ 3D printer (Stratasys Ltd., Edina, MN) with an inner diameter of 5.3 mm. A valve could then be placed inside this tube to verify that it can fit inside a 16 Fr catheter.

Results

The CAD model of the proposed valve was analyzed and its volume and length were found to be 438 mm^3 and 25 mm respectively. The minimum French size the valve could fit into was calculated using Equation (12) to be 14.2, making 15 Fr its actual estimate when rounded up to the next whole number. A prototype valve was placed inside the 16 Fr tube to verify that it meets the specification (see Figure 74).



Figure 74: 10mm valve placed in 16 Fr (5.3 mm) inner diameter tube.

Summary

Table 14 summarizes the design specifications and the results of the verification testing that was performed. The proposed valve met every design requirement for which verification testing was performed.

Table 14: Summary of design specifications and verification testing results for the proposed venous valve.

	Metric	Units	Specification	Valve Performance*
1	Reflux rate under a 30 mmHg pressure head	mL/min	≤ 8	0.44 ± 0.26
2	Reflux rate under a 160 mmHg pressure head	mL/min	≤ 8	0.30 ± 0.27
3	Smallest diameter in which the valve remains competent	mm	≤ 8.5	8^{Ψ}
4	Reflux rate under a 30 mmHg pressure head after 500,000 cycles	mL/min	≤ 8	$0.03 \pm 0.06^{\Psi}$
5	Reflux rate under a 160 mmHg pressure head after 500,000 cycles	mL/min	≤ 8	$0.04 \pm 0.05^{\Psi}$
6	Leaflet closing time	s	< 0.5	0.067 ± 0
7	Distal pressure rise 30 seconds after a simulated calf flexion	%	≤ 10	7 ± 1
8	Outflow resistance added by the valve under a 15 mmHg pressure head	mmHg*min/L	< 5	2.3 ± 1.0
9	Fluid behind leaflets washes out under 400 mL/min	Binary	1	1^{Ψ}
10	Smallest diameter in which a valve does not buckle	mm	≤ 8.5	6.5^{Ψ}
11	Maximum shear rate on the valve walls with an inlet flow rate of 1600 mL/min	s^{-1}	< 3500	2300
12	Material does not elicit inflammatory response or foreign body reaction when placed in the bloodstream	Binary	1	1
13	Material passes biocompatibility tests specified by ISO and USFDA	Binary	1	1
14	Material is less thrombogenic than Dacron	Binary	1	1
15	Time to occlusion when running heparinized (3.5 mL/L) porcine blood in a flow loop	Hours	> 3	$> 3^{\Psi}$
16	Minimum catheter size the valve can fit in	Fr	≤ 16	16
17	Ratio of the valve length that contacts the vein wall to the vein diameter	NA	≥ 1.5	1.5

* Mean \pm Standard Deviation

Ψ N=1

CHAPTER 6: PROPOSED VALIDATION TESTING AND SIZING

Purposes

While verification testing confirmed that the proposed valve met all the design specifications for an effective prosthetic venous valve, validation testing is needed to confirm that the valve meets the needs of the user with its intended use [197].

Animal Testing

The long term safety, patency, and relative thrombogenicity of a proposed valve in a human can be inferred by testing it in an animal model. Replacement venous valves have historically been tested in sheep, pigs, dogs, and goats with complications, if occurring, such as valve migration, thrombus formation, neointimal hyperplasia, fibrous encapsulation, and inflammation developing within 12 weeks [12, 94, 107-110, 115, 117, 118, 121, 125, 127-129, 134, 145]. In animal studies longer than 12 weeks, complications did not develop or worsen after 12 weeks [115, 127, 131].

The ovine external jugular vein (EJV) is a potential site of implantation to test the proposed valve. This vein has an average diameter of 12.0 with a standard deviation of 1.4 mm, which is comparable to the average size of the human femoral vein, 11.84 mm [115, 151]. Valves are naturally present in the sheep EJV and close to prevent peripheral venous hypertension when hydrostatic or central venous pressure increases [198]. Thus a prosthetic venous valve placed in this location is expected to periodically cycle, such as when the sheep drops its head below its heart while eating.

Proposed Methods (Animal Study)

A study was designed to evaluate the patency, fixation, and biocompatibility of the proposed prosthetic venous valve in the external jugular veins (EJV) of sheep. In studies where replacement valves remained patent for 12 weeks, 9-16 sheep were used [121, 131]. For this study to be comparable to these studies, 12 sheep may be used to account for potential biologic variance.

Each sheep will have two valves surgically implanted, one in each EJV. Each sheep will be anesthetized prior to surgery. To implant the valves, approximately 2 inches of each EJV will be exposed by a longitudinal incision. A stented valve will be inserted into each vein through a small venotomy and expanded by a balloon until fixed in position. Each venotomy and longitudinal incision will be closed with sutures. Each sheep will then recover from the anesthesia and be given local analgesics to minimize pain and discomfort.

To decrease the risk of thrombosis during and after surgery, the following regiment of anticoagulation will be given to each sheep. During manufacturing valves will be impregnated with less than 5 mL of 3.2% sodium citrate which will be slowly expelled after implantation. During surgery, each sheep will receive 100 U/kg of heparin. After surgery, 325 mg of buffered aspirin will be daily administered to each sheep.

Valve patency and position, and biocompatibility will be the primary endpoints of the study. The study will last for a maximum of 12 weeks. The position of and flow through each valve will be evaluated every two weeks by venogram, as described by Midha [145]. The sheep will be anesthetized during each venogram. Sheep will be euthanized after 12 weeks or when both of its implanted valves are no longer patent. The valve will be deemed biocompatible if inflammation or fibrin encapsulation does not occur. Each sheep will be observed daily for any

signs of discomfort or abnormal behavior. If a sheep loses more than 20% of its baseline weight prior to surgery it will be euthanized to prevent unnecessary distress.

After a sheep is sacrificed, the vein segments containing the implanted valves will be removed. Each segment will be gently washed with saline to decrease the risk of post-mortem clotting and placed in formalin for preservation. The valves will be examined by gross sectioning and histology performed as described by Midha [145].

Protocol 2002062-102415BA, which details the above procedures, was approved by the Institutional Animal Care and Use Committee of Emory University on October 24, 2012.

Human Testing

If the proposed valve meets the primary endpoints of animal testing, the valve will then be ready for human testing. The following describes the recommended protocol to implant and evaluate the valve in human subjects.

Location

Minimum Distance Between Valves

The minimum distance between two prosthetic valves placed in the same vein segment will be determined by the minimum pressure needed to close an individual valve. The proposed valve will flutter open and closed when a low level of backpressure is applied, resulting in a pulsing sensation. As flow pulsation in the saphenous vein has been correlated with increased symptom severity in individuals with CVI, leaflet fluttering should be avoided [199].

The average minimum closing pressure of the proposed valve was found by visually measuring the minimum height of water needed to close the valve and calculating the applied hydrostatic pressure. Three valves each underwent this procedure three times and the mean and standard deviation for the minimum water height and corresponding hydrostatic pressure required to close each valve is shown in Table 15. The mean minimum closing pressure for three valves was approximately 10 mmHg, which would occur under a column of blood (density = 1056 kg/m³) 13 cm high [193]. This suggests that valves of this design should be implanted at least 13 cm apart.

Table 15: Experimental results of the minimum height of water required to close a valve. The applied hydrostatic pressure and the height of blood needed to cause this pressure (equivalent to the minimum distance between valves in a vein) were calculated.

Valve	Minimum Water Height Needed to Close the Valve (cm) (mean ± stdev)	Hydrostatic Pressure (mmHg) (mean ± stdev)	Minimum Distance Between Valves in a vein (cm)
A	13.7 ± 0.6	10.1 ± 0.4	13 ± 1
B	13.3 ± 0.6	9.8 ± 0.4	13 ± 1
C	13.3 ± 0.6	9.8 ± 0.4	13 ± 1
Average	13.4	9.9	13

Potential Vein Segments and Implantation Sites

Labropoulos recorded the number of refluxing segments in the deep veins for 94 patients with venous ulcers (see Table 16) [42]. Reflux in the Popliteal vein accounted for the largest percentage of refluxing segments (42%), followed by the CFV (29%), calf veins (17%), and the femoral vein (12%). The deep veins in the calf are approximately 2-3 mm in diameter and are much smaller than the other deep veins which are roughly 9-14 mm in diameter [200]. To reduce

the number of different valve sizes to be produced and keep manufacturing costs low, the CFV, femoral, and popliteal veins will be the sites of implantation for the proposed valve. Valves that fit in these three veins will be able to correct 83% of the refluxing deep venous segments for individuals with venous ulcers.

Table 16: Occurrence of reflux in deep vein segments in ulcerated limbs (data from [42]).

Vein	Number of Refluxing Segments	Percent
CFV	26	29
Femoral	11	12
Popliteal	37	42
Calf Veins	15	17

In the surgical correction of deep venous valves, usually only one incompetent valve is corrected with sites of repair being the most proximal valve in the CFV, femoral, or popliteal vein [43, 98, 99, 201-204]. While the majority of valve repairs have been in the CFV, surgical correction of the popliteal vein is becoming more popular among surgeons [154]. However, Tripathi found a statistically significant increase in ulcer healing rate when the surgical correction of deep venous valves was performed in multiple venous segments compared to singular valve repair, irrespective of the site of valve repair (see Table 17) [45]. This suggests that reflux should be corrected in each refluxing vein segment to achieve the greatest symptom improvement. However, it may be prudent to implant valves only in the CFV in the initial clinical trial to avoid the development of significant complications in the event of valve occlusion. If validation testing shows that the proposed valve is unlikely to clot in the CFV, valves may also be placed in incompetent femoral and popliteal veins.

Table 17: Comparison of ulcer healing rates for the surgical correction of single and multiple deep venous valves with primary and secondary incompetence (data from [45]).

Incompetence Type	% Ulcer Healing		Difference
	Single valve repaired	Valves repaired in 2-3 incompetent venous segments	
Primary	57	72.9	15.9
Secondary	46	54.7	8.7

A functioning valve in the most proximal end of an incompetent vein would likely restore competence to a greater portion of the vein than when placed in a more distal location. Native valves are typically located 0.5-2 cm distal to junctions with other veins and periodically in between (see Figure 75) [205]. Assuming validation testing shows that the proposed valve is unlikely to clot in the CFV, it is suggested that the replacement valve be placed 0.5-2 cm below the most proximal end of each refluxing CFV, femoral, and popliteal vein (see Figure 75). After the initial valve is placed, Doppler ultrasound may be used to determine if additional valves need to be implanted distal to the initial valve. When reflux greater than 3 mL/min is present during a Valsalva maneuver, additional valves may be placed between vein junctions within the same vein segment with a minimum of 13 mm between valves to ensure that these additional valves can close. Prior to implantation, a specific implantation site for the most proximal valve in each incompetent vein segment should be determined by venogram or ultrasound.

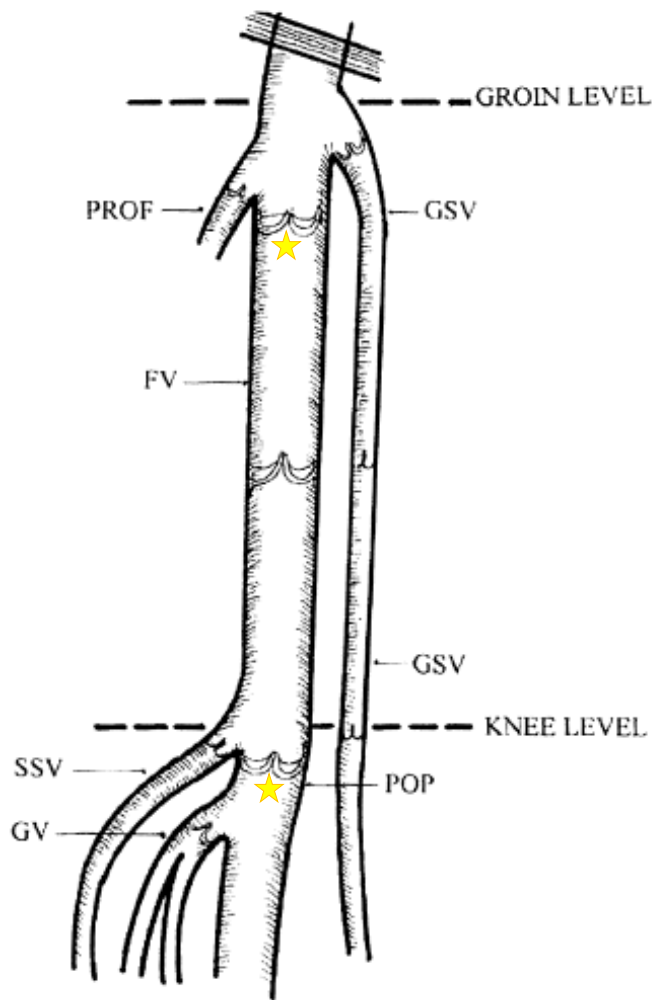


Figure 75: Schematic of deep vein junctions between the groin and below the knee (image from [32]) Stars indicate the proposed locations of the prosthetic valve to be implanted in the femoral and popliteal veins.

Proposed Methods (Human Study)

Sample Size

As the data to be analyzed is paired and will not be normal, the Wilcoxon signed-rank statistic for paired data may be used to determine statistical significance compared to baseline values [206, 207]. This statistic is commonly used to determine significance in VCS scores and hemodynamic parameters [38, 52].

G*Power was used to determine the sample size with the following inputs [208, 209]: The significance level, also referred to as the type 1 error alpha, was set to 0.05. As the VCS score changes in discrete increments of 1, the effect size to be discerned in the test was set to 1. The desired power of the test is 0.95. With the aforementioned criteria, the suggested sample size is 15 subjects. As there is a risk of losing contact with some subjects, the actual number of subjects recruited for the study may be more than 15 to ensure that enough subjects remain in contact for statistical significance to be determined.

Inclusion Criteria

Subjects selected for the study will have a severe case of CVI that is resistant to conservative treatment, specifically compression stockings, with a VCS score of 7 or higher. Each will have the presence of deep venous reflux, with reflux lasting more than 2 seconds in the CFV and have a VFI 10 mL/s or greater.

Exclusion Criteria

Potential subjects will be excluded based on the following criteria: The presence of venous obstruction of any grade level, as manifested by an outflow resistance 15 mmHg*min/L or greater, as venous stenting would be a more appropriate procedure [48]. Occurrence of thrombosis in the last 24 months, as this would increase the likelihood of thrombosis occurring in the valve clotting. Individuals with the presence of another disease requiring treatment such as diabetes or another cardiovascular disease. Individuals with a high risk of developing complications from heparin or aspirin.

Implantation

Prior to implantation, subjects will have their VCS score, VFI, AVP, EF, and outflow resistance measured. Prior to the procedure, the diameter of the CFV where the valve will be implanted may be measured using Doppler ultrasound. The guidelines found in Chapter 6 of this manuscript regarding valve sizing will be followed to determine the size of valves to be implanted. Patients will be given local anesthesia and 5000 units of heparin in preparation for the procedure [88]. Guided by ultrasound, a valve may be percutaneously delivered by catheter 0.5-2 cm below the most proximal end of the CFV and expanded with a balloon. Additional valves may be implanted in the CFV at least 13 cm apart, to ensure that valves will be able to close, at locations where Doppler ultrasound reveals reflux to exceed 3 mL/min when patients perform a Valsalva maneuver. Patients will take 81 mg of Aspirin daily indefinitely after implantation to reduce the risk of thrombus formation [88].

Endpoints

Primary endpoints to evaluate the safety and functionality of the proposed valve after being implanted in a human are as follows:

- Valve patency, which may be determined by Doppler ultrasound in the supine position. A few prosthetic venous valves implanted into humans have been reported, with most failing to demonstrate long term competency and patency [110, 116, 124, 126]. Of these valves, the longest reported to remain competent and patent was 16 months, which serves as a benchmark for other prosthetic venous valves [126].
- Valve competency, which may be determined by Doppler ultrasound during a Valsalva maneuver with the subject in the 15° reverse Trendelenburg position. Valves taking

longer than 0.5 seconds to close are typically deemed incompetent in clinical practice, thus the valve will be deemed competent if it closes in less than 0.5 seconds [30-34]. The benchmark for competency is 16 months [126].

- Valve position, as determined by ultrasound. A valve that is not fixed in position after implantation has the risk of migrating to the lungs.
- Valve biocompatibility, as determined by the absence of inflammation or fibrin encapsulation.

Secondary endpoints to evaluate the valve's impact on a subject's symptoms and vein hemodynamics, and to allow comparison to other treatments of CVI are as follows:

- VCS score, which will quantify the change in severity of a subject's symptoms and allow comparison with other treatments for CVI. For example, Cesarone reported the average VCS score in 31 individuals with CVI to decrease from 8.4 to 5.7 after eight weeks when treated with compression therapy [61]. As VCS scores are discrete, the proposed valve would be as effective for treating CVI as compression stockings if the average VCS score in the proposed human study is 6 or less after 8 weeks.
- AVP, which may be determined by needle in the dorsal foot vein during tiptoe exercises with the methods used by Nicolaides [18]. This will quantify any changes in a subject's venous hypertension, which is the primary characteristic of individuals with CVI.
- VFI, which may be measured by PG with the methods used by Araki [36]. This will quantify the effectiveness of the proposed valve to reduce venous reflux.
- EF, which may be determined by PG with the methods used by Araki [36]. This will determine if the valve influences the effectiveness of the calf muscle pump, which is one of the main contributing factors to venous hypertension in CVI.

- Outflow resistance, which may be determined by PG and a needle in the dorsal foot vein with the methods used by Neglen [48]. This will detect if an outflow obstruction, another contributor to the venous hypertension seen in individuals with CVI, has developed in a subject. An outflow resistance above 15 mmHg*min/L would indicate that something, such as the valve or DVT, has obstructed venous outflow and that additional corrective procedures, such as venous stenting, may need to be proscribed.

Primary and secondary endpoints will be measured at baseline, 8 weeks, as well as 6, 12, and 18 months after implantation.

Valve Sizing

Determining Vein Diameter for Sizing

To determine the range of vein sizes in which the proposed valve can fit, a baseline reference for the vein diameter must first be defined because veins are distensible. Sizing the valve in terms of a vein's fully distended diameter is advantageous so that fixation by stent expansion can be ensured. In this chapter, D^* will refer to the fully distended diameter of the vein.

Minimum Vein Diameter

The smallest diameter in which a valve can remain competent will determine the minimum diameter, D_{min}^* , it can be implanted into. The distensibility of a vein, α , can be quantified by dividing a vein's D^* by the diameter of the vein at rest, D_{rest} :

$$\alpha = \frac{D^*}{D_{rest}} \quad (13)$$

The D_{min}^* a valve can be placed in is

$$D_{min}^* = \alpha * SCD \quad (14)$$

Where SCD is the smallest diameter in which the valve can remain competent. The SCD of the 9 mm valve design that underwent verification testing was 8 mm. Assuming the ratio of valve diameter to SCD remains constant when the valve is scaled in size, Equation (14) can be stated in terms of the original outer diameter of the valve, V_{Di} :

$$D_{min}^* = 0.9\alpha V_{Di} \quad (15)$$

Equation (15) can be used to find the smallest D^* in which a valve can be placed and remain competent and is a function of the vein's distensibility and the initial diameter of the valve.

Maximum Diameter

The largest diameter in which a valve can remain competent without tearing during stent expansion will determine the maximum vein diameter, D_{max}^* , it can be placed in. Weaver defined the stretch ratio of a circular test section as [177]:

$$\lambda = \frac{C_f}{C_i} \quad (16)$$

Where C_f is the final circumference of the test section and C_i is its initial circumference.

Equation (16) can be rewritten as:

$$\lambda = \left(\frac{D_f}{D_i}\right)^2 \quad (17)$$

Where D_f is the final diameter of the circular test section and D_i is its initial diameter.

Solving Equation (17) for the final diameter yields:

$$D_f = D_i\sqrt{\lambda} \quad (18)$$

For the present application, D_f would be equal to D_{max}^* , D_i the valve's unexpanded diameter V_{Di} , and λ the allowable stretch ratio. Weaver determined that a cylindrical 20 wt% PVA section opened at a slow rate will fail at an average stretch ratio of 3.08 [177]. Dividing by a safety factor of 1.25 yields a safe stretch ratio of 2.46. It is assumed that a stented valve needs to be capable of expanding to a diameter at least 15% larger than the vein it is inserted into to be fixed in place [68]. These constraints can be imposed on Equation (18):

$$1.15D_{max}^* = V_{Di}\sqrt{2.46} \quad (19)$$

Solving for D_{max}^* , Equation (19) becomes:

$$D_{max}^* = 1.4V_{Di} \quad (20)$$

Equation (20) is only a function of the initial diameter of the valve and can be used to find the largest D^* a valve can be placed into and remain fixed in position with low risk of tearing.

The risk of leaflet prolapse increases the larger the valve expands. An experimental test was performed to ensure that the leaflets of a valve will not prolapse when expanded to 1.4 times its initial diameter. Using Equation (20), D_{max}^* for a 9 mm valve was calculated to be 12.6 mm (see Figure 76). A stented 9 mm valve was then expanded inside a 13 mm tube, the nearest available sized tubing larger than its D_{max}^* . A pressure head of 160 mmHg was applied proximal to the valve with a column of water 220 cm above the valve's shoulder. The leaflets closed

without prolapsing. This suggests that D_{max}^* is limited more by the risk of tearing than by prolapse for this valve design and that the leaflets will not prolapse if Equation (20) is followed.

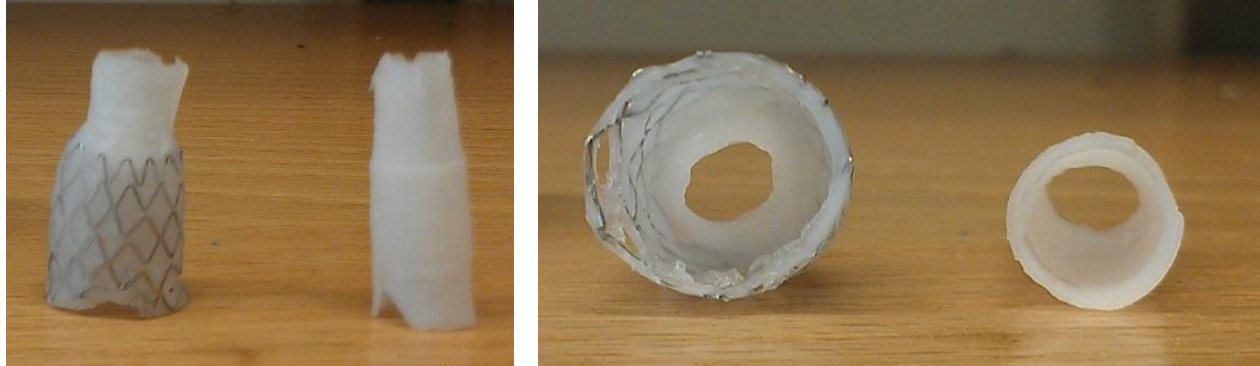


Figure 76: Views of a stented 9 mm valve expanded to 12 mm (approximately the size of the largest vein diameter this valve is suggested to be placed in) compared to an unexpanded valve.

Stent Size

It is assumed that a stented valve needs to be capable of expanding to a diameter at least 15% larger than the vein it is inserted into to be fixed in place [68]. Thus the fully expanded diameter of a valve's stent, D_{stent} , needs to be 15% larger than the valve's D_{max}^* , which can be found by modifying Equation (20):

$$D_{stent} = 1.15 * 1.4V_{Di} \quad (21)$$

Which simplifies to:

$$D_{stent} = 1.6V_{Di} \quad (22)$$

Valve Sizing for Sheep

Bia measured the mean cross sectional area of the sheep EJV to increase by 2%, which corresponds to a diameter change of less than 1%, as the internal pressure increased from 75 to 130 mmHg [210]. This suggests that the distensibility of the sheep EJV can be neglected. Thus

D^* for a sheep EJV is the diameter of the pressurized vein at rest which can be measured, such as by venogram, prior to implantation.

The mean sheep EJV diameter is 12.0 mm and has a standard deviation of 1.4 mm [115]. Assuming the diameters of this vein have a normal distribution, 95.5% of these veins will be within two standard deviations of the mean, 9.2-14.8 mm. The smallest sheep EJV diameter, $D_{min,sheep}^*$, in which a valve can remain competent can be found by substituting $\alpha = 1$, which corresponds to a non-distensible vein, into Equation (15):

$$D_{min,sheep}^* = 0.9V_{Di} \quad (23)$$

Equation (20) regulates the largest sheep EJV diameter, $D_{max,sheep}^*$, a valve can be safely placed in.

A single valve size which is capable of fitting into most sheep EJV diameters is desirable to reduce the number of stents to be acquired and valves to be manufactured. A valve which can fit in the highest percentage of sheep EJV diameters will have its minimum and maximum D^* be the same distance away from the mean:

$$12.0 \text{ mm} - D_{min,sheep}^* = D_{max,sheep}^* - 12.0 \text{ mm} \quad (24)$$

Substituting Equations (20) and (23) into Equation (24) yields:

$$12.0 \text{ mm} - 0.9V_{Di} = 1.4V_{Di} - 12.0 \text{ mm}$$

Solving for V_{Di} :

$$V_{Di} = 10.4 \text{ mm}$$

This suggests that a valve of the proposed design scaled to have an outer diameter of 10.4 mm will fit the highest percentage of sheep EJV diameters. Equations (20) and (23) indicate that

a 10.4 mm valve would fit into sheep EJVs with diameters ranging from 9.4 to 14.6 mm which accounts for 94% of the expected vein diameters, assuming normality (see Figure 77). Equation (22) indicates that a stent capable of expanding to 17 mm stent would need to be placed in a 10.4 mm valve.

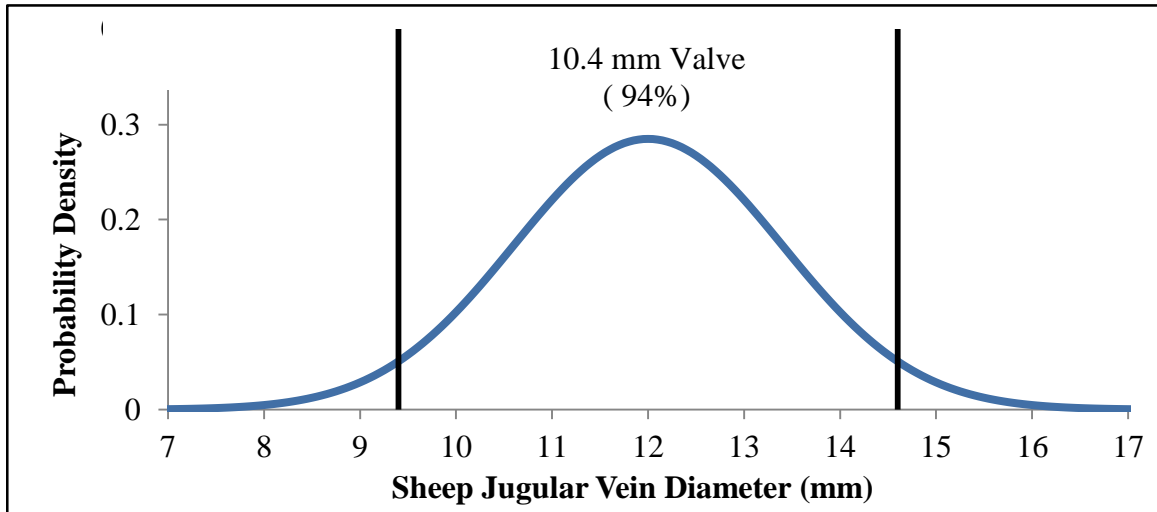


Figure 77: Probability density, assuming normality, of the sheep jugular vein diameter. A 10.4 mm diameter valve would fit into diameters ranging from 9.4 to 14.6 mm, which covers 94% of the expected diameter sizes.

Valve Sizing for Humans

In humans, the Valsalva maneuver can be used to cause veins to distend, with greater dilation occurring when the individual is inclined in the reverse Trendelenburg position than in the supine position [151, 211, 212]. The diameter of a human vein in the 15% reverse Trendelenburg position during a Valsalva maneuver is assumed to be D^* , the fully distended diameter of the vein. The vein diameter may be visualized and measured by venogram or ultrasound. The methods used by Fronck are an example of using duplex ultrasound to take this measurement [151].

Fronek measured the mean diameter of the CFV of individuals at rest in the supine position and during a Valsalva maneuver in the 15% reverse Trendelenburg position (D^*) [151]. On the average, D^* was 21% larger than the diameter of the vein at rest and had a mean diameter of 14.27 mm with a standard deviation of 2.49 mm [151]. Hertzberg measured the popliteal vein of individuals at rest in the supine position to be 6.8 mm with a standard deviation of 2.11 mm [213]. Assuming that the diameter of the popliteal vein also distends from rest by 21% during a Valsalva maneuver in the 15% reverse Trendelenburg position, the popliteal vein's mean D^* is 8.2 mm. The standard deviation of D^* for the popliteal vein is assumed to remain the same as when resting, 2.11 mm. Assuming a normal distribution, 95.5% of the D^* s of the CFV and popliteal veins will be within two standard deviations of their means, 9.3-19.3 mm and 4.0-12.4 mm respectively.

The smallest vein diameter, $D_{min,human}^*$, in which a valve can remain competent can be found by substituting $\alpha = 1.21$, which corresponds to a 21% distention from rest, into Equation (15):

$$D_{min,human}^* = 1.1V_{Di} \quad (25)$$

Equations (25) and (20) can be used to find the D^* range for a stented valve of the proposed design of any scale for a human. From this information, a set of valve sizes can be specified which will fit into the CFV, femoral, and popliteal veins of the general population. As the femoral vein is typically smaller than the CFV and larger than the popliteal vein in an individual, it is assumed that a set of valves that fits at least 90% of the CFV and popliteal veins in the general population will also service the femoral veins encountered.

A proposed set of 5 valve sizes is shown in Table 18 which will cover 90-96% of the probable range of CFV and popliteal vein diameters of the general population. This set was developed by attempting to satisfy the following criteria:

- 1) Service at least 90% of both the CFV and the popliteal veins to ensure adequate coverage of the general population.
- 2) Offer continuous size coverage throughout the entire set to ensure that valves within the set will also fit the femoral veins of the general population.
- 3) Each individual valve size is to service at least 15% of at least one vein type to warrant its production.
- 4) Have the overlap of two valve D^* ranges occur in multiples of 0.5 mm to make it easier for a surgeon to discern which valve size to use.

To simplify the selection process, each valve was named from the NATO phonetic alphabet, with Alpha corresponding to the smallest valve size and Echo the largest valve size (see Table 18). Assuming normality, the probability of each vein's D^* occurring in the range of each valve was calculated using Minitab v 13.2 (Minitab, Inc, State College, PA) and is shown in Table 18, Figure 79, and Figure 78. The CFV will primarily be serviced by the largest three valves, and the popliteal by the smallest 3 valves (see Table 18, Figure 78 and Figure 79).

A guide for surgeons to select the appropriately sized valve is shown in Table 19. In the event of a measurement for D^* being on the boundary of two valve sizes, it is recommended that the larger valve size be chosen to ensure the correct fixation and to keep the shear rates low. For example, it is recommended that a vein with a D^* of 14.5 mm have the Echo valve placed inside of it. The guide in Table 19 also displays the maximum expanded diameter of the stent to be

housed inside each valve, indicating the size of balloon for surgeons to use during insertion.

These stent sizes were found using Equation (22).

The flow rate through the popliteal vein is approximately 30% of that through the CFV [214]. While the valves best suited to fit inside the popliteal vein are much smaller than the one analyzed in the CFD simulation in Chapter 4, an elevated shear rate will likely not occur because of the lower flow rate.

Table 18: Suggested set of valve sizes with the calculated minimum and maximum D^* of each.

Valve Name	Valve Diameter (mm)	Min Diameter* (mm)	Max Diameter* (mm)	% of CFV diameters serviced	% of Popliteal diameters serviced
Alpha	5	5.5	7.0	0	18
Bravo	6.4	7.0	9.0	2	36
Charlie	8.2	9.0	11.5	12	30
Delta	10.4	11.4	14.6	40	6
Echo	13.2	14.5	18.5	42	0
	Entire Set	5.5	18.5	96	90

Table 19: Sizing guide for the suggested valve set.

Diameter* (mm)	Valve	Fully Expanded Stent Diameter (mm)
5.5-7	Alpha	8
7-9	Bravo	10
9-11.5	Charlie	13
11.5-14.5	Delta	17
14.5-18.5	Echo	21

*Diameter measured by ultrasound during a Valsalva maneuver in the 15% reverse Trendelenburg position. In the event of the diameter falling on the boundary of two valve sizes, the larger size should be selected.

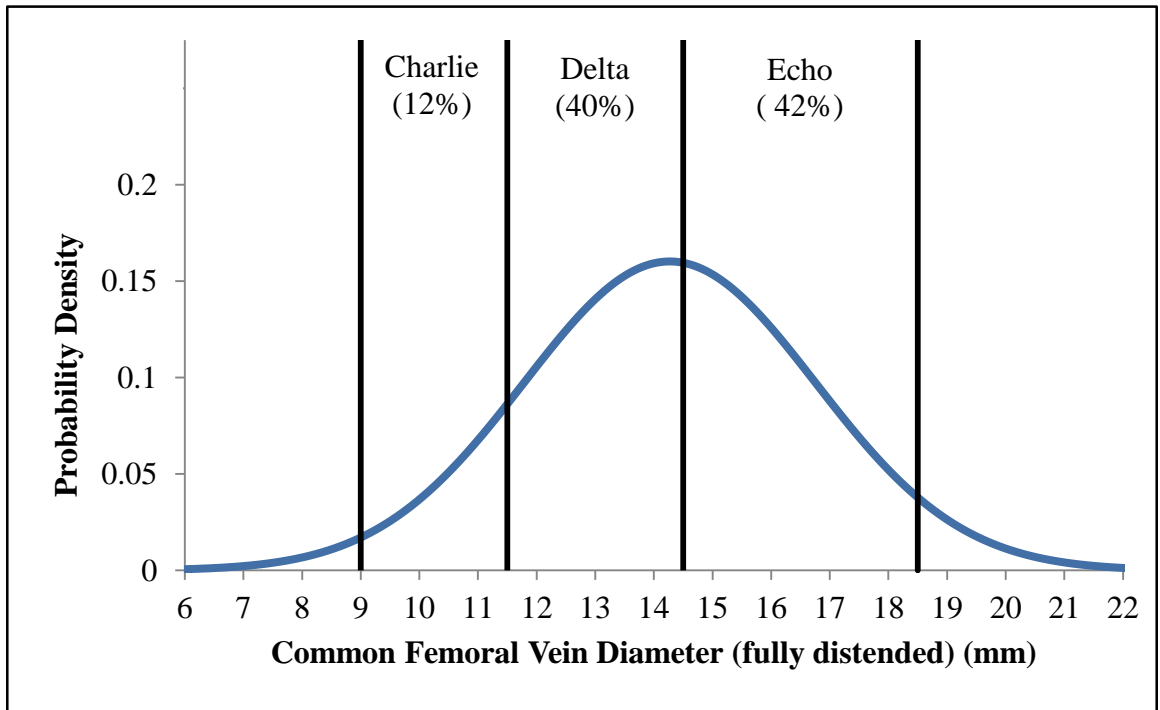


Figure 78: Probability density, assuming normality, of the CFV's fully distended diameter. The percent probability of a diameter falling in the range of selected valve sizes is indicated.

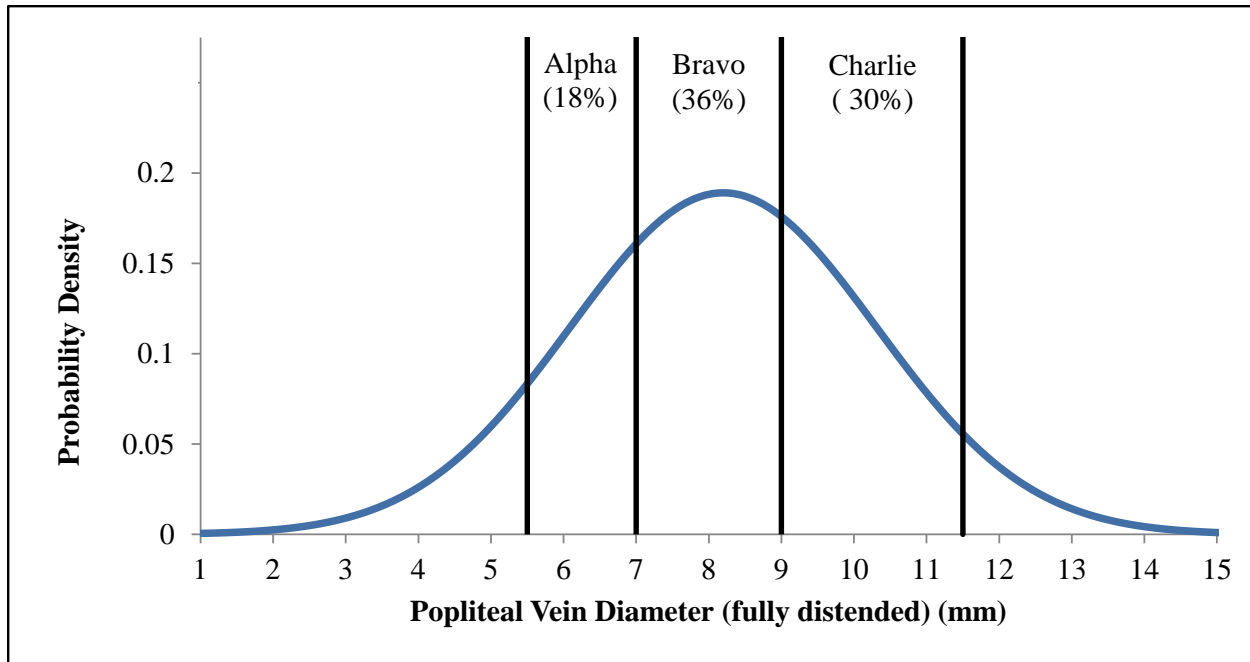


Figure 79: Probability density, assuming normality, of the popliteal vein's fully distended diameter. The percent probability of a diameter falling in the range of selected valve sizes is indicated.

Clinician Procedure

A flow chart for the role of clinicians in implantation and evaluation of the proposed valve is shown in Figure 80. Clinicians will identify where valves should be implanted by identifying refluxing vein segments and then visualizing implantation sites using venogram or ultrasound. The diameter at the implantation site of each vein will be measured in the 15° reverse Trendelenburg position using venogram or ultrasound. Table 19 will be used to select the appropriate valve size to be implanted in each location. The valves may then be percutaneously delivered via catheter and the valve's stents will then be expanded by balloon. Additional valves may be implanted in the same vein segment at least 13 cm apart at locations where Doppler ultrasound reveals reflux to exceed 3 mL/min when patients perform a Valsalva maneuver. After the procedure the primary endpoints will be assessed for each implanted valve, and the secondary endpoints will be measured for each limb at 8 weeks and 6, 12, and 18 months.

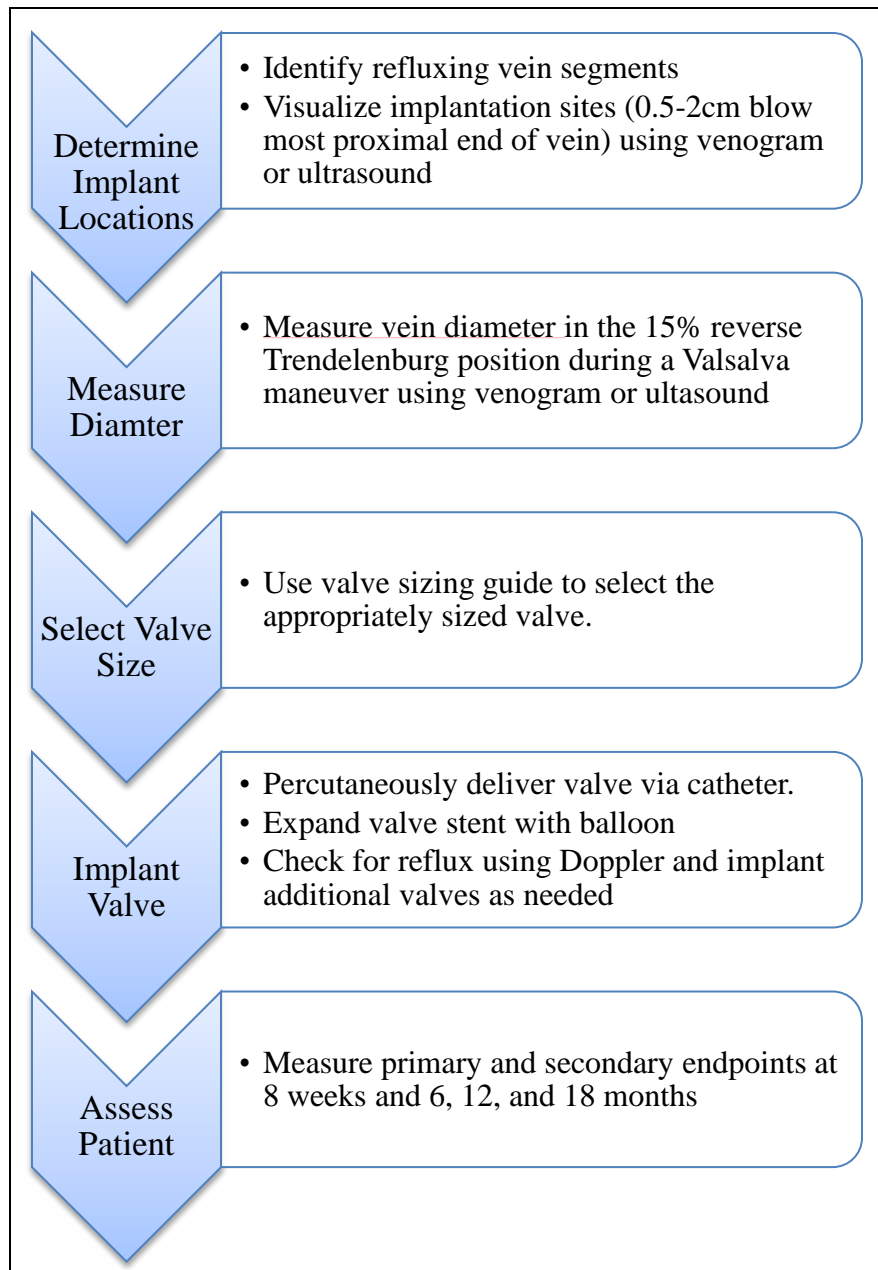


Figure 80: Flow chart for clinicians for human testing.

CHAPTER 7: EVALUATION AND DISCUSSION

Valve Design Evaluation

The proposed valve met every design specification for an effective prosthetic venous valve. On the average, the valve allows less than 0.5 mL/min of reflux at low and high retrograde pressures even after 500,000 cycles, suggesting that it will reduce the reflux of individuals with venous reflux by more than 99.6% [32]. The valve closes in less than 0.07 seconds and allows the distal pressure to rise to an average of 7% of the equilibrium pressure 30 seconds after a simulated ankle flexion. The valve increases the outflow resistance an average of 2.3 mmHg*min/L which is much less than venous obstructions which increase the outflow resistance by at least 5 mmHg*min/L [48]. The valve can fit in a 16 French catheter and is capable of percutaneous delivery. The base of the valve is 1.5 times the diameter of the vein it is to be implanted which will help it to be oriented correctly upon deployment.

Thus far the valve has demonstrated that it has low thrombogenicity. The maximum shear rate in the valve after a Valsalva maneuver is approximately 2300 s^{-1} , which puts it at low risk for shear induced thrombosis. Fluid behind the valve's leaflets is ejected with a forward flow rate of 400 mL/min, suggesting that thrombus formation will not occur at this location when an individual is at rest in the supine position. The material of the valve, PVA, has passed the ISO and USFDA biocompatibility tests and has been shown to be less thrombogenic than Dacron in previous testing [144, 165, 175]. PVA is also capable of drug delivery and can elute anti-coagulation drugs, such as citrate [145]. A stented valve remained patent in a porcine blood flow loop for 3 hours, demonstrating that its short term patency is at least equivalent to the Midha valve which had previously held the record for the longest occlusion time in such a loop.

Valves of the proposed design can function and expand into veins with fully distended diameters that are 1.1-1.4 times the valve's initial diameter. With this versatility, a 10.4 mm valve is expected to fit in 94% of sheep EJVs, and a set of 5 valves is expected to fit in 90-96% of the CFV, femoral, and popliteal veins.

While many prosthetic venous valves have been developed, only a handful have reported experimental testing results. While the experimental methods for testing these valves has differed, an attempt has been made to briefly compare their performances (see Table 20) [102, 123, 132, 137, 140, 142, 143, 145]. Only three valves, the Sathe valve, Moriyama valve, and the valve presented in this work, have demonstrated their ability to reduce reflux below 3 mL/min (see Figure 81); however, only the present valve did not increase the outflow resistance to venous obstruction levels [142, 143]. While the maximum shear rate during forward flow has not been calculated for most valves, shear induced platelet aggregation is expected to be a common failure mode for many previously developed prosthetic venous valves due to their relatively small orifices or sharp changes in geometry.

As the prosthetic venous valve presented in this work is the only valve to meet every design specification for an effective prosthetic venous valve, this valve shows the most potential to be a minimally invasive treatment for deep venous reflux.

Table 20: Performance comparison of prosthetic venous valves which underwent experimental testing (data extracted from [102, 122, 123, 132, 137, 140, 142, 143, 145]). The valve presented in this work is referred to as "Tanner".

Metric	Specification	Tanner	Taheri	PVVB	Akron Gen 2	Akron Gen 3	bPVV	oPVV	Liu	Sathe	Midha
Reflux rate (mL/min)	≤ 8	0.3-0.4	145	40-120	87.5	14.25	2.04	30.8	12-16	< 0.3	30.8
Reflux rate after fatigue (mL/min)	≤ 8	< 0.1	-	-	-	-	-	-	-	< 0.3	41.1
Leaflet closing time (s)	< 0.5	0.067	-	0.43-0.49	1.38**	-	-	-	-	-	-
Distal pressure rise 30 seconds after a simulated calf flexion (%)	≤ 10	7	-	-	-	-	~10	100	-	-	-
Increased outflow resistance by the valve (mmHg*min/L)	< 5	2.3	333*	322*	1.37-2.33	1.15-4.66	> 372	> 46	-	324.6	7.3
Fluid behind leaflets washes out under forward flow	Yes	Yes	-	-	-	-	Yes***	No***	-	-	Yes***
Smallest diameter valve can be placed in without buckling (mm)	≤ 8.5	6.5	-	-	-	-	-	-	-	-	10
Maximum shear rate during forward flow (s ⁻¹)	< 3500	2300	-	-	7600	-	-	-	-	> 10E3	3000
Time to occlusion when running heparinized (3.5 mL/L) porcine blood in a flow loop (Hours)	> 3	> 3	-	-	-	-	-	-	-	0.3	> 3

*Resistance of the testing system not reported so the total resistance of the valve and the testing system are presented.

**Only the results for a 2:1 scale mockup of the prototype valve were reported

***Applied flow rate was higher than 400 mL/min

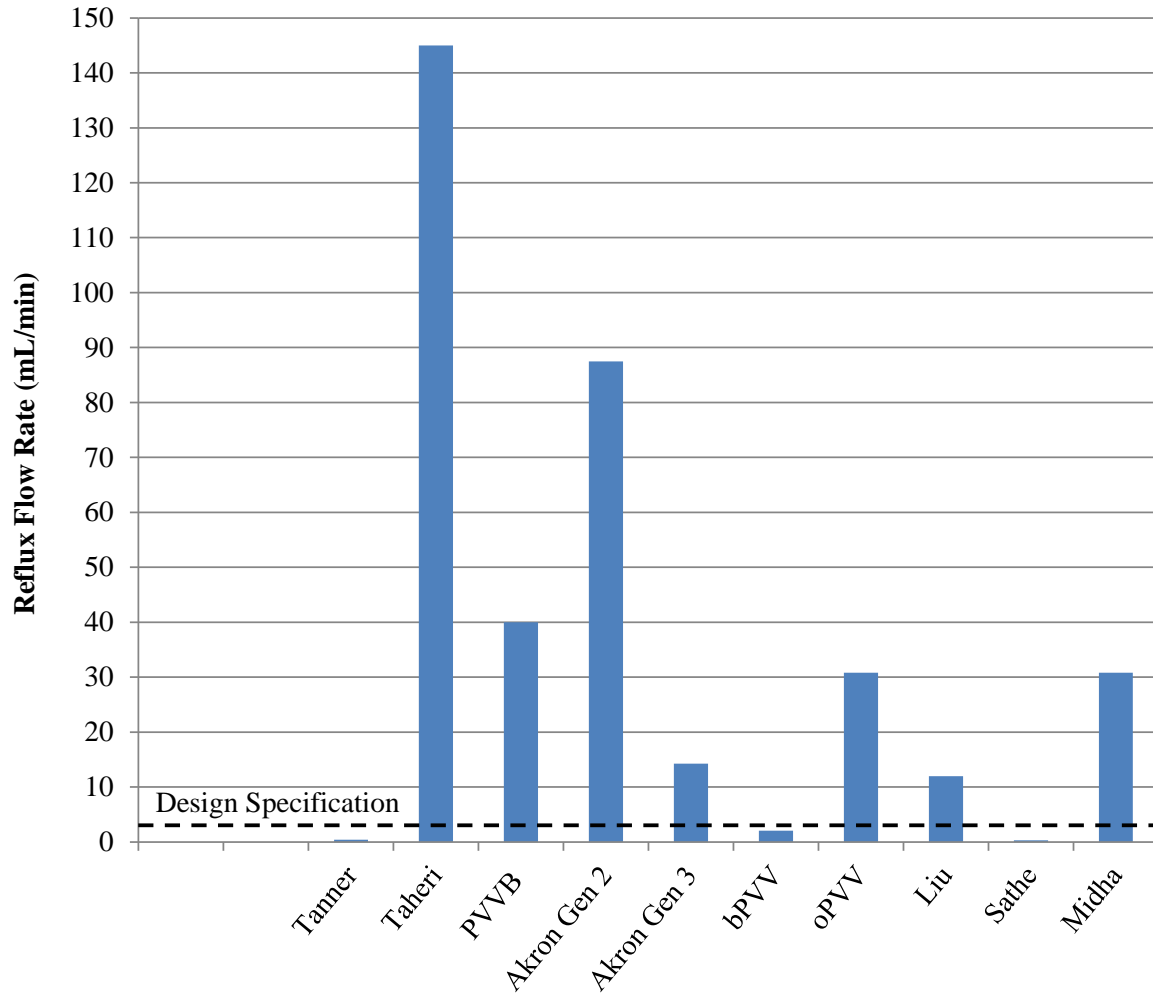


Figure 81: Comparison of reflux flow rate of prosthetic venous valves which underwent experimental testing (data extracted from [102, 122, 123, 132, 137, 140, 142, 143, 145]). The valve presented in this work is referred to as "Tanner".

Main Contributions:

The present work made novel contributions in the field of prosthetic venous valve development in the areas of valve design, design specifications, verification testing, computational analysis, and valve placement.

Valve Design

Novel features of the valve include the slits in the leaflet corners to improve sealing and the shape of the leaflets to help prevent prolapse. The transition of the valve orifice from being elliptical to lemon shaped from the shoulder to half the height of the leaflets, which helps to prevent leaflet prolapse, and then remaining lemon shaped, which promotes sealing, is also unique. The design of a valve which can expand from its initial diameter by more than 40% is also original.

Design Specifications and Verification Testing

Previous design specifications for reflux have been based on the volume ejected from the calf muscle pump or the amount of flow through the femoral vein when at rest in the supine position [143, 145]. However, the specification for competency in this work was made relative to the amount of reflux seen in individuals with venous reflux, ensuring that a prosthetic valve that meets this specification will reduce the amount of reflux below the level that will contribute to CVI symptoms. Measuring the reflux by weight, which increased the precision of the test, was unique to this work. Additionally, specifications for the diameter of a constricted vein in which a valve is to remain competent and not buckle have not heretofore been proposed or verified in testing.

A specification for the closing time of a prosthetic valve is unique to this work as well as measuring the closing time using a visual recording. While previous researchers have recorded the rise in distal pressure after a simulated calf flexion, a definitive design specification has not previously been proposed for this test [142]. A design specification for outflow resistance, which

ensured that the valve did not impede flow to the level of venous obstruction, had not been previously proposed.

A similar washout test was performed for the Midha valve which applied a 75mmHg pressure head using water [145]. The resulting forward flow rate in Midha's washout test was approximately 2700 mL/min, which is higher than the maximum flow of 1600 mL/min seen in the femoral vein, which biased the test towards washing out [137, 145, 151]. The washout test in the present work used a forward flow rate of 400 mL/min, corresponding to the flow rate of a subject in the supine position, being the situation where the valve is most likely to develop stagnant flow. Additionally, a glycerol solution with a similar viscosity as blood was used as the working fluid, further making the washout test in the present work more indicative of flow behind the valve's leaflets in a human vein.

A stented prosthetic venous valve had not been placed in a porcine blood flow loop before. A mathematical model to estimate the minimum catheter size in which a prosthetic venous valve can fit had not been previously proposed.

Computational Analysis

To date, this is the first work to use a finite element simulation to analyze a prosthetic venous valve. The material properties of 20 wt% PVA undergoing 4 freeze-thaw cycles at a slow thawing rate used in the finite element simulation had not been previously estimated.

While other CFD simulations of prosthetic valves inside the femoral vein have been performed, this was the first to use the deformed geometry of the valve when expanded by a stent in the vein (see Figure 47), the physiologic maximum flow rate of 1600 mL/min, or a fully

developed flow profile at the inlet to decrease the computational burden of the model [137, 139, 145].

Valve Placement

A method to determine the minimum distance between implanted valves in the same venous segment has not heretofore been set forth for any prosthetic venous valve. This work is the first to propose a method to determine the diameters in which a valve can be placed and maintain full functionality. The suggestion of a set of vein valve sizes which could service the CFV, femoral, and popliteal veins is also a novel contribution, as well as the creation of a guide for surgeons to select the correct valve size.

Future Work

Additional fatigue testing of the proposed valve should be performed to determine if the valve will fail from fatigue before 9 million cycles, the expected number of cycles the valve will undergo in its lifetime, at a frequency of 0.67 Hz [143].

After stents of the appropriate size are obtained the animal study can be performed. If animal testing indicates that the valve will be successful in human testing, an IRB protocol to test the valve in humans should be prepared. After IRB approval, the proposed human study could then be performed.

While a set of valves for the CFV, femoral, and popliteal veins was proposed, a set of valves which can service the superficial and perforating veins could be developed which would allow the valve to treat multisystem reflux. Human testing using the valve to correct multisystem

reflux could then be pursued. A stented valve also has the potential to treat outflow obstruction in addition to venous reflux in subjects, which could be researched further.

While the shoulder of the proposed valve provided a visual cue to align a stent inside the valve correctly during manufacturing, it did not act as a ledge to stop the stent from protruding into the leaflets. Another method to help align the stent during manufacturing could likely be found, and the shoulder should be removed. The removal of the shoulder would reduce the bulk of the valve and potentially allow the valve to fit into a smaller catheter size. However, the removal of the shoulder will likely change the smallest diameter in which the valve can remain competent and this verification test would need to be performed again.

REFERENCES

1. Nicolaides, A.N., *Investigation of Chronic Venous Insufficiency : A Consensus Statement*. *Circulation*, 2000. **102**(20): p. e126-e163.
2. Meissner, M.H., et al., *The hemodynamics and diagnosis of venous disease*. *J Vasc Surg*, 2007. **46 Suppl S**: p. 4S-24S.
3. Sherwood, L., *Human physiology: from cells to systems*2012: Brooks/Cole Publishing Company.
4. Vasquez, M.A., et al., *Revision of the venous clinical severity score: venous outcomes consensus statement: special communication of the American Venous Forum Ad Hoc Outcomes Working Group*. *J Vasc Surg*, 2010. **52**(5): p. 1387-96.
5. Lee, A.J., et al., *Lifestyle factors and the risk of varicose veins: Edinburgh Vein Study*. *Journal of clinical epidemiology*, 2003. **56**(2): p. 171.
6. Fowkes, F., et al., *Lifestyle risk factors for lower limb venous reflux in the general population: Edinburgh Vein Study*. *International journal of epidemiology*, 2001. **30**(4): p. 846-852.
7. Laurikka, J.O., et al., *Risk indicators for varicose veins in forty-to sixty-year-olds in the Tampere varicose vein study*. *World journal of surgery*, 2002. **26**(6): p. 648-651.
8. Chiesa, R., et al., *Demographic factors and their relationship with the presence of CVI signs in Italy: the 24-cities cohort study*. *European journal of vascular and endovascular surgery: the official journal of the European Society for Vascular Surgery*, 2005. **30**(6): p. 674.
9. Beebe-Dimmer, J.L., et al., *The epidemiology of chronic venous insufficiency and varicose veins*. *Ann Epidemiol*, 2005. **15**(3): p. 175-84.
10. Criqui, M.H., et al., *Chronic Venous Disease in an Ethnically Diverse Population The San Diego Population Study*. *American journal of epidemiology*, 2003. **158**(5): p. 448-456.
11. Phillips, T., et al., *A study of the impact of leg ulcers on quality of life: financial, social, and psychologic implications*. *Journal of the American Academy of Dermatology*, 1994. **31**(1): p. 49-53.
12. Taheri, S.A. and R.O. Schultz, *Experimental prosthetic vein valve long-term results*. *Angiology*, 1995. **46**(4): p. 299-303.

13. McGuckin, M., et al., *Validation of venous leg ulcer guidelines in the United States and United Kingdom*. The American journal of surgery, 2002. **183**(2): p. 132-137.
14. Ruckley, C., *Socioeconomic impact of chronic venous insufficiency and leg ulcers*. Angiology, 1997. **48**(1): p. 67-69.
15. Callam, M., et al., *Chronic ulcer of the leg: clinical history*. British medical journal (Clinical research ed.), 1987. **294**(6584): p. 1389-1391.
16. Shrestha, L.B. *Life expectancy in the United States*. 2005. Congressional Information Service, Library of Congress.
17. Callam, M., et al., *Chronic leg ulceration: socio-economic aspects*. Scottish medical journal, 1988. **33**(6): p. 358.
18. Nicolaides, A.N., et al., *The relation of venous ulceration with ambulatory venous pressure measurements*. Journal of Vascular Surgery, 1993. **17**(2): p. 414-419.
19. McCaughan, J.J., et al., *In vitro observations of greater saphenous vein valves during pulsatile and nonpulsatile flow and following lysis*. Journal of Vascular Surgery, 1984. **1**(2): p. 356-361.
20. van Bemmelen, P.S., et al., *The mechanism of venous valve closure: its relationship to the velocity of reverse flow*. Archives of Surgery, 1990. **125**(5): p. 617.
21. Lurie, F., R.L. Kistner, and B. Eklof, *The mechanism of venous valve closure in normal physiologic conditions*. Journal of Vascular Surgery, 2002. **35**(4): p. 713-717.
22. Lurie, F., et al., *Mechanism of venous valve closure and role of the valve in circulation: a new concept*. Journal of Vascular Surgery, 2003. **38**(5): p. 955-961.
23. Qui, Y., et al., *Fluid dynamics of venous valve closure*. Annals of biomedical engineering, 1995. **23**(6): p. 750-759.
24. Moore, D.J., P.D. Himmel, and D.S. Sumner, *Distribution of venous valvular incompetence in patients with the postphlebotic syndrome*. Journal of Vascular Surgery, 1986. **3**(1): p. 49-57.
25. Hanrahan, L.M., et al., *Distribution of valvular incompetence in patients with venous stasis ulceration*. Journal of Vascular Surgery, 1991. **13**(6): p. 805-812.

26. Cesarone, M., et al., *'Real' Epidemiology of Varicose Veins and Chronic Venous Diseases: The San Valentino Vascular Screening Project*. *Angiology*, 2002. **53**(2): p. 119-130.
27. Shull, K.C., et al., *Significance of popliteal reflux in relation to ambulatory venous pressure and ulceration*. *Archives of Surgery*, 1979. **114**(11): p. 1304.
28. PERRIN, M., et al., *Evaluation of the new severity scoring system in chronic venous disease of the lower limbs: an observational study conducted by French angiologists*. *Phlebology*, 2006. **13**(1): p. 6-16.
29. Raju, S., et al., *Ambulatory venous hypertension: component analysis in 373 limbs*. *Vascular and endovascular surgery*, 1999. **33**(3): p. 257-266.
30. van Bemmelen, P.S., et al., *Quantitative segmental evaluation of venous valvular reflux with duplex ultrasound scanning*. *Journal of Vascular Surgery*, 1989. **10**(4): p. 0425-0431.
31. Labropoulos, N., et al., *Definition of venous reflux in lower-extremity veins*. *Journal of Vascular Surgery*, 2003. **38**(4): p. 793-798.
32. Neglen, P., et al., *Hemodynamic and clinical impact of ultrasound-derived venous reflux parameters*. *J Vasc Surg*, 2004. **40**(2): p. 303-10.
33. Danielsson, G., et al., *Deep axial reflux, an important contributor to skin changes or ulcer in chronic venous disease*. *Journal of Vascular Surgery*, 2003. **38**(6): p. 1336-1341.
34. Iafrati, M.D., et al., *Correlation of venous noninvasive tests with the Society for Vascular Surgery/International Society for Cardiovascular Surgery clinical classification of chronic venous insufficiency*. *Journal of vascular surgery : official publication, the Society for Vascular Surgery*, 1994. **19**(6): p. 1001-1007.
35. Christopoulos, D. and A. Nicolaides, *Noninvasive diagnosis and quantitation of popliteal reflux in the swollen and ulcerated leg*. *The Journal of cardiovascular surgery*, 1988. **29**(5): p. 535.
36. Araki, C.T., et al., *The significance of calf muscle pump function in venous ulceration*. *Journal of Vascular Surgery*, 1994. **20**(6): p. 872-879.
37. Fukuoka, M., T. Sugimoto, and Y. Okita, *Prospective evaluation of chronic venous insufficiency based on foot venous pressure measurements and air plethysmography findings*. *Journal of Vascular Surgery*, 2003. **38**(4): p. 804-811.

38. Christopoulos, D., et al., *Air-plethysmography and the effect of elastic compression on venous hemodynamics of the leg*. Journal of Vascular Surgery, 1987. **5**(1): p. 148-159.
39. Christopoulos, D., et al., *Pathogenesis of venous ulceration in relation to the calf muscle pump function*. Surgery, 1989. **106**(5): p. 829.
40. Myers, K.A., et al., *Duplex ultrasonography scanning for chronic venous disease: patterns of venous reflux*. Journal of Vascular Surgery, 1995. **21**(4): p. 605-612.
41. Labropoulos, N., et al., *The role of the distribution and anatomic extent of reflux in the development of signs and symptoms in chronic venous insufficiency*. Journal of Vascular Surgery, 1996. **23**(3): p. 504-510.
42. Labropoulos, N., et al., *Venous hemodynamic abnormalities in patients with leg ulceration*. The American journal of surgery, 1995. **169**(6): p. 572-574.
43. Raju, S. and R. Fredericks, *Valve reconstruction procedures for nonobstructive venous insufficiency: Rationale, techniques, and results in 107 procedures with two- to eight-year follow-up*. Journal of Vascular Surgery, 1988. **7**(2): p. 301-310.
44. Morano, J. and S. Raju, *Chronic venous insufficiency: assessment with descending venography*. Radiology, 1990. **174**(2): p. 441-444.
45. Tripathi, R., M. Abbas, and N. Durrani, *Five-Year Experience of Valvular Reconstructions for Nonhealing Leg Ulceration due to Deep Venous Reflux: Lessons Learned*. Perspectives in vascular surgery and endovascular therapy, 2002. **15**(2): p. 87-100.
46. Mozes, G. and P. Gloviczki, *New discoveries in anatomy and new terminology of leg veins: clinical implications*. Vascular and endovascular surgery, 2004. **38**(4): p. 367-374.
47. Nam, K.H., et al., *Velocity field measurements of valvular blood flow in a human superficial vein using high-frequency ultrasound speckle image velocimetry*. Int J Cardiovasc Imaging, 2012. **28**(1): p. 69-77.
48. Neglen, P. and S. Raju, *Detection of outflow obstruction in chronic venous insufficiency*. Journal of Vascular Surgery, 1993. **17**(3): p. 583-589.
49. Shiman, M.I., et al., *Venous ulcers: A reappraisal analyzing the effects of neuropathy, muscle involvement, and range of motion upon gait and calf muscle function*. Wound Repair and Regeneration, 2009. **17**(2): p. 147-152.

50. Criado, E., et al., *The role of air plethysmography in the diagnosis of chronic venous insufficiency*. Journal of Vascular Surgery, 1998. **27**(4): p. 660-670.
51. Bergan, J.J., et al., *Chronic venous disease*. New England Journal of Medicine, 2006. **355**(5): p. 488-498.
52. Vasquez, M.A., et al., *The utility of the Venous Clinical Severity Score in 682 limbs treated by radiofrequency saphenous vein ablation*. J Vasc Surg, 2007. **45**(5): p. 1008-1014; discussion 1015.
53. Kakkos, S.K., et al., *Validation of the new venous severity scoring system in varicose vein surgery*. Journal of Vascular Surgery, 2003. **38**(2): p. 224-228.
54. Rutherford, R.B., et al., *Venous severity scoring: An adjunct to venous outcome assessment*. Journal of Vascular Surgery, 2000. **31**(6): p. 1307-1312.
55. Meissner, M.H., C. Natiello, and S.C. Nicholls, *Performance characteristics of the venous clinical severity score*. Journal of Vascular Surgery, 2002. **36**(5): p. 889-895.
56. Gillet, J.L., M.R. Perrin, and F.A. Allaert, *Clinical presentation and venous severity scoring of patients with extended deep axial venous reflux*. J Vasc Surg, 2006. **44**(3): p. 588-94.
57. Padberg Jr, F.T., et al., *Hemodynamic and clinical improvement after superficial vein ablation in primary combined venous insufficiency with ulceration*. Journal of vascular surgery: official publication, the Society for Vascular Surgery [and] International Society for Cardiovascular Surgery, North American Chapter, 1996. **24**(5): p. 711.
58. Masuda, E.M., et al., *The effect of ultrasound-guided sclerotherapy of incompetent perforator veins on venous clinical severity and disability scores*. J Vasc Surg, 2006. **43**(3): p. 551-6; discussion 556-7.
59. Mekako, A.I., et al., *A nonrandomised controlled trial of endovenous laser therapy and surgery in the treatment of varicose veins*. Ann Vasc Surg, 2006. **20**(4): p. 451-7.
60. Vasquez, M.A. and C.E. Munschauer, *Venous Clinical Severity Score and quality-of-life assessment tools: application to vein practice*. Phlebology, 2008. **23**(6): p. 259-75.
61. Cesarone, M.R., et al., *Improvement of signs and symptoms of chronic venous insufficiency and microangiopathy with Pycnogenol: a prospective, controlled study*. Phytomedicine, 2010. **17**(11): p. 835-9.

62. Marston, W.A., et al., *Endovenous saphenous ablation corrects the hemodynamic abnormality in patients with CEAP clinical class 3–6 CVI due to superficial reflux*. *Vascular and endovascular surgery*, 2006. **40**(2): p. 125-130.
63. Hartung, O., et al., *Mid-term results of endovascular treatment for symptomatic chronic nonmalignant ilio caval venous occlusive disease*. *J Vasc Surg*, 2005. **42**(6): p. 1138-44; discussion 1144.
64. Yamaki, T., et al., *Prospective randomised comparative study of visual foam sclerotherapy alone or in combination with ultrasound-guided foam sclerotherapy for treatment of superficial venous insufficiency: preliminary report*. *Eur J Vasc Endovasc Surg*, 2012. **43**(3): p. 343-7.
65. Padberg Jr, F., M.V. Johnston, and S.A. Sisto, *Structured exercise improves calf muscle pump function in chronic venous insufficiency: a randomized trial*. *Journal of vascular surgery: official publication, the Society for Vascular Surgery [and] International Society for Cardiovascular Surgery, North American Chapter*, 2004. **39**(1): p. 79.
66. Choi, J.H., H.-C. Park, and J.H. Joh, *The occlusion rate and patterns of saphenous vein after radiofrequency ablation*. *Journal of the Korean Surgical Society*, 2013. **84**(2): p. 107-113.
67. Raju, S. and P. Neglén, *Chronic venous insufficiency and varicose veins*. *New England Journal of Medicine*, 2009. **360**(22): p. 2319-2327.
68. Eberhardt, R.T. and J.D. Raffetto, *Chronic venous insufficiency*. *Circulation*, 2005. **111**(18): p. 2398-2409.
69. Motykie, G., et al., *Evaluation of therapeutic compression stockings in the treatment of chronic venous insufficiency*. *Dermatologic surgery*, 1999. **25**(2): p. 116-120.
70. Agu, O., G. Hamilton, and D. Baker, *Graduated compression stockings in the prevention of venous thromboembolism*. *British journal of surgery*, 1999. **86**(8): p. 992-1004.
71. FRANKS, P.J., et al., *Risk factors for leg ulcer recurrence: a randomized trial of two types of compression stocking*. *Age and Ageing*, 1995. **24**(6): p. 490-494.
72. Raju, S., K. Hollis, and P. Neglen, *Use of compression stockings in chronic venous disease: patient compliance and efficacy*. *Ann Vasc Surg*, 2007. **21**(6): p. 790-795.

73. Erickson, C.A., et al., *Healing of venous ulcers in an ambulatory care program: the roles of chronic venous insufficiency and patient compliance*. Journal of Vascular Surgery, 1995. **22**(5): p. 629-636.
74. Jull, A., et al., *Factors influencing concordance with compression stockings after venous leg ulcer healing*. Journal of Wound Care, 2004. **13**(3): p. 90-92.
75. Kiev, J., et al., *Patient compliance with fitted compression hosiery monitored by photoplethysmography*. Arch Phys Med Rehabil, 1990. **71**(6): p. 376-379.
76. Gohel, M.S. and A.H. Davies, *Pharmacological agents in the treatment of venous disease: an update of the available evidence*. Current Vascular Pharmacology, 2009. **7**(3): p. 303-308.
77. Gohel, M. and A. Davies, *Pharmacological treatment in patients with C4, C5 and C6 venous disease*. Phlebology, 2010. **25**(suppl 1): p. 35-41.
78. Perrin, M. and A. Ramelet, *Pharmacological treatment of primary chronic venous disease: rationale, results and unanswered questions*. European journal of vascular and endovascular surgery, 2011. **41**(1): p. 117-125.
79. Gloviczki, P., et al., *The care of patients with varicose veins and associated chronic venous diseases: clinical practice guidelines of the Society for Vascular Surgery and the American Venous Forum*. J Vasc Surg, 2011. **53**(5 Suppl): p. 2S-48S.
80. Lane, T.R., et al., *Cyanoacrylate glue for the treatment of great saphenous vein incompetence in the anticoagulated patient*. Journal of Vascular Surgery: Venous and Lymphatic Disorders, 2013.
81. Min, R.J., N. Khilnani, and S.E. Zimmet, *Endovenous laser treatment of saphenous vein reflux: long-term results*. Journal of Vascular and Interventional Radiology, 2003. **14**(8): p. 991-996.
82. Lv, W., et al., *Analysis of a Series of Patients with Varicose Vein Recurrence*. The Journal of International Medical Research, 2012. **40**(3): p. 1156-1165.
83. Rivlin, S., *The surgical cure of primary varicose veins*. British journal of surgery, 2005. **62**(11): p. 913-917.
84. Royle, J.P., *Recurrent varicose veins*. World journal of surgery, 1986. **10**(6): p. 944-953.

85. Dwerryhouse, S., et al., *Stripping the long saphenous vein reduces the rate of reoperation for recurrent varicose veins: five-year results of a randomized trial*. Journal of Vascular Surgery, 1999. **29**(4): p. 589-592.
86. Winterborn, R.J., C. Foy, and J.J. Earnshaw, *Causes of varicose vein recurrence: late results of a randomized controlled trial of stripping the long saphenous vein*. Journal of Vascular Surgery, 2004. **40**(4): p. 634-639.
87. Neglen, P., M. Berry, and S. Raju, *Endovascular surgery in the treatment of chronic primary and post-thrombotic iliac vein obstruction*. European journal of vascular and endovascular surgery, 2000. **20**(6): p. 560-571.
88. Neglén, P. and S. Raju, *Balloon dilation and stenting of chronic iliac vein obstruction: technical aspects and early clinical outcome*. Journal Information, 2000. **7**(2).
89. Neglen, P., et al., *Stenting of the venous outflow in chronic venous disease: long-term stent-related outcome, clinical, and hemodynamic result*. J Vasc Surg, 2007. **46**(5): p. 979-990.
90. Raju, S., R. Darcey, and P. Neglén, *Unexpected major role for venous stenting in deep reflux disease*. Journal of Vascular Surgery, 2010. **51**(2): p. 401.
91. Raju, S. and P. Neglén, *Percutaneous recanalization of total occlusions of the iliac vein*. Journal of Vascular Surgery, 2009. **50**(2): p. 360-368.
92. Delis, K.T., et al., *Successful iliac vein and inferior vena cava stenting ameliorates venous claudication and improves venous outflow, calf muscle pump function, and clinical status in post-thrombotic syndrome*. Annals of surgery, 2007. **245**(1): p. 130.
93. Maleti, O. and M. Perrin, *Reconstructive surgery for deep vein reflux in the lower limbs: techniques, results and indications*. Eur J Vasc Endovasc Surg, 2011. **41**(6): p. 837-48.
94. Ofenloch, J.C., et al., *Endoscopic Venous Valve Transplantation with a Valve–Stent Device*. Ann Vasc Surg, 1997. **11**(1): p. 62-67.
95. Neglen, P. and S. Raju, *Venous reflux repair with cryopreserved vein valves*. J Vasc Surg, 2003. **37**(3): p. 552-7.
96. Dalsing, M.C., et al., *A multicenter, phase I evaluation of cryopreserved venous valve allografts for the treatment of chronic deep venous insufficiency*. Journal of Vascular Surgery, 1999. **30**(5): p. 854-866.

97. Maleti, O. and M. Lugli, *Neovalve construction in postthrombotic syndrome*. J Vasc Surg, 2006. **43**(4): p. 794-9.
98. Kistner, R. and M. Sparkuhl, *Surgery in acute and chronic venous disease*. Surgery, 1979. **85**(1): p. 31.
99. Taheri, S., et al., *Indications and results of vein valve transplant*. The Journal of cardiovascular surgery, 1986. **27**(2): p. 163.
100. Perrin, M., *Reconstructive surgery for deep venous reflux: a report on 144 cases*. Cardiovascular Surgery, 2000. **8**(4): p. 246-255.
101. Dotter, C.T. *Interventional radiology--review of an emerging field*. in *Seminars in roentgenology*. 1981.
102. Taheri, S.A., et al., *Experimental prosthetic vein valve*. The American journal of surgery, 1988. **156**(2): p. 111-114.
103. Taheri, S.A., et al., *Experimental prosthetic vein valve*. International angiology: a journal of the International Union of Angiology, 1989. **8**(1): p. 7.
104. Taheri, S.A., *Experimental Prosthetic Vein Valve*. Vascular and endovascular surgery, 1997. **31**(3): p. 395-398.
105. McLachlin, A.D., et al., *Valve replacement in the recanalized incompetent superficial femoral vein in dogs*. Annals of surgery, 1965. **162**(3): p. 446.
106. GERLOCK Jr, A.J., T.J. PHIFER, and J.C. McDONALD, *Venous Prosthetic Valves The First Step Toward an Investigation in the Canine Model*. Investigative radiology, 1985. **20**(1): p. 42-44.
107. Hill, R., et al., *Development of a prosthetic venous valve*. Journal of biomedical materials research, 1985. **19**(7): p. 827-832.
108. Dalsing, M.C., et al., *An early experience with endovascular venous valve transplantation*. Journal of vascular surgery: official publication, the Society for Vascular Surgery [and] International Society for Cardiovascular Surgery, North American Chapter, 1996. **24**(5): p. 903.
109. Gomez-Jorge, J., A.C. Venbrux, and C. Magee, *Percutaneous Deployment of a Valved Bovine Jugular Vein in the Swine Venous System: A Potential Treatment for Venous Insufficiency*. Journal of Vascular and Interventional Radiology, 2000. **11**(7): p. 931-936.
110. Pavcnik, D., et al., *Percutaneous management of chronic deep venous reflux: review of experimental work and early clinical experience with bioprosthetic valve*. Vascular Medicine, 2008. **13**(1): p. 75-84.

111. Thorpe, P., F. Osse, and L. Correa. *The valve-stent: development of a percutaneous prosthesis for treatment of valvular insufficiency*. in *The 12th Annual Meeting of the American Venous Forum, Phoenix, AZ, USA*. 2000.
112. Hasaniya, N., *In vitro construction of totally autogenous venous valve: Early experience*. *Phlebology*, 2002. **16**(4): p. 142-144.
113. Pavcnik, D., et al., *Aortic and venous valve for percutaneous insertion*. *Minimally Invasive Therapy & Allied Technologies*, 2000. **9**(3-4): p. 287-292.
114. Pavcnik, D., et al., *Square stent: a new self-expandable endoluminal device and its applications*. *Cardiovascular and interventional radiology*, 2001. **24**(4): p. 207-217.
115. Pavcnik, D., et al., *Percutaneous bioprosthetic venous valve: a long-term study in sheep*. *Journal of Vascular Surgery*, 2002. **35**(3): p. 598-602.
116. Pavcnik, D., et al., *Percutaneous prosthetic venous valves: current state and possible applications*. *Techniques in Vascular and Interventional Radiology*, 2003. **6**(3): p. 137-142.
117. Pavcnik, D., et al., *Second-generation percutaneous bioprosthetic valve: a short-term study in sheep*. *Journal of Vascular Surgery*, 2004. **40**(6): p. 1223-1227.
118. Pavcnik, D., et al., *Significance of spatial orientation of percutaneously placed bioprosthetic venous valves in an ovine model*. *J Vasc Interv Radiol*, 2005. **16**(11): p. 1511-6.
119. Pavcnik, D., *Update on Venous Valve Replacement: Long-Term Clinical Results*. *Vascular*, 2006. **14**(Suppl 1): p. S106.
120. Pavcnik, D., et al. *Percutaneous Therapy for Deep Vein Reflux*. in *Seminars in Interventional Radiology*. 2005. Thieme Medical Publishers.
121. Pavcnik, D., et al., *Percutaneous autologous venous valve transplantation: short-term feasibility study in an ovine model*. *J Vasc Surg*, 2007. **46**(2): p. 338-45.
122. Lee, D., et al., *In vitro testing of venous valves*. *ASAIO transactions/American Society for Artificial Internal Organs*, 1991. **37**(3): p. M266.
123. DeLaria, G.A., et al., *Hemodynamic evaluation of a bioprosthetic venous prosthesis*. *Journal of Vascular Surgery*, 1993. **18**(4): p. 577-586.

124. Serino, F., *Preliminary clinical experiences with VenPro PVVB*. Updating course in vascular pathology of surgical interest. In deep venous surgery and new technologies. Pisa, Italy, 2002.
125. de Borst, G.J., et al., *A percutaneous approach to deep venous valve insufficiency with a new self-expanding venous frame valve*. Journal of Endovascular Therapy, 2003. **10**(2): p. 341-349.
126. Gale, S.S., et al., *Percutaneous venous valve bioprosthesis: initial observations*. Vascular and endovascular surgery, 2004. **38**(3): p. 221-224.
127. Kucher, T., et al., *Endovascular delivery of vein segments with valves versus direct anastomosis*. Journal Information, 2005. **12**(3).
128. Teebken, O., et al., *Tissue-engineered bioprosthetic venous valve: a long-term study in sheep*. European journal of vascular and endovascular surgery, 2003. **25**(4): p. 305-312.
129. Teebken, O.E., et al., *Preclinical development of tissue-engineered vein valves and venous substitutes using re-endothelialised human vein matrix*. Eur J Vasc Endovasc Surg, 2009. **37**(1): p. 92-102.
130. Wei, Z., et al., *[Comparison between canine decellularized venous valve stent combined with endothelial progenitor cells and native venous valve on venous valve closure mechanism in normal physiological conditions]*. Chinese journal of reparative and reconstructive surgery, 2009. **23**(10): p. 1260.
131. Dijkstra, M.L., et al., *PS134. Endovenous Valve Transfer for Chronic Venous Hypertension*. Journal of Vascular Surgery, 2012. **55**(6): p. 61S.
132. Liu, C., et al., *Fabrication of tissue engineered vein containing valve scaffolds*. Zhonghua yi xue za zhi, 2012. **92**(15): p. 1054.
133. Wen, Y., et al., *Construction of Tissue-Engineered Venous Valves in Vitro Using Two Types of Progenitor Cells and Decellularized Scaffolds Category: Original*. Open Tissue Engineering and Regenerative Medicine Journal, 2012. **5**: p. 9-16.
134. Uflacker, R. *Percutaneously introduced artificial venous valve: experimental use in pigs*. in *The 1993 Annual Meeting of the Western Angiographic & Interventional Society*. 1993.
135. Nadzeyka, I., et al., *Development of a Percutaneous Implantable Venous Valve Prosthesis made from Polyurethane*. ICI meeting 2011, Tel-Aviv, 2011.

136. de Borst, G.J. and F.L. Moll, *Percutaneous Venous Valve Designs for Treatment of Deep Venous Insufficiency*. Journal of Endovascular Therapy, 2012. **19**(2): p. 291-302.
137. Rittgers, S.E., M.T. Oberdier, and S. Pottala, *Physiologically-based testing system for the mechanical characterization of prosthetic vein valves*. Biomed Eng Online, 2007. **6**: p. 29.
138. Oberdier, M.T. and S.E. Rittgers, *The design, development, and evaluation of a prototypic, prosthetic venous valve*. Biomed Eng Online, 2008. **7**: p. 25.
139. Raja, V., *Computational Fluid Dynamics Analysis of a Prototypic, Prosthetic Venous Valve*, 2007, University of Akron.
140. Anim, K., *Design, Development, Testing, and Evaluation of a Prosthetic Venous Valve*, 2010, University of Akron.
141. Sathe, R.D., *Design and development of a novel implantable prosthetic vein valve*. 2006.
142. Moriyama, M., et al., *Evaluation of prosthetic venous valves, fabricated by electrospinning, for percutaneous treatment of chronic venous insufficiency*. J Artif Organs, 2011. **14**(4): p. 294-300.
143. Sathe, R.D. and D.N. Ku, *Flexible Prosthetic Vein Valve*. Journal of Medical Devices, 2007. **1**(2): p. 105.
144. Farrell, L.L.A.C., *Prosthetic Vein Valve: Delivery and In Vitro Evaluation*. 2007.
145. Midha, P.A., *Long-term patency of a polymer vein valve*. 2009.
146. US Food and Drug Administration. Title 21: Food and Drugs. Chapter I: Food and Drug Administration, Department of Health and Human Services. Subchapter H: Medical Devices. 21CFR part 820: Quality System Regulation., 1996.
147. Vasdekis, S.N., G.H. Clarke, and A.N. Nicolaides, *Quantification of venous reflux by means of duplex scanning*. Journal of Vascular Surgery, 1989. **10**(6): p. 0670-0677.
148. Höjensgard, I., *Static and Dynamic Pressures in Superficial and Deep Veins of the Lower Extremity in Man*. Acta physiologica Scandinavica, 1953. **27**(1): p. 49-67.
149. Stick, C., U. Hiedl, and E. Witzleb, *Venous pressure in the saphenous vein near the ankle during changes in posture and exercise at different ambient*

- temperatures*. European journal of applied physiology and occupational physiology, 1993. **66**(5): p. 434-438.
150. Alimi, Y., P. Barthelemy, and C. Juhan, *Venous pump of the calf: a study of venous and muscular pressures*. Journal of Vascular Surgery, 1994. **20**(5): p. 728-735.
 151. Fronek, A., et al., *Common femoral vein dimensions and hemodynamics including Valsalva response as a function of sex, age, and ethnicity in a population study*. J Vasc Surg, 2001. **33**(5): p. 1050-6.
 152. Dickson, B.C., *Venous thrombosis: on the history of Virchow's triad*. Univ Toronto Med J, 2004. **81**(3): p. 166-171.
 153. Victor, R.G. and D.R. Seals, *Reflex stimulation of sympathetic outflow during rhythmic exercise in humans*. American Journal of Physiology-Heart and Circulatory Physiology, 1989. **257**(6): p. H2017-H2024.
 154. Wilson, N. and D. Rutt, *Repair and replacement of deep vein valves in the treatment of venous insufficiency*. British journal of surgery, 1991. **78**(4): p. 388-394.
 155. Savage, B., E. Saldívar, and Z.M. Ruggeri, *Initiation of platelet adhesion by arrest onto fibrinogen or translocation on von Willebrand factor*. Cell, 1996. **84**(2): p. 289-297.
 156. Hellums, J.D., *1993 Whitaker Lecture: biorheology in thrombosis research*. Annals of biomedical engineering, 1994. **22**(5): p. 445-455.
 157. Bark, D.L., A.N. Para, and D.N. Ku, *Correlation of thrombosis growth rate to pathological wall shear rate during platelet accumulation*. Biotechnology and Bioengineering, 2012.
 158. Zydney, A.L. and C.K. Colton, *Augmented solute transport in the shear flow of a concentrated suspension*. PCH, PhysicoChem. Hydrodyn, 1988. **10**: p. 77.
 159. Markou, C., et al., *The role of high wall shear rate on thrombus formation in stenoses*. ASME-PUBLICATIONS-BED, 1993. **26**: p. 555-555.
 160. Badimon, L., et al., *Influence of arterial damage and wall shear rate on platelet deposition. Ex vivo study in a swine model*. Arterioscler Thromb Vasc Biol, 1986. **6**(3): p. 312-320.
 161. Barstad, R.M., et al., *A perfusion chamber developed to investigate thrombus formation and shear profiles in flowing native human blood at the*

- apex of well-defined stenoses. Arterioscler Thromb Vasc Biol, 1994. 14(12): p. 1984-1991.*
162. Barstad, R., P. Kierulf, and K. Sakariassen, *Collagen induced thrombus formation at the apex of eccentric stenoses: a time course study with non-anticoagulated human blood. Thrombosis and haemostasis, 1996. 75(4): p. 685-692.*
 163. Para, A., et al., *Rapid Platelet Accumulation Leading to Thrombotic Occlusion. Annals of biomedical engineering, 2011. 39(7): p. 1961-1971.*
 164. Onuki, Y., et al., *A review of the biocompatibility of implantable devices: current challenges to overcome foreign body response. J Diabetes Sci Technol, 2008. 2(6): p. 1003-1015.*
 165. Ku, D.N., *New soft tissue Implants using organic elastomers. Biomedical Engineering Systems and Technologies, 2009: p. 85-95.*
 166. Marascalco, P.J., et al., *Development of standard tests to examine viscoelastic properties of blood of experimental animals for pediatric mechanical support device evaluation. ASAIO J, 2006. 52(5): p. 567-74.*
 167. Windberger, U., et al., *Whole blood viscosity, plasma viscosity and erythrocyte aggregation in nine mammalian species: reference values and comparison of data. Experimental Physiology, 2003. 88(3): p. 431-440.*
 168. Brookshier, K.K. and J. Tarbell, *Effect of hematocrit on wall shear rate in oscillatory flow: do the elastic properties of blood play a role? Biorheology, 1991. 28(6): p. 569.*
 169. Para, A.N., *Preventing rapid platelet accumulation under very high shear stress. 2012.*
 170. Rachel, E.S., et al., *Percutaneous endovascular abdominal aortic aneurysm repair. Ann Vasc Surg, 2002. 16(1): p. 43-49.*
 171. Ku, D.N., L.G. Braddon, and D.M. Wootton, *Poly (vinyl alcohol) cryogel, 1999, US Patent 5981826.*
 172. Ku, D.N., *Poly (vinyl alcohol) hydrogel, 2001, US Patent 6,231,605.*
 173. Weaver, J.D., *Development of a polyvinyl alcohol cryogel covered stent. 2010.*
 174. Miyake, H., et al., *New small-caliber antithrombotic vascular prosthesis: Experimental study. Microsurgery, 1984. 5(3): p. 144-150.*
 175. Weaver, J.D. and D.N. Ku, *Biomaterial testing for covered stent membranes: Evaluating thrombosis and restenosis potential. Journal of*

- Biomedical Materials Research Part B: Applied Biomaterials, 2011. **100**(1): p. 103-110.
176. Nuttelman, C.R., et al., *Attachment of fibronectin to poly (vinyl alcohol) hydrogels promotes NIH3T3 cell adhesion, proliferation, and migration.* Journal of biomedical materials research, 2001. **57**(2): p. 217-223.
 177. Weaver, J.D. and D.N. Ku, *Mechanical Evaluation of Polyvinyl Alcohol Cryogels for Covered Stents.* Journal of Medical Devices, 2010. **4**(3): p. 031002.
 178. Fromageau, J., et al., *Characterization of PVA cryogel for intravascular ultrasound elasticity imaging.* Ultrasonics, Ferroelectrics and Frequency Control, IEEE Transactions on, 2003. **50**(10): p. 1318-1324.
 179. Fromageau, J., et al., *Estimation of polyvinyl alcohol cryogel mechanical properties with four ultrasound elastography methods and comparison with gold standard testings.* Ultrasonics, Ferroelectrics and Frequency Control, IEEE Transactions on, 2007. **54**(3): p. 498-509.
 180. Duboeuf, F., et al. *Static mechanical assessment of elastic Young's modulus of tissue mimicking materials used for medical imaging.* in *Engineering in Medicine and Biology Society, 2007. EMBS 2007. 29th Annual International Conference of the IEEE.* 2007. IEEE.
 181. Stammen, J.A., et al., *Mechanical properties of a novel PVA hydrogel in shear and unconfined compression.* Biomaterials, 2001. **22**(8): p. 799-806.
 182. Williams, S., *Mechanical testing of a new biomaterial for potential use as a vascular graft and articular cartilage replacement.* MStthesis, Georgia Institute of Technology, 1998. **10**.
 183. Duboeuf, F.o., et al., *Investigation of PVA cryogel Young's modulus stability with time, controlled by a simple reliable technique.* Medical Physics, 2009. **36**(2): p. 656.
 184. Xie, L., et al., *Controlled mechanical and swelling properties of poly(vinyl alcohol)/sodium alginate blend hydrogels prepared by freeze-thaw followed by Ca²⁺ crosslinking.* Journal of Applied Polymer Science, 2012. **124**(1): p. 823-831.
 185. Holloway, J.L., A.M. Lowman, and G.R. Palmese, *Aging behavior of PVA hydrogels for soft tissue applications after in vitro swelling using osmotic pressure solutions.* Acta Biomater, 2012.
 186. Cournane, S., et al., *Assessment of the accuracy of an ultrasound elastography liver scanning system using a PVA-cryogel phantom with*

- optimal acoustic and mechanical properties*. Physics in medicine and biology, 2010. **55**(19): p. 5965.
187. Gupta, S., S. Goswami, and A. Sinha, *A combined effect of freeze--thaw cycles and polymer concentration on the structure and mechanical properties of transparent PVA gels*. Biomed Mater, 2012. **7**(1): p. 015006.
 188. Depp, M.M.R., *PVA cryogel optimization and diffusion studies*. 1998.
 189. Sollier, E., et al., *Rapid prototyping polymers for microfluidic devices and high pressure injections*. Lab on a Chip, 2011. **11**(22): p. 3752-3765.
 190. Dormandy, J., *Clinical significance of blood viscosity*. Annals of the Royal College of Surgeons of England, 1970. **47**(4): p. 211.
 191. Pedley, T.J. and X. Luo, *Fluid mechanics of large blood vessels*. 1995.
 192. Berger, S. and L. Jou, *Flows in stenotic vessels*. Annual Review of Fluid Mechanics, 2003. **32**(1): p. 347.
 193. Cho, Y. and K. Kensey, *Effects of the non-Newtonian viscosity of blood on flows in a diseased arterial vessel. Part 1: Steady flows*. Biorheology, 1991. **28**(3-4): p. 241.
 194. Kundu, P. and I. Cohen, *Fluid Mechanics*. 2004, 2008, Elsevier Academic Press.
 195. Johnston, B.M., et al., *Non-Newtonian blood flow in human right coronary arteries: steady state simulations*. J Biomech, 2004. **37**(5): p. 709-20.
 196. Lesser, A.J., *Fatigue Behavior of Polymers*. Encyclopedia Of Polymer Science and Technology, 2002.
 197. Kinsel, D., *Design control requirements for medical device development*. World Journal for Pediatric and Congenital Heart Surgery, 2012. **3**(1): p. 77-81.
 198. Lu, W., et al., *The ovine jugular vein as a model for interventional radiology procedures*. Radiology and Oncology, 2008. **42**(2): p. 59-65.
 199. Lattimer, C.R., et al., *Saphenous pulsation on duplex may be a marker of severe chronic superficial venous insufficiency*. J Vasc Surg, 2012. **56**(5): p. 1338-43.
 200. Haenen, J., et al., *Venous duplex scanning of the leg: range, variability and reproducibility*. Clinical Science, 1999. **96**: p. 271-277.
 201. Eriksson, I. and B. Almgren, *Surgical reconstruction of incompetent deep vein valves*. Upsala journal of medical sciences, 1988. **93**(2): p. 139-143.

202. Nash, T., *Long term results of vein valve transplants placed in the popliteal vein for intractable post-phlebotic venous ulcers and pre-ulcer skin changes*. J Cardiovasc Surg, 1988. **29**(6): p. 712-6.
203. Sottiurai, V., *Comparison of surgical modalities in the treatment of recurrent venous ulcer*. International angiology: a journal of the International Union of Angiology, 1990. **9**(4): p. 231.
204. Sottiurai, V.S., *Current surgical approaches to venous hypertension and valvular reflux*. International Journal of Angiology, 1996. **5**(1): p. 49-54.
205. Muhlberger, D., L. Morandini, and E. Brenner, *Venous valves and major superficial tributary veins near the saphenofemoral junction*. J Vasc Surg, 2009. **49**(6): p. 1562-9.
206. Wilcoxon, F., *Individual comparisons by ranking methods*. Biometrics Bulletin, 1945. **1**(6): p. 80-83.
207. Wilcoxon, F., et al., *Critical values and probability levels for the Wilcoxon rank sum test and the Wilcoxon signed rank test* 1963: Lederle Laboratories Division, American Cyanamid.
208. Faul, F., et al., *G* Power 3: A flexible statistical power analysis program for the social, behavioral, and biomedical sciences*. Behavior research methods, 2007. **39**(2): p. 175-191.
209. Faul, F., et al., *Statistical power analyses using G* Power 3.1: Tests for correlation and regression analyses*. Behavior research methods, 2009. **41**(4): p. 1149-1160.
210. Bia, D., et al., *In vitro model to study arterial wall dynamics through pressure-diameter relationship analysis*. Latin American applied research, 2005. **35**(3): p. 217-224.
211. Beddy, P., et al., *Valsalva and gravitational variability of the internal jugular vein and common femoral vein: ultrasound assessment*. Eur J Radiol, 2006. **58**(2): p. 307-9.
212. Rippey, J.C., O. Pascu, and I. Jacobs, *Abdominal compression effectively increases the size of the common femoral vein, as measured by ultrasonography*. Ann Emerg Med, 2008. **52**(4): p. 446-52.
213. Hertzberg, B., et al., *Sonographic assessment of lower limb vein diameters: implications for the diagnosis and characterization of deep venous thrombosis*. American Journal of Roentgenology, 1997. **168**(5): p. 1253-1257.

214. Delis, K.T., et al., *Lower limb venous haemodynamic impairment on dependency: quantification and implications for the "economy class" position.* THROMBOSIS AND HAEMOSTASIS-STUTTGART-, 2004. **91**(5): p. 941-950.